reactions

MDPI

Review

Transformations of Glycerol into High-Value-Added Chemical Products: Ketalization and Esterification Reactions

Federico M. Perez , Martin N. Gatti , Gerardo F. Santori and Francisco Pompeo *

Centro de Investigación y Desarrollo en Ciencias Aplicadas (CINDECA), Facultad de Ciencias Exactas, Universidad Nacional de La Plata (UNLP)—CONICET, Calle 47, 257, La Plata 1900, Argentina; federico.perez@ing.unlp.edu.ar (F.M.P.); martin.gatti@ing.unlp.edu.ar (M.N.G.); santori@quimica.unlp.edu.ar (G.F.S.)

* Correspondence: fpompeo@quimica.unlp.edu.ar

Abstract: Biomass allows us to obtain energy and high-value-added compounds through the use of different physical and chemical processes. The glycerol obtained as a by-product in the synthesis of biodiesel is considered a biomass compound that has the potential to be used as a raw material to obtain different chemical products for industry. The development and growth of the biodiesel industry allows for the projection of glycerol biorefineries around these plants that efficiently and sustainably integrate the biodiesel production process together with the glycerol transformation processes. This work presents a review of the ketalization and esterification of glycerol to obtain solketal and acetylglycerols, which are considered products of high added value for the chemical and fuel industry. First, the general aspects and mechanisms of both reactions are presented, as well as the related chemical equilibrium concepts. Subsequently, the catalysts employed are described, classifying them according to their catalytic nature (zeolites, carbons, exchange resins, etc.). The reaction conditions used are also described, and the best results for each catalytic system are presented. In addition, stability studies and the main deactivation mechanisms are discussed. Finally, the work presents the kinetic models that have been formulated to date for some of these systems. It is expected that this review work will serve as a tool for the advancement of studies on the ketalization and esterification reactions that allow for the projection of biorefineries based on glycerol as a raw material.

Keywords: glycerol; ketalization; esterification; solketal; acetylglycerols

check for updates

Citation: Perez, F.M.; Gatti, M.N.; Santori, G.F.; Pompeo, F. Transformations of Glycerol into High-Value-Added Chemical Products: Ketalization and Esterification Reactions. *Reactions* **2023**, *4*, 569–634. https://doi.org/10.3390/reactions4040034

Academic Editors: Diogo M.F. Santos, Margarida Gonçalves, Catarina Nobre and Paulo Brito

Received: 31 July 2023
Revised: 30 August 2023
Accepted: 27 September 2023
Published: 8 October 2023

1. Introduction

In recent years, the growing demand for energy has led scientists to investigate new ways of obtaining energy that, in addition to enabling economic and social development, are eco-compatible and sustainable over time.

In this context, biomass resources that originate from natural and renewable organic resources serve as energy sources, in addition to allowing the production of high-value-added products such as fine chemicals, materials and other consumer goods [1].

According to the way it is obtained, biomass can be classified as primary, secondary, or tertiary, as shown in Figure 1 [2]. Primary biomass is that which is obtained directly from the natural ecosystem, such as leaves and the branches of a tree, for energy utilization. Secondary biomass is that which is obtained as a residue or by-product of human activity, such as waste from the agri-food industry (bagasse, husks, etc.) or forestry and livestock waste. Finally, tertiary biomass is biomass that has been previously processed before use, such as biogas, biodiesel, bioethanol, etc.

There are different ways in which fuels and energy can be obtained from biomass, and these can be categorized into three main processes:

- Thermal conversion to produce heat and electricity.
- Generation of gaseous fuels, such as methane and hydrogen.

- Generation of liquid fuels, such as ethanol and biodiesel.

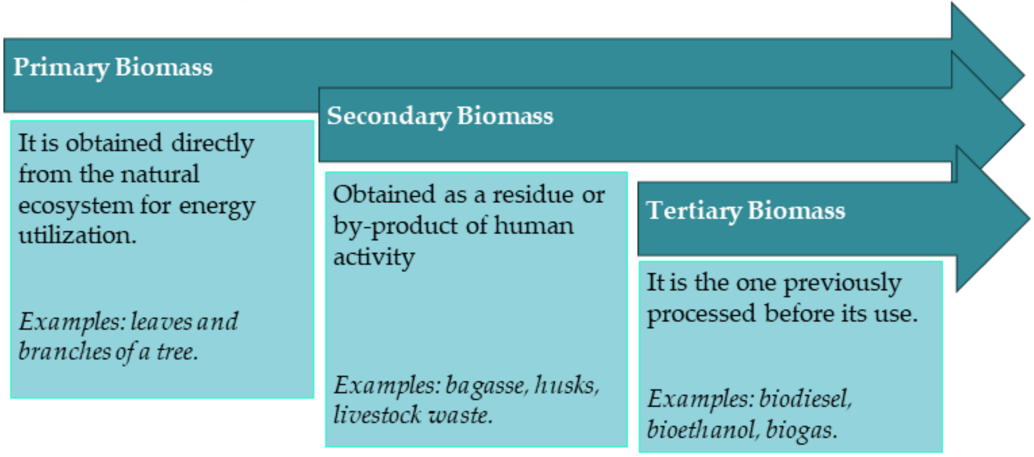

Figure 1. Main glycerol applications.

It is also possible to obtain value-added compounds from biomass through different physical and chemical processes, such as extraction, biochemical conversion and liquefaction, which allow us to visualize the great potential that biomass has for synthesizing a wide range of products of interest. This is the example of the fermentation of glucose (obtained from starch, cellulose, etc.) to obtain lactic acid, whose subsequent polymerization is useful for the synthesis of biodegradable polymers or the dehydration of glucose to obtain 5-hydroxymethylfurfural (HMF), a compound from which a wide variety of interesting products can be synthesized from the industrial point of view [3].

Of all the possible processes for biomass conversion, the production of liquid biofuels has been one of the most developed valorization routes at the international level, being exploited mainly by those countries with a large availability of biomass. Biofuels can be classified as first, second, third or fourth generation, whose characteristics are summarized in Figure 2 [4].

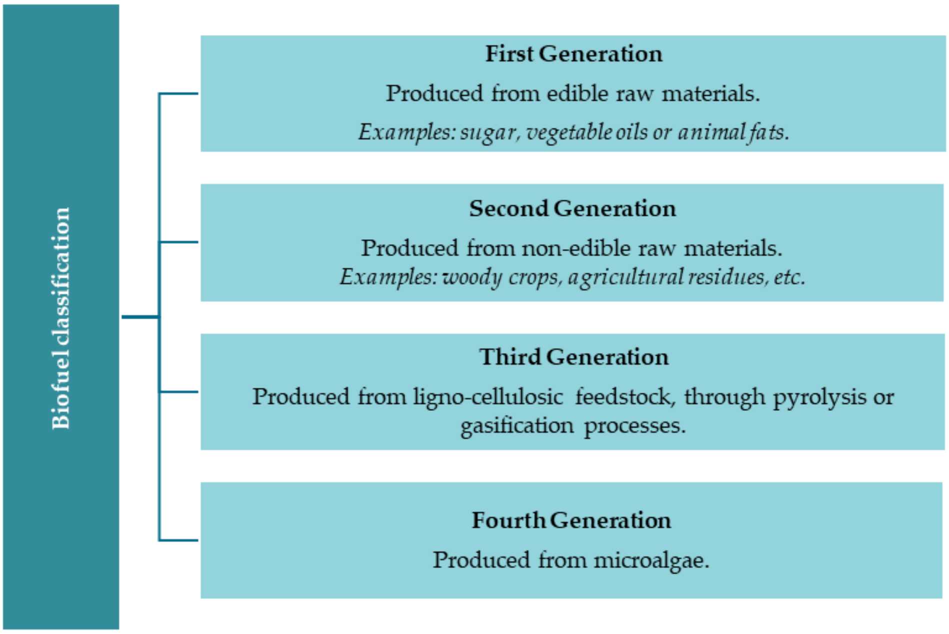

Figure 2. Biofuels' classification according to the raw material employed for their synthesis [4].

Among the first-generation biofuels, biodiesel obtained from soybean oil and bioethanol obtained from sugarcane and corn are the two most widely used types of biofuels in the world.

In particular, biodiesel is a mixture of long-chain fatty acid esters produced from the triglyceride transesterification reaction in the presence of catalysts [5]. Transesterification is an equilibrium reaction in which triglycerides react with a short-chain alcohol (R′OH) ($R' = CH_{3-}/CH_3CH_{2-}/CH_3CH_2CH_{2-}$), usually methanol, in the presence of a catalyst, producing three molecules of fatty acid methyl esters (FAME) and one molecule of glycerol (Scheme 1). The equilibrium is shifted towards the products by carrying out the reaction with excess methanol [4].

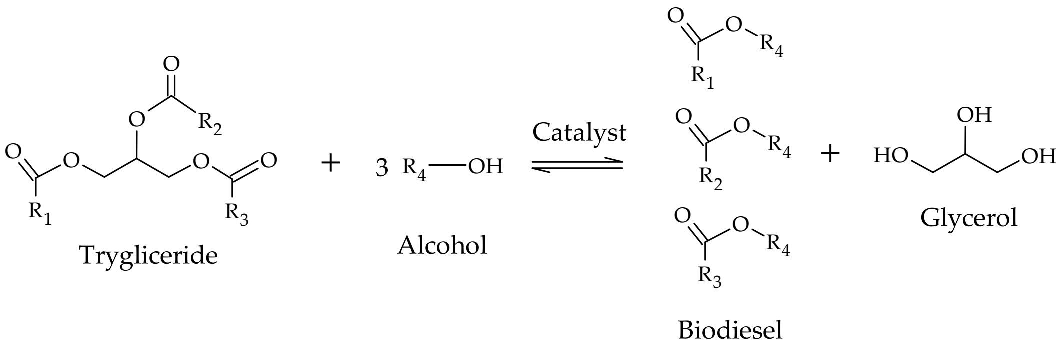

Scheme 1. Transesterification of triglycerides with short-chain alcohols to obtain biodiesel.

Between 2010 and 2021, global biodiesel production has experienced a 240% increase (Figure 3), mainly due to government policies aimed at favoring the use of biofuels [6].

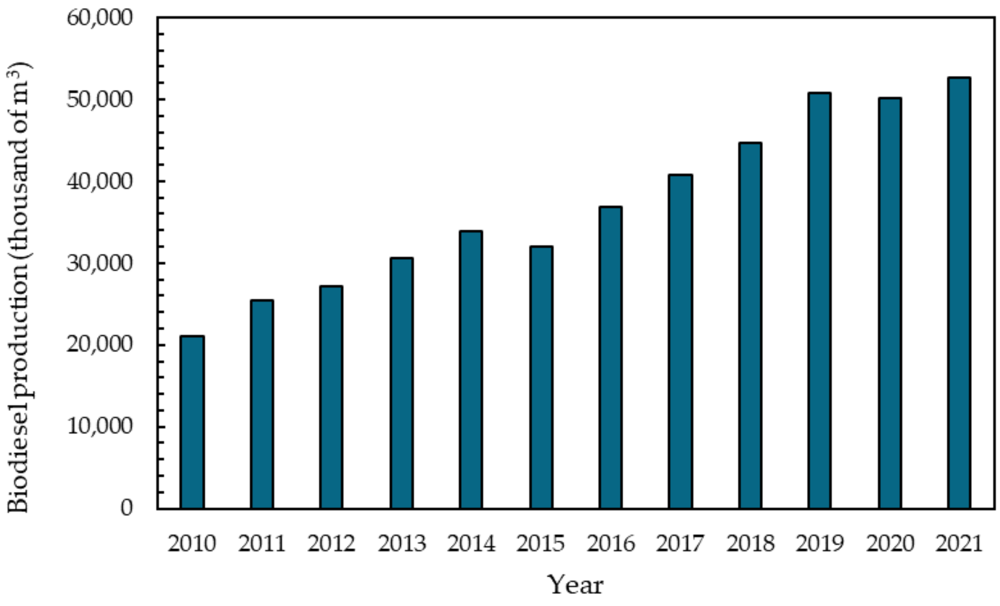

Figure 3. Annual evolution for 2010–2021 of world biodiesel production.

In terms of production distribution, only five countries account for 53% of world's biodiesel production: Indonesia (16%), the United States (13%), Brazil (11%), Germany (8%) and France (5%). The remaining 47% of production is distributed among other countries, with the participation of Argentina, Spain, the Netherlands, Thailand and Malaysia being noteworthy (Figure 4a) [7].

In terms of consumption, the statistics show a relatively decentralized participation. Of the total number of consuming countries, 52% of consumption is concentrated in the United States (14%), Indonesia (13%), Brazil (12%), France (8%) and Germany (5%). The remaining 48% is distributed among the other countries of the world, with a notable participation of Spain, Sweden, Thailand, United Kingdom, Italy and Argentina (Figure 4b) [7].

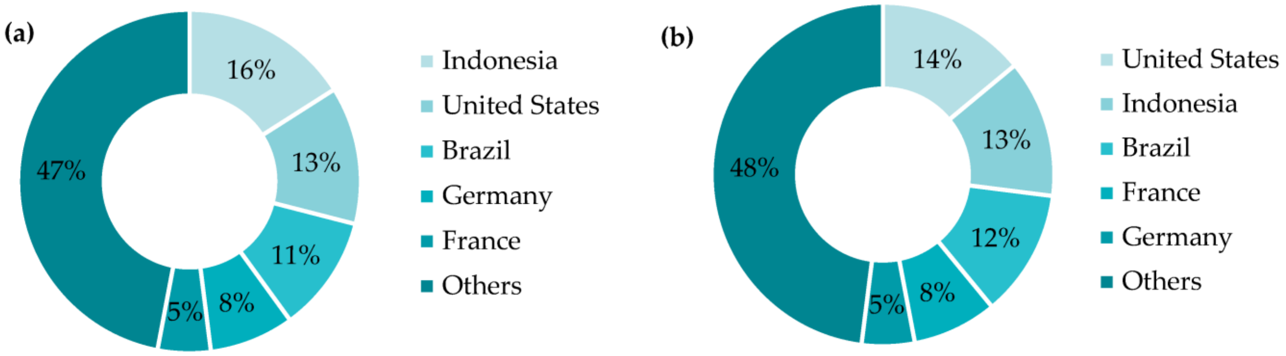

Figure 4. (**a**) Distribution of world biodiesel production. (**b**) Distribution of world biodiesel consumption.

In the triglyceride transesterification reaction, approximately 10 wt.% glycerol is obtained as a by-product, called crude glycerol, with a degree of purity between 55 and 90 wt.% depending on the source of triglycerides used, the catalyst employed and the conditions of the synthesis process. Generally, the impurities encountered include traces of unreacted triglycerides and short-chain alcohol, biodiesel, grade acids, soaps and other minority compounds [4].

Crude glycerol can be further refined for use in various applications, which will establish the specifications it must meet. Once treated, it can be used in the food and beverage industry as a humectant, sweetener and preservative; and in the cosmetics industry as an ingredient in toothpastes, lotions, shaving creams, deodorants, makeup and creams. It has also been reported to be used in the pharmaceutical industry as an active agent in veterinary drugs [4].

Despite its wide variety of uses, they do not satisfy the total supply of glycerol. The surplus has oversaturated these markets, devaluing the price of glycerol and favoring its use as a raw material for the generation of other value-added products [8].

In this sense, the reactivity of glycerol makes it a platform molecule for the production of a wide variety of industrial chemical compounds (Figure 5), such as glyceric acid [9], polyglycerols [10], esters [11], ethers [12], synthesis gas [13], epichlorohydrin [14], glycerol carbonate [15], acrolein [16], glycols [17] and cyclic ketals [18].

Of all the possible glycerol conversion reactions, ketalization and esterification in the presence of catalysts have gained relevance in recent years, due to the particular interest in the products obtained from each one [19,20].

Glycerol ketalization is carried out in the presence of acetone, while esterification is usually carried out in the presence of acetic acid. The reaction products are different for each of them: while ketalization leads to the formation of solketal, esterification leads to the formation of acetylglycerols (Scheme 2).

With respect to solketal, its synthesis at the laboratory level has been known since the end of the 19th century; however, interest in its large-scale production was driven by the development of renewable energies towards the end of the 20th century.

Due to the novelty of the compound, there are very few tabulated data for its physicochemical properties [21]. Various uses of solketal have been reported, and many of them are in the research stage. One of the most promising uses is as a fuel additive to replace ethers with anti-knock properties, such as MTBE (methyl tert-butyl ether), TAME (tert-amyl methyl ether) and ETBE (ethyl tert-butyl ether) [22]. Reportedly, the addition of solketal to naphtha between 1 and 5% by volume leads to a significant decrease in gum formation and improves octane [23]. Its use as a green solvent has also been reported, since its polarity and hydrophobicity are in the order of traditional solvents, such as ethanol, 2-propanol, acetonitrile and ethyl acetate, thus allowing for its application as a binder for polyesters, polyacetates, polyacrylates, epoxies, polyurethanes, etc. [24].

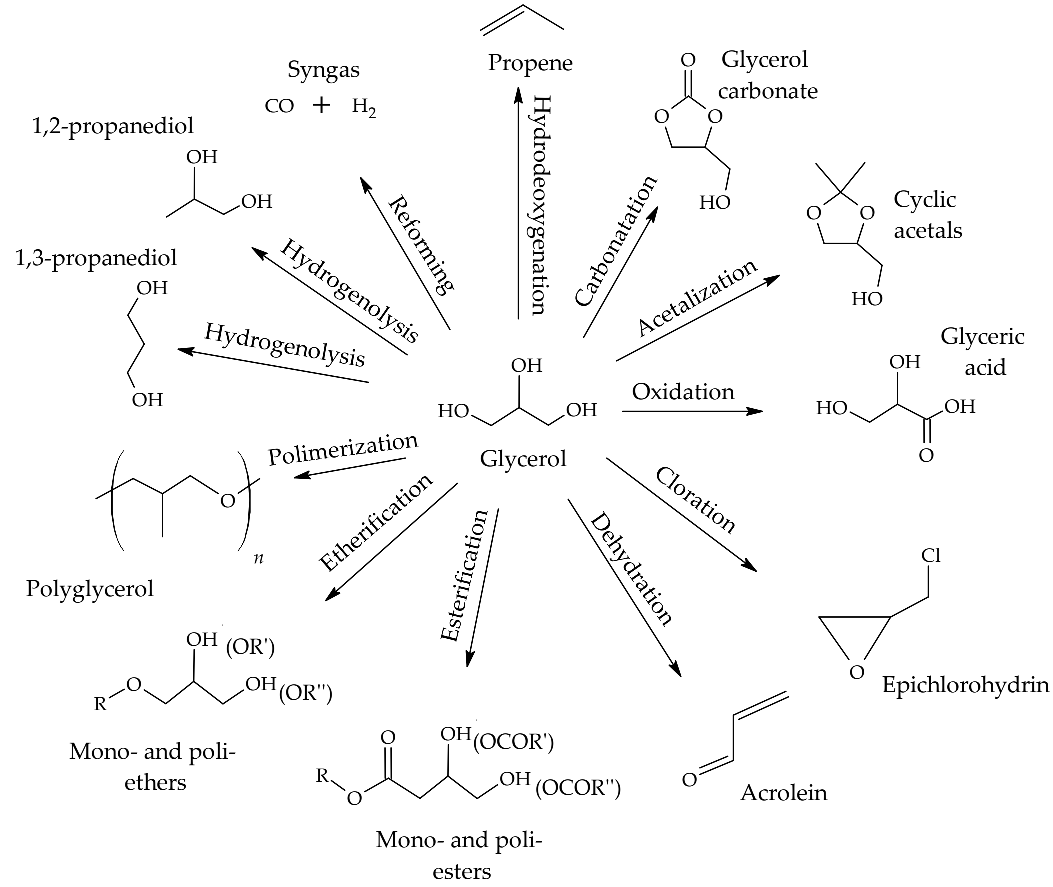

Figure 5. High-added-value products obtained from glycerol conversion reactions.

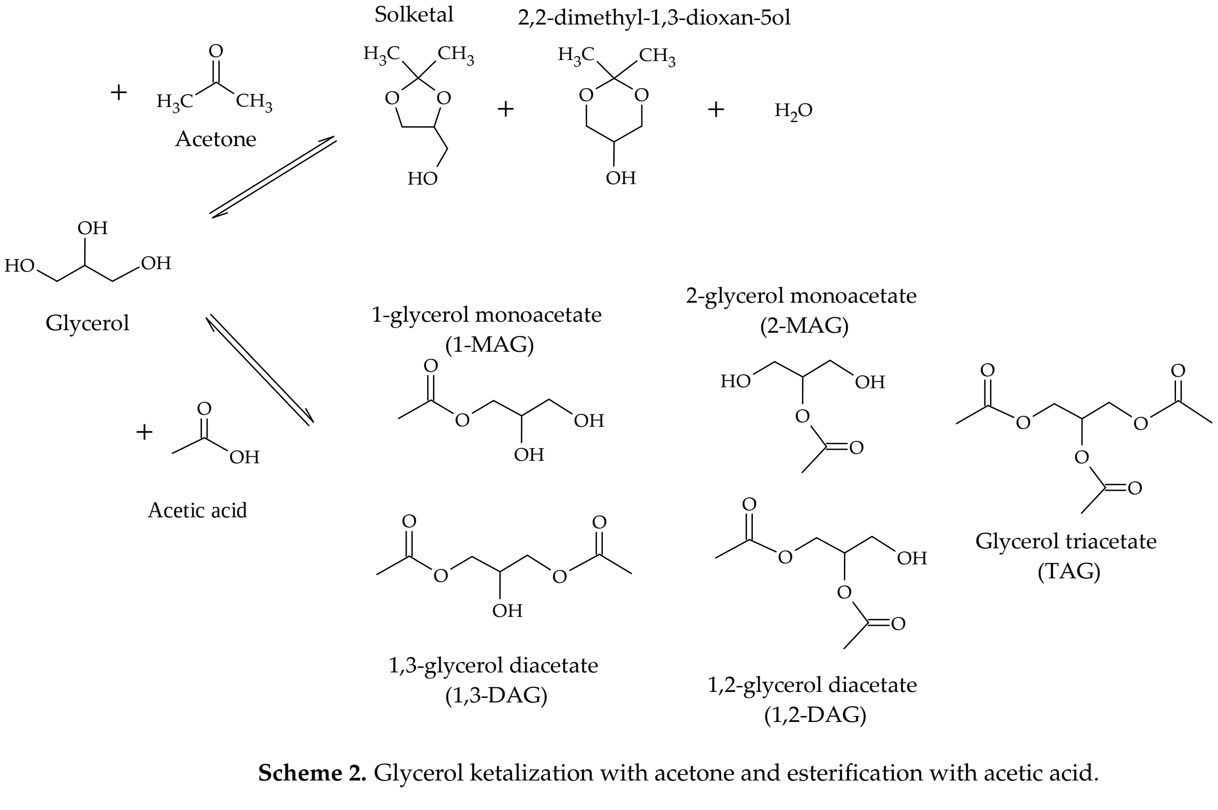

Scheme 2. Glycerol ketalization with acetone and esterification with acetic acid.

With respect to esterification products, they consist of mono-, di- and tri-acetylglycerols, which have diverse industrial applications. Mono-acetylglycerols (MAGs) and di-acetylglycerols (DAGs) have applications in the production of biodegradable polyesters, food additives and the cosmetic industry [25]. In particular, MAGs are used as additives in the pharmaceutical and food industry and for the manufacture of explosives and smokeless gunpowder. DAGs are found in cocoa butter and are used as intermediates in the structural synthesis of lipids. With respect to tri-acetylglycerol (TAG), its use in the production of cosmetics, plasticizers and solvents has been reported [26]. In addition, the FDA (Food and Drug Administration) considers it to be a GRAS (generally recognized as safe) additive, so it is used as a flavoring agent, humectant and solvent in food. In addition, the high O/C ratio in its molecule makes it a promising additive for fuels, improving their performance, facilitating their transport at low temperatures and reducing the emission of harmful gases in their combustion.

Since the 1990s, the biofuel industry began to gain importance, due to the search for new energy sources to replace, at least partially, the energy obtained from fossil fuels. This resulted in an increase in publications related to the ketalization of glycerol to produce solketal (Figure 6a) and the esterification of glycerol to produce acetylglycerols (Figure 6b) [27]. In both cases, an increase in the number of publications from 2000 to the present is observed.

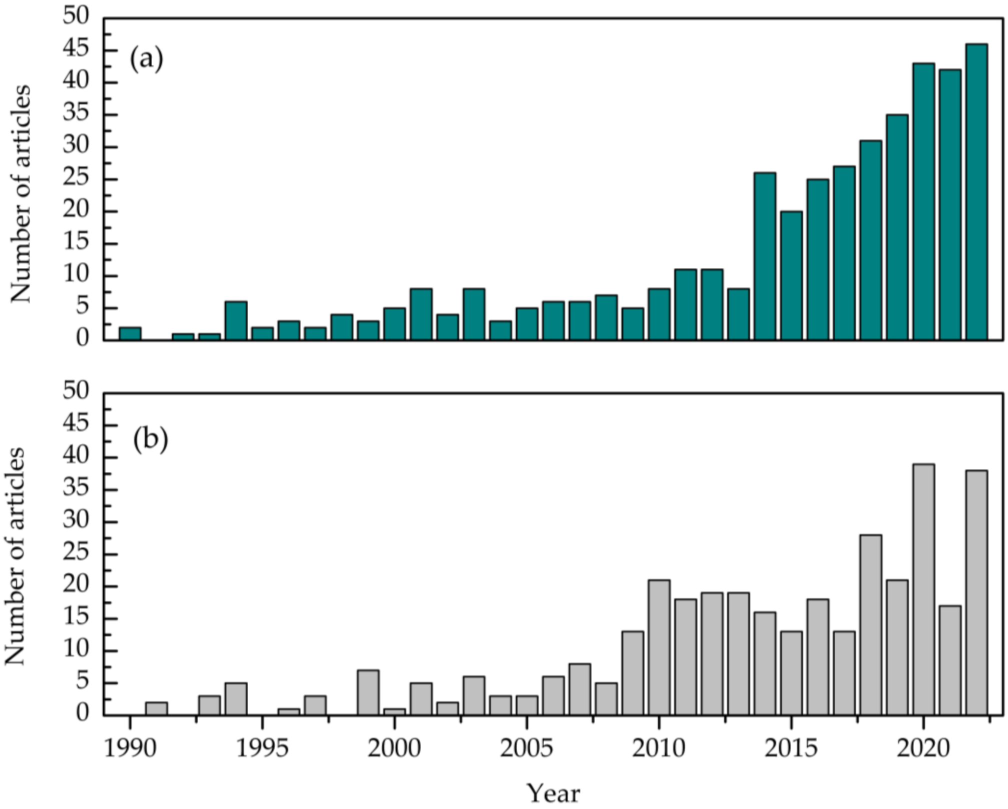

Figure 6. Annual evolution of publications: (**a**) ketalization of glycerol with acetone (**b**) esterification of glycerol with acetic acid. Source: Scopus (March 2023). Search words: (**a**) “Solketal”; (**b**) “Triacetin” and “Glycerol”.

Regarding the countries that have published the largest number of papers on glycerol ketalization, China leads the ranking, followed by Brazil and then India, the United States and France (Figure 7a). As for glycerol esterification, the United States leads the ranking, followed by India and then China, Indonesia and Germany (Figure 7b).

With respect to the review papers, the contribution of those articles dealing with glycerol ketalization to produce solketal has been more noticeable than the contribution of those dealing with esterification to produce acetylglycerols.

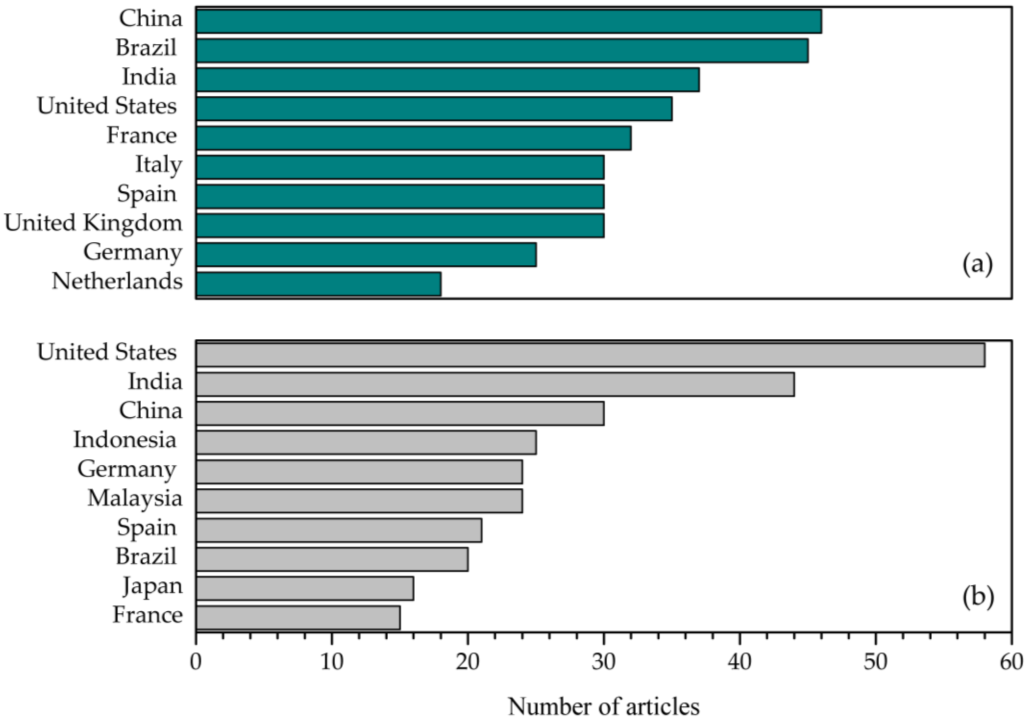

Figure 7. Countries that published the largest number of papers related to the valorization of glycerol through reactions of (**a**) ketalization with acetone and (**b**) esterification with acetic acid. Source: Scopus (March 2023). Search words: (**a**) "Solketal"; (**b**) "Triacetin" and "Glycerol".

Regarding solketal production, the reviews have focused on the reaction mechanism, some aspects of chemical equilibrium [28,29] and the homogeneous and heterogeneous catalysts employed in the synthesis, such as zeolites, supported heteropolyacids, acid ion exchange resins and metal catalysts [28–32]. In addition, in most of these reviews, the influence of operating variables such as temperature, reagent molar ratio and reaction time in batch and continuous flow reactors has also been discussed [28–30,32]. Some papers have also determined the key factors for operation in continuous flow reactors and the use of crude glycerol as an alternative feedstock to analytical glycerol solutions [28,31].

With respect to glycerol esterification, a few review papers have been published in which the topic is generally included with other glycerol transformation reactions [33–35]. In addition to these publications, Nda-Umar et al. reported the results of different heterogeneous catalysts used in glycerol ketalization, such as resins, supported heteropolyacids, functionalized silicas and carbons, metal oxides and clays. Their study focused on the influence of the catalyst to glycerol ratio, temperature and reaction time [36].

The objective of this research was to carry out a literature review study on the catalytic, thermodynamic and kinetic aspects of the esterification reaction of glycerol with acetic acid and acetalization of glycerol with acetone, two conversion reactions that lead to the formation of acetylglycerols and solketal, respectively, which are high-value-added products with potential use in the chemical industry. This article reviews more than 240 references from 1993 up to the present, covering about 30 years of the literature. The work is organized by first presenting both reactions and their mechanisms, emphasizing the chemical equilibrium and its most relevant aspects. Next, the catalysts used are described and classified according to their catalytic nature (zeolites, carbons, exchange resins, etc.). In this section, the effect of the operating variables is described, and the best results for each catalytic system are presented, as well as studies carried out on catalytic stability and the main deactivation mechanisms. Then, for some of these systems, the kinetic models that have been formulated to date are included. Finally, technological aspects related to these reactions are described in view of the future projection of glycerol biorefineries.

2. Reaction Mechanisms

The ketalization and esterification reactions occur in the presence of acid catalysts and can be catalyzed by both Brønsted and Lewis sites. In this section, the proposed mechanisms for these reactions in the presence of both types of sites are briefly described.

2.1. Glycerol Ketalization with Acetone

In a general reaction, an alcohol reacts reversibly with an aldehyde to form acetals or with a ketone to form ketals. In this transformation, two alcohol molecules are attached to the carbonyl group, while one water molecule is removed (Scheme 3).

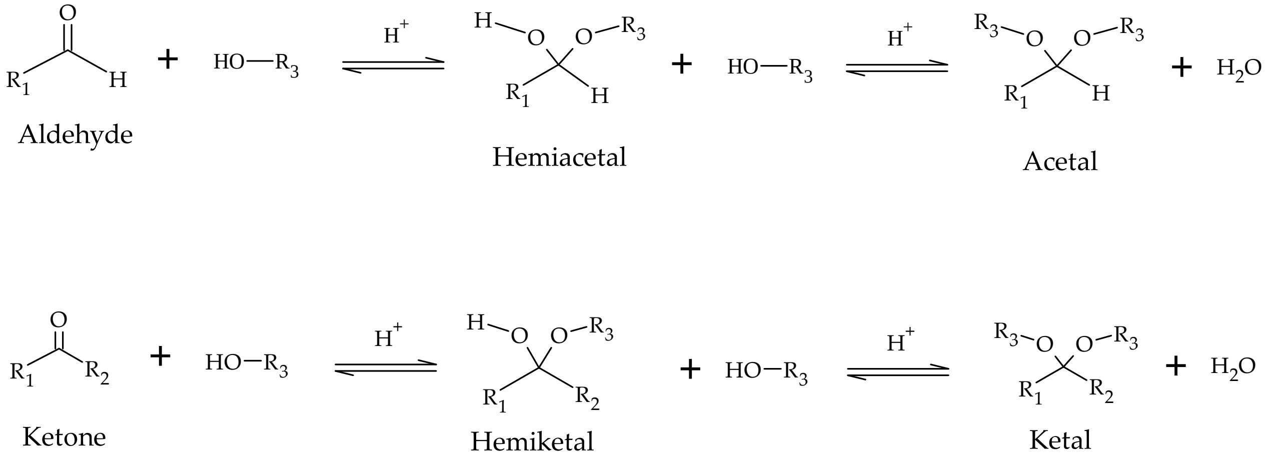

Scheme 3. General ketalization and acetalization reactions.

In the case of glycerol, due to the presence of more than one hydroxyl group in its molecule, the ketalization reaction leads to the formation of five- or six-membered cyclic ketals. In particular, the ketalization of glycerol and acetone leads to the formation of (2,2-dimethyl-1,3-dioxan-4-yl) methanol, known as solketal, and its isomer, 2,2-dimethyl-1,3-dioxan-5ol (Scheme 4).

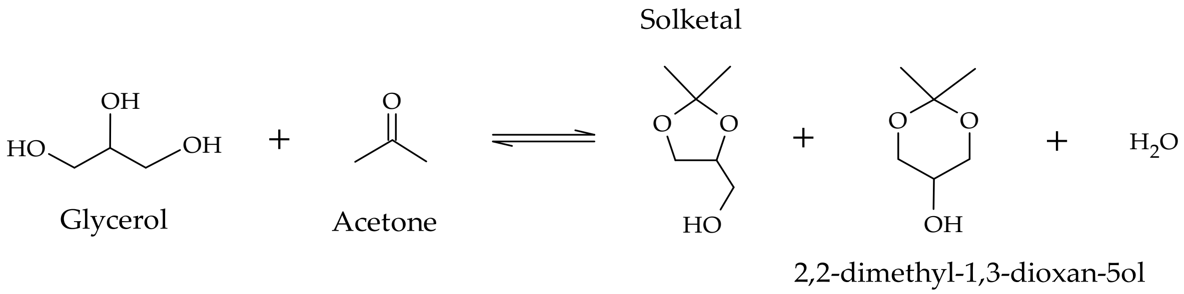

Scheme 4. Glycerol ketalization with acetone.

Solketal is the most abundant of the products formed because the formation of the five-membered ring is thermodynamically favored over the formation of the six-membered ring [37].

Since the reaction is reversible, the composition of the products at equilibrium will depend on the operating conditions under which it is carried out. In several articles, the composition at equilibrium was determined as a function of temperature, using different catalysts, from the estimation of thermodynamic parameters such as enthalpy (ΔH^s), entropy (ΔS^s) and free energy of reaction (ΔG^s). The results obtained for these parameters in each of the papers are summarized in Table 1.

The first authors to report the thermodynamic study of solketal synthesis in liquid phase were Nanda et al. In their study, they employed an Amberlyst 35 resin as catalyst and ethanol as solvent and carried out the tests in a batch reactor operating at 20–50 °C, with a molar ratio of acetone/glycerol (A/G) equal to 2 and 1 wt.% catalyst to glycerol. The results allowed them to estimate the first values for the thermodynamic reaction properties even when considering the ideality of the liquid phase [38]. In contrast, Moreira et al. used the same resin and ethanol as solvent and calculated the thermodynamic equilibrium from experimental data, taking into account the non-ideality of the liquid phase. For this purpose, they studied the effect of the temperature and A/G ratio on the equilibrium conversion and used the UNIFAC method to determine the activity coefficients [39].

Subsequently, other authors determined values for the thermodynamic reaction parameters by using different acid catalysts, such as Hβ zeolites [40], CT-275 exchange resins [41] and sulfated zirconia [42]. Perez et al. carried out a theoretical study of the chemical equilibrium of the synthesis of solketal, taking into account the non-ideality of the liquid phase in order to avoid problems related to transport limitations [43]. All the previously described experiments agree on the exothermic character of the reaction; however, the endergonic or exergonic character of the reaction, depending on the sign of ΔG^s, resulted in being different, and this result could be attributed to the consideration of the non-ideality of the liquid phase.

Table 1. Thermodynamic parameters of the glycerol ketalization reaction with acetone reported by different authors.

ΔH^s (kJ mol^{-1})	ΔG^s (kJ mol^{-1})	ΔS^s (kJ mol^{-1} K^{-1})	Liquid Phase	Reference
-30.0 ± 1.6	-2.1 ± 0.1	-0.1000 ± 0.01	Ideal	[38]
-6.605 ± 0.168	-0.5530	-0.0203	Ideal	[41]
-20.1 ± 1.1	1.4 ± 0.1	-0.0721	Non ideal	[39]
-14.5	0.3777	-0.0499	Ideal	[40]
-11.6 ± 1.1	4.0 ± 0.01	-0.0523	Non ideal	[42]
-6.43	3.36	-0.0328	Non ideal	[43]

Three mechanisms have been proposed for the ketalization of glycerol with acetone, depending on whether the reaction is carried out in the presence of Brønsted or Lewis sites or both.

In the mechanism employing Brønsted sites (Scheme 5), the reaction starts with the protonation of the carbonyl group of acetone due to the presence of protons on the catalyst, which rapidly leads to the formation of a positive pole on the central carbon atom of acetone. Then, a primary hydroxyl group of glycerol that is adsorbed on the surface of the solid attacks the positive charge on the carbon atom of the acetone, leading to the formation of an adsorbed hemiacetal. Subsequently, the removal of a water molecule leads to the formation of an unstable carbocation, which can be attacked by two different oxhydryls of the molecule, leading to the formation of the solketal or its isomer, depending on which oxhydryl attacks the carbon atom. In general, the authors considered that the rate-determining step is the surface reaction leading to the formation of the adsorbed hemiacetal [38,39].

For acid catalysts with Lewis sites, Li et al. proposed a mechanism whereby the active site metal plays a role similar to that of Meerwein–Ponndorf–Verley reduction reactions and Oppenauer oxidation, coordinating and activating the carbonyl group of acetone [44]. Subsequently, the terminal oxhydryl group of glycerol attacks the carbon atom of the carbonyl group, accompanied by the formation of a bond between the β-carbon of glycerol and the oxygen of the carbonyl group, resulting in the intermediate shown in Scheme 6. These two simultaneous steps are followed by consecutive elimination of water to form solketal. This mechanism was also reported by Da Silva et al., who employed SnF_2 as catalysts [45].

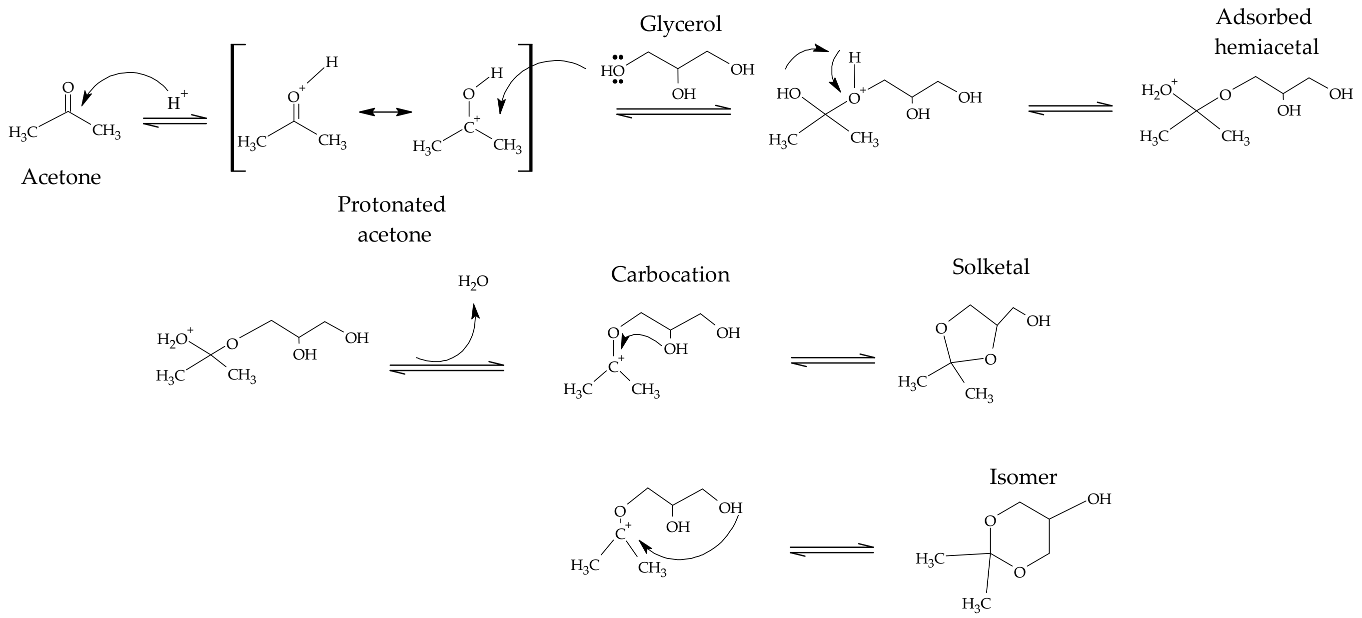

Scheme 5. Brønsted mechanism for the glycerol ketalization with acetone.

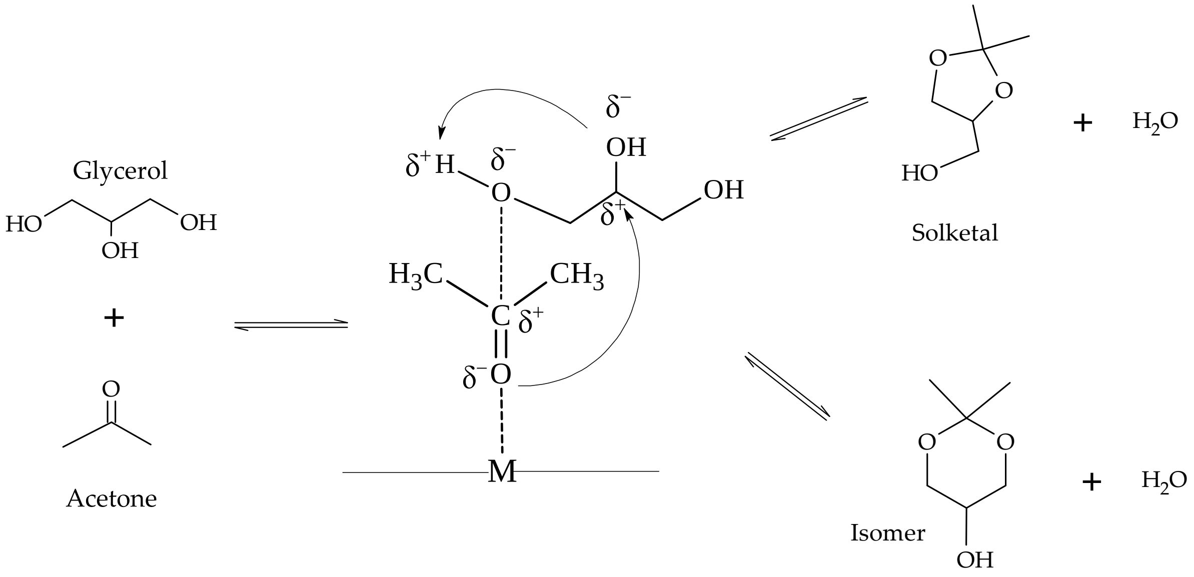

Scheme 6. Lewis's mechanism for the glycerol ketalization with acetone.

Other authors proposed reaction mechanisms in which both Lewis and Brønsted sites are present in the catalyst and are part of the mechanism (Scheme 7). Priya et al. proposed a combined mechanism in which the oxygen of the carbonyl group (-C=O) of the acetone strongly coordinates with the catalyst, forming a positively charged carbonyl carbon. This atom is then attacked by the terminal hydroxyl group of the glycerol (-OH) and forms the tertiary alcohol intermediate. Subsequently, one of the oxhydryl groups of the hemiacetal is protonated by the presence of Brønsted sites on the catalyst, with the consequent loss of a water molecule and the formation of the solketal and its six-membered isomer [46]. A similar mechanism was proposed by Janiszewska et al. [47].

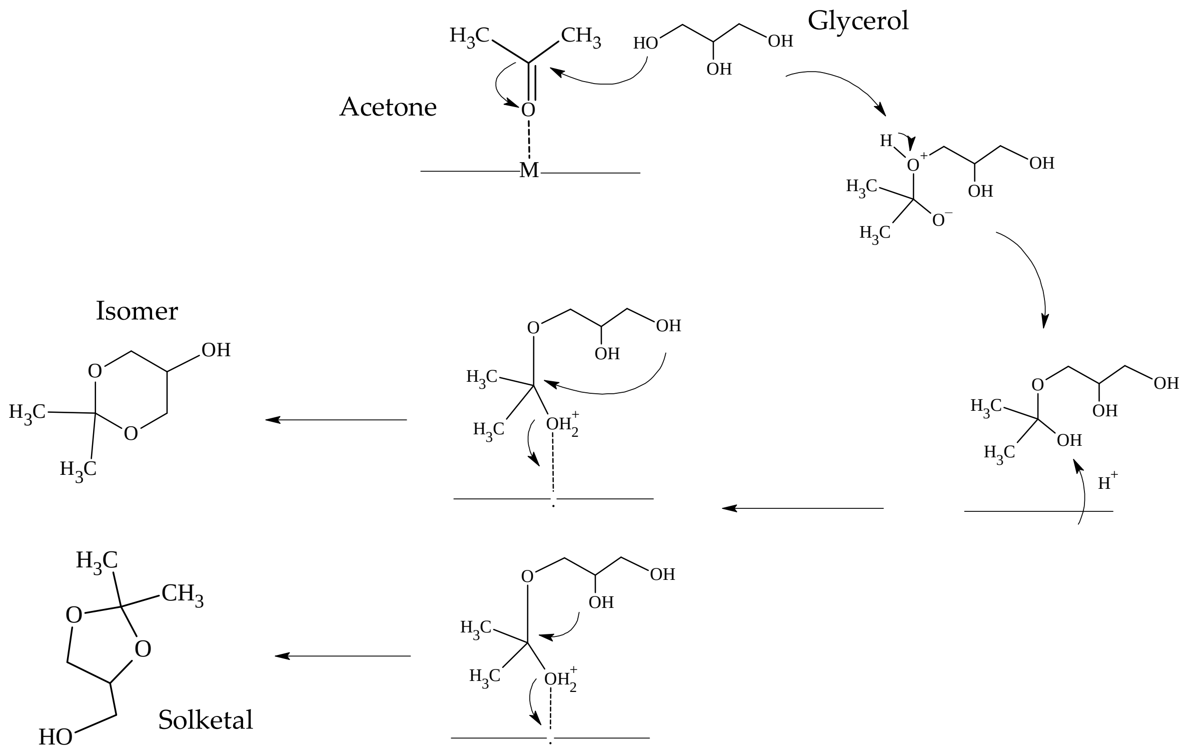

Scheme 7. Combined Lewis–Brønsted mechanism for glycerol ketalization with acetone.

2.2. Glycerol Esterification with Acetic Acid

In general terms, the esterification reaction is carried out in the presence of an alcohol and a carboxylic acid to produce an ester and water (Scheme 8).

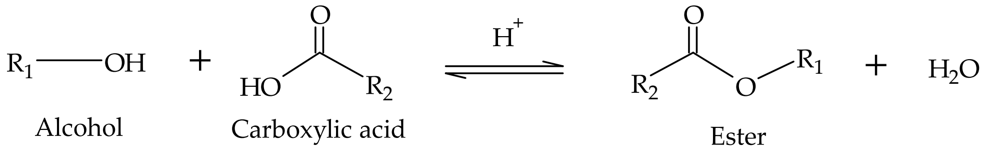

Scheme 8. General esterification reaction.

In the case of glycerol esterification, which is carried out in the presence of acetic acid, the reaction leads to the formation of mono-, di- and tri-esters of glycerol due to the presence of multiple hydroxyl groups on the glycerol molecule (Scheme 9).

Like glycerol ketalization with acetone, glycerol esterification is a reversible reaction and is therefore limited by thermodynamic equilibrium. Previous studies have shown that glycerol conversion decreases with an increasing temperature, revealing the overall exothermicity of the system. However, this variation is not significant, and it is attributed to the slight variation of the specific heat of all compounds with temperature. Furthermore, the AA/G molar ratio affects the glycerol conversion to a greater extent than temperature, showing the largest variation for AA/G molar ratios between 1 and 4. However, the selectivity towards TAG is lower under these conditions, so higher AA/G values should be used to obtain more substituted products [11].

Two mechanisms have been proposed for this reaction, one in the presence of catalysts with Brønsted acid sites and the other for catalysts with Lewis acid sites.

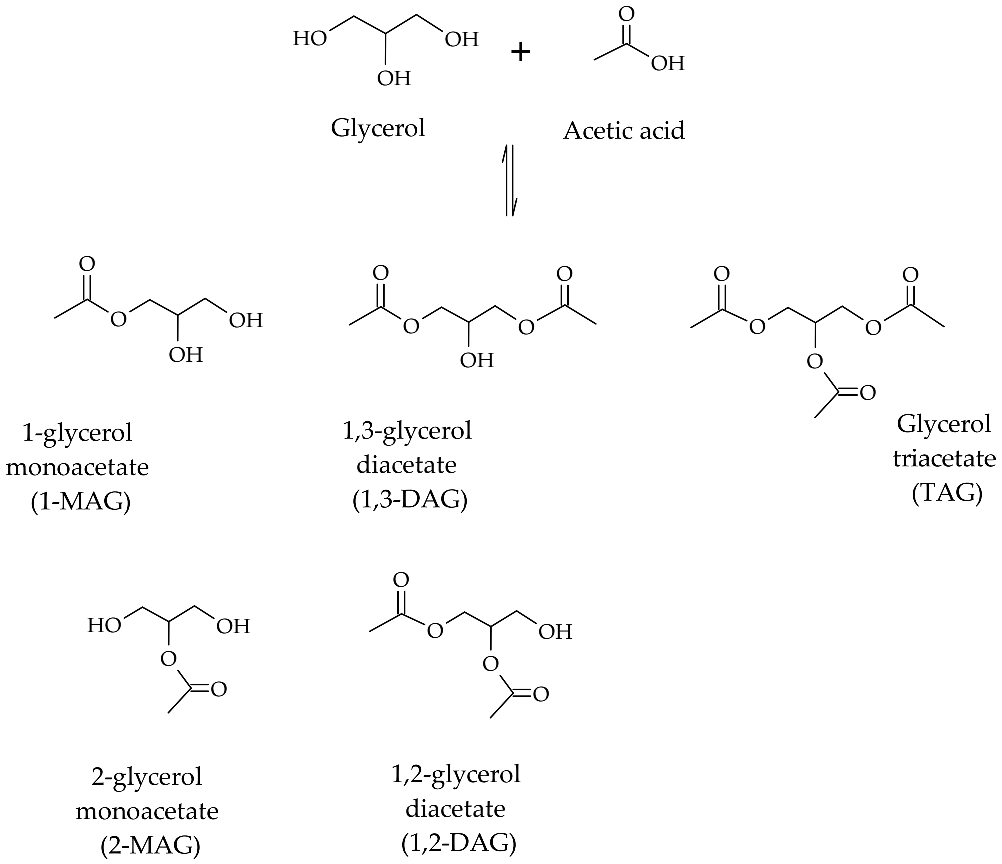

Scheme 9. Glycerol esterification reaction with acetic acid.

Troncea et al. were among the first authors to report the Brønsted mechanism for this reaction (Scheme 10), which corresponds to a traditional Fischer esterification. In this mechanism, the acid site (H^+) activates the carbonyl group (-C=O) of acetic acid, increasing its electrophilicity. Then, the terminal hydroxyl group of the glycerol (-OH) attacks the activated carbonyl, and the transfer of a proton leads to the formation of an activated complex with the consequent formation of water. Removal of the water molecule leads to the formation of MAG, and the mechanism continues sequentially to form DAG and TAG [48]. This mechanism has been reported using various acid catalysts, such as exchange resins [49,50], heteropolyacids [51] and acidified clays [52] that feature Brønsted-type sites only.

With respect to the Lewis-site-catalyzed reaction mechanism, this involves the presence of a Mn^+ metal as an electrophile, facilitating the activation of the carbonyl group (Scheme 11) [53]. In this sense, some authors have reported the use of catalysts that present both Brønsted and Lewis acid sites, such as cesium phosphotungstate [54], Ag-exchanged heteropolyacids [55], mixed oxides [56] and hydroxylated magnesium fluorides [48]. The latter authors have concluded that the presence of acid sites of different types has a double effect: on the one hand, they act as active sites; and, on the other hand, they adsorb water molecules formed during the reaction, leading to higher selectivity values to DAG and TAG [48].

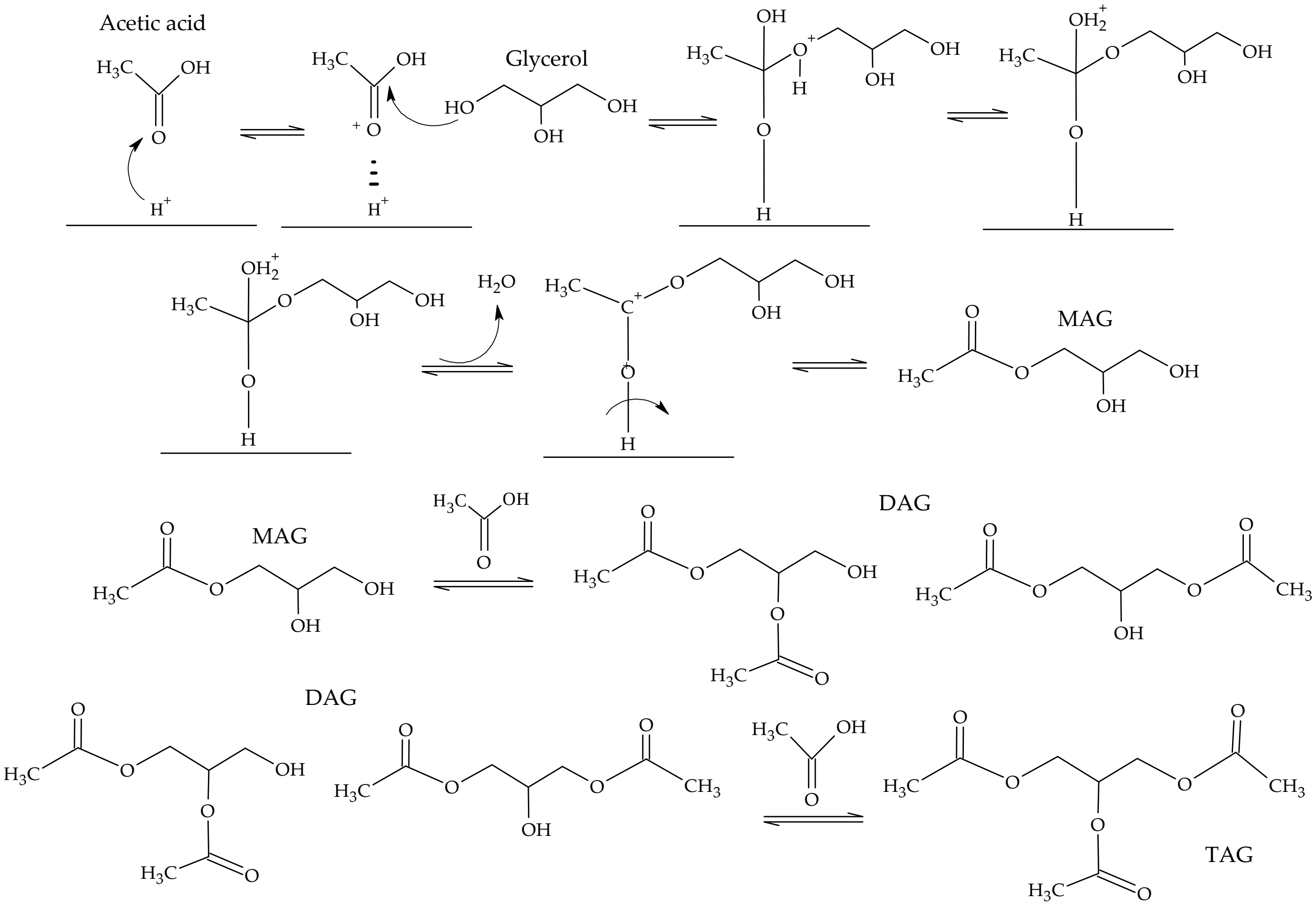

Scheme 10. Glycerol esterification mechanism with acetic acid.

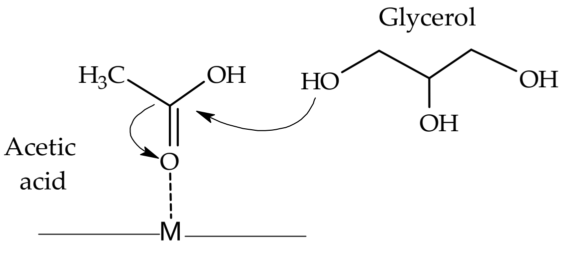

Scheme 11. Activation of the carbonyl group of acetic acid by the presence of a Lewis acid site.

3. Catalysts for Glycerol Ketalization and Esterification

Both the ketalization and esterification reactions are catalyzed by acid sites. In this sense, several catalysts have been reported for both reactions.

In this section, we present the catalysts that have been reported for both reactions, according to their homogeneous or heterogeneous nature and the reaction conditions under which they have been evaluated. For all of them, the results were obtained in batch reactors, since they are the ones most widely used at the laboratory scale to evaluate catalytic performance as a function of the operating variables such as temperature, reaction time and reagents' molar ratio.

3.1. Homogeneous Catalysts

The study of glycerol ketalization reactions with acetone was initiated using organic acids and inorganic salts as homogeneous catalysts. Most of the results were published before the year 2000, and, in particular, no papers have been found studying homogeneous catalysts for the esterification reaction of glycerol with acetic acid, possibly because their study is more recent.

The most reported homogeneous catalyst in solketal synthesis is p-toluensulfonic acid (p-TSA). The first results date back to a Spanish patent (ES 499129A1) which reported the synthesis of solketal, employing an A/G = 1 molar ratio, obtaining a yield of 80%. Similar results, but under other reaction conditions, were later described in another patent (EP 456073B1) in which the yield achieved was 56%.

In 1997, Mushrush et al. carried out the reaction of glycerol ketalization with acetone at room temperature, using an A/G = 4 molar ratio and 3 wt.% p-TSA acid. In order to retain the reaction product water, a 5 Å molecular sieve was also used. After 33 h of reaction, the product mixture was filtered and distilled under vacuum, obtaining a solketal yield of 88% [57].

Subsequently, Bruchmann et al. published a patent (US5917059) in which p-TSA acid was also used as catalyst, carrying out the reaction in different steps. In each one, using an A/G = 4 molar ratio and 0.05 wt.% of catalyst, the excess acetone was removed by distillation, and fresh acetone was added to start another cycle. At the end of the stages, the yield achieved was 99.5% [58]. García et al. also obtained yields of 90% after 16 h, carrying out the same method as Bruchmann et al. but with an A/G = 3 molar ratio and 0.1 wt.% of catalyst [59].

In 2011, Suriyaprapadilok and Kitiyanan carried out the solketal synthesis reaction with an A/G = 6 molar ratio and 1 wt.% of p-TSA acid [60]. After 12 h of reaction under reflux, the glycerol conversion achieved was 82.7%.

Continuing the search for homogeneous catalysts, in 2013 Menezes et al. were the first authors to report the use of $SnCl_2 \cdot 2H_2O$, $SnBr_2$, SnF_2 and $Sn(OAc)_2$ as homogeneous catalysts with Lewis-type acidity in solketal synthesis, and they compared the results with Brønsted-type acids, such as sulfuric acid and p-TSA [61]. The best results were obtained for the $SnCl_2 \cdot 2H_2O$ catalyst, whose behavior was attributed to the fact that it showed a higher tolerance than the rest in the presence of water in the reaction medium. On the other hand, the SnF_2 and $Sn(OAc)_2$ catalysts presented low solubility in the reactive mixture; therefore, they were discarded for future investigations.

On the other hand, Zaher et al. used iron chloride as a catalyst ($FeCl_3 \cdot 6H_2O$) and obtained a 100% glycerol conversion after 10 min of reaction, demonstrating the high efficiency of this catalyst [62].

Recently, Nascimento et al. carried out the solketal synthesis reaction by using CO_2 at high pressure as a catalyst. They reported that CO_2 dissolved in alcohols at high pressure, leading to the formation of carbonic acids in a reversible manner, enabling the occurrence of acid-site-catalyzed reactions. When the system was decompressed after the reaction, the carbonic acid decomposed and re-formed CO_2, leaving only the reaction products and unreacted reactants in the liquid phase. The best results were obtained for a temperature of 115 °C, a pressure of 4.3 MPa and a reaction time of 4.2 h, conditions that allowed for a glycerol conversion of 60.6% to be reached [63].

Table 2 summarizes the homogeneous catalysts and the operating conditions under which they were employed, arranged in increasing order according to the yield obtained at solketal.

Due to environmental complications and operational difficulties related to the separation of homogeneous catalysts from the reaction medium and corrosion phenomenon, they have been replaced by solid catalysts [64]. For this reason, many authors currently report homogeneous catalysts only for the purpose of comparison with different synthesized solids.

Table 2. Homogeneous catalysts employed in glycerol ketalization with acetone.

Catalyst	T (°C)	A/G	t (h)	m_c/m_{gly}	X (%)	S_S (%)	Y_S (%)	Ref.
$CO_{2\ \text{dissolved}}$	115	2.0	4.2	NR	60.6	NR	NR	[63]
$SnCl_2 \cdot 2H_2O$	RT	4.0	2.0	0.02	81	98	79.0	[61]

Table 2. *Cont.*

Catalyst	T (°C)	A/G	t (h)	m_c/m_{gly}	X (%)	S_S (%)	Y_S (%)	Ref.
p-TSA	RT	6.0	12.0	0.01	82.7	100	82.7	[60]
p-TSA	RT	4.0	33.0	0.03	NR	NR	88.0	[57]
p-TSA	RT	3.0	16.0	0.002	NR	NR	90.0	[59]
$FeCl_3 \cdot 6H_2O$	RT	0.87	0.17	0.001	100	97	97.0	[62]
p-TSA	RT	4.0	12.0	0.001	NR	NR	99.5	[58]

RT, room temperature; A/G, acetone/glycerol molar ratio; m_c/m_{gly}, catalyst/glycerol molar ratio; X, glycerol conversion; S_s, selectivity towards solketal; Y_s, yield of solketal.

3.2. Ionic Liquids

As a replacement for organic acids and inorganic salts, some authors have evaluated the use of ionic liquids as catalysts in both the ketalization and esterification reactions. These substances are organic salts composed of a cation and an anion and have a melting point of less than 100 °C. The most commonly used cations and anions in the reactions of glycerol ketalization with acetone and glycerol esterification with acetic acid are shown in Figure 8.

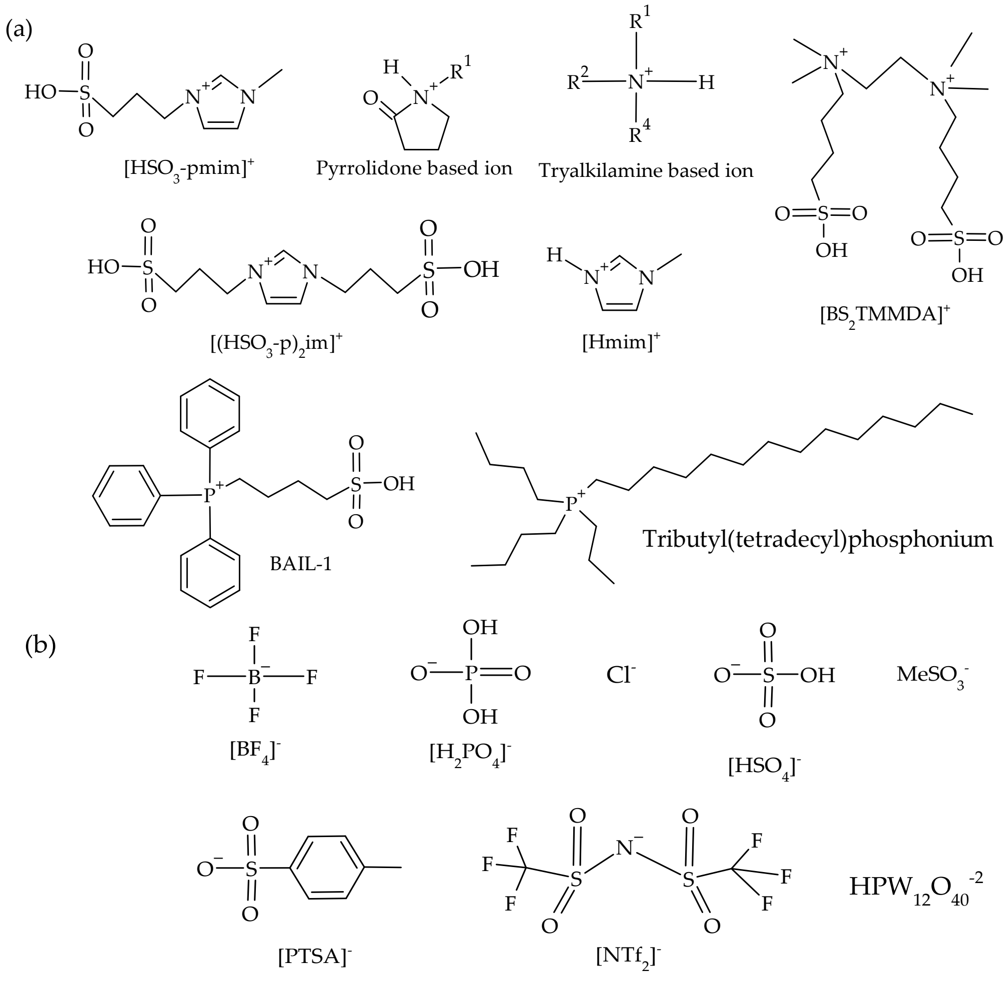

Figure 8. Cations (**a**) and anions (**b**) reported as ions in the synthesis of ionic liquids as catalysts in the esterification and ketalization reactions of glycerol.

Ionic liquids initially emerged as alternative solvents to volatile organic solvents because they are environmentally friendly. However, they are currently finding diverse applications in the areas of catalysis, electrochemistry, spectroscopy and materials science [65]. The interest in using this type of catalysts lies in their ease of separation from the reaction medium, their ability to be reused and their low corrosiveness, which differentiates them from inorganic acids [66].

3.2.1. Glycerol Ketalization with Acetone

Gui et al. were the first to carry out the reaction of glycerol ketalization with acetone, using ionic liquids with Brønsted acidity as catalysts, due to the presence of -SO_3H groups in the molecule. The authors synthesized two different catalysts, BAIL-1 and BAIL-2, which showed similar results in the reaction; the glycerol conversion achieved with the BAIL-1 catalyst was slightly higher. After 30 min, 100% glycerol conversion was achieved, with 98% selectivity towards solketal, maintaining the activity after four reaction cycles [67].

On the other hand, Ji et al. also used an ionic liquid $[P(C_4H_9)_3C_{14}H_{29}][TsO]$ called TTPT. After 20 min of reaction, a solketal yield of 86% was achieved. This catalyst was reused 10 times, with negligible loss of activity, highlighting the advantage of this type of catalyst over inorganic and organic acids [66]. Table 3 summarizes these results.

Table 3. Ionic liquids employed in glycerol ketalization with acetone.

Catalyst	T (°C)	A/G	t (h)	m_c/m_{gly}	X (%)	S_S (%)	Y_S (%)	Ref.
TTPT	30	6.0	0.50	0.05	NR	NR	86.0	[66]
BAIL-1	RT	15.0	0.25	0.14	96.0	98.5	94.6	[67]

RT, room temperature; A/G, acetone/glycerol molar ratio; m_c/m_{gly}, catalyst/glycerol molar ratio; X, glycerol conversion; S_s, selectivity towards solketal; Y_s, yield of solketal; NR, not reported.

3.2.2. Glycerol Esterification with Acetic Acid

With respect to the esterification reaction of glycerol with acetic acid, Li et al. carried out a comparative study of different ionic liquids as catalysts, using the same cation $[HSO_3\text{-}pmim]^+$ and modifying the anion. In this sense, $[HSO_4]^-$, $[PTSA]^-$, $[H_2PO_4]^-$, $[BF_4]^-$ and Cl^- anions were used, determining that the $[HSO_3\text{-}pmim][HSO_4]$ catalyst allows the best yields to TAG (96.3%) to be obtained, even higher than H_2SO_4, due to the high acidic strength and to the fact that the TAG formed cannot dissolve in the ionic liquid and forms another phase, thus facilitating the progress of the reaction [68].

Liu et al. studied the effect of the amounts of the alkyl sulfonic groups present in the liquids on the activity of the catalysts. When the authors compared them with H_2SO_4, the catalysts containing only one alkyl sulfonic group showed a lower activity than H_2SO_4, while those containing two alkyl sulfonic groups showed a higher activity than this inorganic acid. In addition, the type of anion also influenced the activity: those liquids containing $[HSO_4]^-$ and $[NTf_2]$-groups showed a higher activity than those containing a tosylate anion, $[Tos]^-$. Thus, the combination of two alkyl sulfonic groups with a $[HSO_4]^-$ anion led to an ionic liquid with higher Brønsted-type acidity, leading to the $[(HSO_3\text{-}p)_2im][HSO_4]$ catalyst, which proved to be the most active one, in agreement with the results reported by Li et al. [69].

Keogh et al. synthesized ionic liquids based on n-alkyl pyrrolidone and trialkyl amines cations and $HSO_4{}^-$ as an anion. The alkyl groups employed were CH_3, C_2H_5, C_3H_7, C_4H_9 and C_8H_{17}. The results showed that the ionic liquids based on n-alkyl pyrrolidines turned out to be more active than the others, probably due to the higher density of acid sites. Moreover, the catalyst containing CH_3 as the alkyl group ($[H\text{-}NMP][HSO_4]$) presented the highest selectivity towards DAG and TAG [70]. The authors also remarked that the activity towards TAG formation was higher for those ionic liquids based on trialkyl amines that are more substituted, as was also reported by Liu et al. This behavior could be due to the higher hydrophobicity of these compounds, which caused the water generated during the reaction to be expelled, favoring the progress of the reaction.

Finally, Guang et al. synthesized ionic liquids based on heteropolyacids functionalized with sulfonic acid. The results indicated that the $[BS_2TMEDA]HPW_{12}O_{40}$ catalyst exhibited the highest catalytic activity and selectivity over TAG compared to the commercial catalysts

$H_3PW_{12}O_{40}$, H_2SO_4 and Amberlyst 15, and this result was attributed to its higher average acidity of the -SO3H groups and carbon chain length [71].

Table 4 summarizes the best results of the use of ionic liquids as catalysts in the esterification of glycerol with acetic acid.

Table 4. Ionic liquids employed in glycerol esterification with acetic acid.

Catalyst	T (°C)	AA/G	t (h)	m_c/m_{gly}	X (%)	S_{MAG} (%)	S_{DAG} (%)	S_{TAG} (%)	Ref.
$[HSO_3\text{-}pmim][HSO_4]$	90	8.0	6.0	0.411	NR	NR	NR	96.3	[68]
$[(HSO_3\text{-}p)_2im][HSO_4]$	100	5.0	1.0	0.002	95.7	32.8	52.1	15.1	[69]
$[H\text{-}NMP][HSO_4]$	100	6.0	0.5	0.106	99.0	12.0	58.0	30.0	[70]
$[BS_2TMEDA]HPW_{12}O_{40}$	120	7	8	0.06	100	1	28.1	70.9	[71]

AA/G, acetic acid/glycerol molar ratio; m_c/m_{gly}, catalyst/glycerol mass ratio; X, glycerol conversion; $S_{MAG/DAG/TAG}$, selectivity towards MAG/DAG/TAG; NR, not reported.

3.3. Zeolites

For ketalization and esterification reactions, certain types of zeolites have proven to be active materials due to their acidic, textural and physicochemical properties.

With respect to acidity, the protonated form of zeolites allows both reactions to be catalyzed by Brønsted sites. The spatial distribution of the sites according to the surface determines the site density and its function.

With respect to the textural properties, the pore diameter determines the selectivity of the zeolites towards the bulkier reaction products. Table 5 shows the maximum sizes that molecules should have to diffuse inside the pores of some zeolites reported in the ketalization and esterification reactions. The data were extracted from the IZA database [72].

Table 5. Maximum diameter of a particle to diffuse in the pores of some zeolites.

Zeolite Code	Average Pore Diameter (Å)	Dimensions of a Molecule so that It Can Diffuse Inside the Pores (Å)
MFI	6.36	4.70 × 4.46 × 4.46
BEA	6.68	5.95 × 5.95 × 5.95
FAU	11.24	7.35 × 7.35 × 7.35
MOR	6.70	1.57 × 2.95 × 6.45
FER	6.31	1.56 × 3.40 × 4.69

Last but not least, physicochemical properties such as the surface chemical affinity and crystal size are some of the variables that also influence catalytic activity.

A discussion on the influence of all of these properties on both reactions follows in the next section.

3.3.1. Glycerol Ketalization with Acetone

Da Silva et al. were among the first authors to report the use of zeolites for the acetylation of glycerol with acetone [24]. In their study, they compared the activity of Beta (BEA), USY (FAU) and ZSM-5 (MFI) zeolites. The catalytic results showed that, under the same reaction conditions, the activity followed the order Beta > USY > ZSM5. The low activity of the ZSM-5 zeolite was attributed to the small pore size, which would lead to the reaction only taking place on the outer surface of the catalyst, where the least number of active sites was located. The good activity of Beta and Y zeolites, unlike ZSM-5, was subsequently confirmed by several authors, who also attributed this behavior to the larger pore size of these zeolites [73–77].

Following these results, Manjunathan et al. employed a Mordenite type zeolite (MOR) and obtained glycerol conversions of 8% due to the small pore size of these zeolites [73]. Rossa et al. employed a ferrierite-type zeolite (FER) and reported lower activity than the H-BEA zeolite (45% glycerol conversion), the result also being a consequence of the low porosity of this material [77].

In order to improve the textural properties of zeolites, various treatments have been employed, such as the use of strong bases to partially remove Si^{+4} ions. Following this method, Kowalska-Kus et al. modified the structure of ZSM-5 (MFI), mordenite (MOR) and β (BEA) zeolites by treating them with 0.2 M NaOH. The fresh zeolites, named MFI-1-P (Si/Al = 12), MFI-2-P (Si/Al = 27), MOR-P (Si/Al = 17) and BEA-P (Si/Al = 12), were treated with the strong base solution and subsequently with NH_4NO_3 solutions to achieve ion exchange. They were then calcined to transform them into their protonated form. These zeolites were named MFI-1-AT (Si/Al = 9.2), MFI-2-AT (Si/Al = 13.2), BEA-AT (Si/Al = 9.3) and MOR-AT (Si/Al = 10.8) [75]. Of all the untreated commercial zeolites, the MOR-P and BEA-P materials presented higher conversion to glycerol (67 and 72%, respectively). This is due to the higher percentage of mesoporosity (32% for both materials). On the other hand, the zeolites MFI-1-P and MFI-2-P presented lower conversions (18 and 38%, respectively), due to the lower percentage of mesoporosity (10 and 12%, respectively). The partial removal of silicon in MOR-P and BEA-P zeolites led to an increase in glycerol conversion up to 81%. On the other hand, the desilication process of MFI-1-P, MFI-2-P zeolites led to an increase in glycerol conversion up to values of 30 and 80%, respectively. Other authors have reported that desilylation is more effective in materials presenting a Si/Al ratio between 25 and 50 [78], so that the large increase in conversion in the MFI-2-P material could be due to this characteristic. Thus, it has been demonstrated that the porosity of zeolites can be increased by the desilication method with strong bases, as this improves their activity in solketal synthesis.

Recently, Saini et al. carried out a desilication of a mordenite-type zeolite via treatment with NaOH at different concentrations. The authors reported that the porosity of the materials increased as the severity of the treatment increased, while the number of strong acid sites first increased and then decreased, a behavior that also affected the activity of the solids. In this sense, the zeolite treated with 0.5 M NaOH (MOR0.5) exhibited a higher number of strong acid sites, leading to higher activity [79].

In addition to porosity, the crystal size of zeolites also turns out to be an activity-determining property in solketal synthesis. Manjunathan et al. synthesized two types of beta zeolite with different crystal sizes, named H-Beta-1 and H-Beta-2. Zeolite H-Beta-1, with an average crystal size of 135 nm, led to 86% glycerol conversion, while zeolite H-Beta-2, with an average crystal size of 450 nm, achieved 38% conversion, even though the acidity of zeolite H-Beta-1 (1.51 mmol g^{-1}) was 20% lower than that of H-Beta-2 (1.8 mmol g^{-1}). This showed that crystal size predominates over acidity, and this result was attributed to the fact that molecules diffuse more easily in smaller particle sizes due to the shorter pores [73].

Because the generation of water as a by-product limits the extent of the reaction, some authors altered the Si/Al ratio of zeolites to modify the affinity of zeolites for water and shift the thermodynamic equilibrium condition. Zeolites with low silica content are hydrophilic because the structure is highly negatively charged, and many positive ions are found to be charge compensating. In contrast, zeolites with a high silica content have a hydrophobic character. Consequently, high Si/Al ratios lead to the hydrophobic behavior of the material. However, it is necessary to take into account that the acidity of zeolites is associated with the presence of aluminum ions, so that high Si/Al ratios also lead to a lower content of active sites.

Da Silva et al. compared the activity of zeolite beta (Si/Al = 16) with zeolite USY (Si/Al = 2.8) under the same reaction conditions, such that the number of active sites in the reaction is the same. The beta zeolite led to a 90% conversion, while the USY led to a 60% conversion. This result was attributed to the high Si/Al ratio of the beta zeolite and its higher hydrophobicity [80].

The Si/Al ratio can also be modified by acid treatment so as to partially remove Al^{+3} ions. Venkatesha et al. treated a beta zeolite in its protonated form (Si/Al = 25) with different organic acids of 1 M concentration (p-TSA, phenoldisulfonic acid and methanesulfonic acid) to partially remove aluminum ions [81]. The samples thus treated were named 1.0pTSABEA

(Si/Al = 48), 1.0PDSABEA (Si/Al = 96) and 1.0MSABEA (Si/Al = 69), respectively. After 30 min of reaction, the glycerol conversion achieved with the untreated beta zeolite was 76%; with 1.0pTSABEA, it was 82%; with 1.0PDSABEA, it was 80%; and with 1.0MSABEA, it was 84%. This increase in conversion was accompanied by an increase in selectivity towards solketal, with the 1.0PDSABEA sample being the most selective one, so that it was used to study the effect of acid concentration on material properties and activity. It was observed that as the acid concentration increased, the Si/Al ratio increased due to the loss of aluminum ions from the structure. While this led to a decrease in the total acidity of the samples, treatment with organic acids led to an increase in the contribution of strong sites and an increase in pore volume. The combination of these two factors, coupled with the increase in hydrophobicity, led to an increase in catalyst conversion and selectivity.

Some authors have modified the surface of zeolites to improve water tolerance, without the need to attack the solid with acids or bases to partially remove Al^{+3} or Si^{+4} ions, respectively. Ferreira et al. synthesized supported Nb_2O_5 catalysts, using NaY, HY and HUSY zeolites as supports, via the incipient wetting impregnation method [82]. The synthesized catalysts were named Nb5-NaY, Nb5-HY, Nb5-HUSY, Nb15-NaY, Nb15-HY and Nb15-HUSY, and the subscript indicated the percentage of Nb present in the catalyst. Both fresh NaY and HY catalysts and their supported variants did not exhibit activity in solketal synthesis. On the one hand, the low activity of the NaY zeolite was due to the weak strength of the sites and its hydrophilic character, properties that failed to be improved by the incorporation of Nb. As for the HY catalyst, it possesses almost 20% of medium and strong sites. However, the hydrophilic character of the material and the small pore size made it impossible for the reaction to proceed completely. Its supported variant showed no activity due to the small pore size. On the other hand, with the HUSY zeolite, a 29% conversion was obtained at 70 °C and 3 h of reaction, while its supported variants presented an increase in conversion to values above 60% under the same conditions. The activity of this zeolite was due to the presence of a certain degree of mesoporosity compared to the rest of the materials, a property that was improved through the addition of Nb to the support.

Rahaman et al. modified the surface of a HY zeolite by incorporating an organosilane surfactant (n-octadecyl-trichlorosilane, OTS) with the aim of increasing the hydrophobicity of the material and improving the interaction of the reactive phases, thus minimizing the resistance to matter transport [83]. The synthesized material was named OTS-HY. The conversion of the unmodified HY catalyst after 1 h of reaction and 30 °C was 28%, with a solketal selectivity of 88%, while the OTS-HY catalyst reached a conversion of 89%, with a solketal selectivity of 95%, within the same period of time and under the same reaction conditions. This behavior was due to the fact that the groups incorporated into the OTS-HY material made it possible to form a stable emulsion that favored the miscibility of the phases at 30 °C. This made it possible to achieve the same activity as the unmodified HY zeolite at 50 °C, a temperature at which the miscibility of the reactants is improved.

Recently, Li et al. synthesized a NaY zeolite with Fe^{+3} ion exchange at different concentrations by the cation exchange method. The authors demonstrated that higher Fe^{+3} contents led to higher glycerol conversions, and this result was attributed to an increase in the strength of the acid sites generated. Furthermore, they observed that these solids only dispersed in the glycerol phase, disfavoring the contact between both reagents and the catalyst. For this reason, some catalysts were modified with chlorotrimethylsilane (CTS) to improve the dispersion of the catalyst in both phases and favor the transport of matter between the reagents and the solid, reporting a clear increase in the activity of the solids [84]. The authors reported that the turnover frequency (TOF) was 18 times higher for the catalyst modified with CTS compared to the unmodified catalyst.

Table 6 summarizes the best results employing zeolites in the reaction of glycerol ketalization with acetone, ordered according to the solketal yield.

Table 6. Zeolites employed in glycerol ketalization with acetone.

Catalyst	T (°C)	A/G	t (h)	m_c/m_{gly}	X (%)	S_S (%)	Y_S (%)	Ref.
H-Mordenite	28	2.0	1.0	0.05	8.0	80.0	6.4	[73]
MFI-1-P	70	1.0	NR	0.01	18.0	72.0	13.0	[75]
H-ZSM-5	28	2.0	1.0	0.05	19.5	85.0	16.6	[73]
ZSM-5	70	1.2	0.67	0.25	20.0	100.0	20.0	[80]
MFI-2-P	70	1.0	NR	0.01	38.0	75.0	28.5	[75]
H-FER	50	4.0	1.0	0.01	45.4	97.5	44.3	[77]
USY	70	1.2	0.67	0.16	60.0	100.0	60.0	[80]
Beta zeolite	30	1.0	0.5	0.54	76.0	83.0	63.0	[81]
Nb_5-HUSY	40	2.0	3.0	0.02	66.0	98.0	64.7	[82]
MOR-P	70	1.0	NR	0.01	67.0	98.0	65.7	[75]
BEA-P	70	1.0	NR	0.01	72.0	98.0	70.5	[75]
H-BEA	60	4.0	1.0	0.05	72.6	98.3	71.4	[76]
H-Y	28	2.0	1.0	0.05	74.2	98.2	72.8	[73]
1.0pTSABEA	30	1.0	0.5	0.54	82.0	90.0	73.8	[81]
Beta zeolite	30	6.0	1.0	0.14	90.0	86.0	77.4	[74]
1.0MSABEA	30	1.0	0.5	0.54	84.0	93.0	78.1	[81]
MFI-2-AT	70	1.0	NR	0.01	81.0	98.0	79.4	[75]
1.0PDSABEA	30	1.0	0.5	0.54	80.0	100	80.0	[81]
OTS-HY	30	12.0	1.0	0.05	89.0	95.0	84.5	[83]
H-Beta-1	28	2.0	1.0	0.05	86.0	98.5	84.7	[73]
Beta zeolite	70	1.2	0.67	0.19	90.0	100	90.0	[80]
MOR0.5	60	10.0	4.0	0.25	99.0	99.0	99.0	[79]

A/G, acetone/glycerol molar ratio; m_c/m_{gly}, catalyst/glycerol molar ratio; X, glycerol conversion; S_s, selectivity towards solketal; Y_s, yield of solketal, NR, not reported.

3.3.2. Glycerol Esterification with Acetic Acid

Zeolites have also been employed as catalysts in the esterification reaction of glycerol with acetic acid, with the pore size being the property of zeolites that most influences product selectivity.

Gonçalves et al. compared the activity of H-ZSM-5 and HUSY zeolites with a K-10 montmorillonite. The results showed that the former was less active and also presented lower selectivity towards the most substituted products (DAG and TAG). The authors attributed this behavior to the smaller pore size presented by these zeolites, causing diffusional problems for the DAG and TAG molecules, which turned out to be very bulky [85]. The same behavior was observed by Dalla Costa et al., who reported a higher selectivity towards DAG and TAG (60 and 30%, respectively) if a sulfonic-acid-functionalized mesoporous silica (pore size of 32 Å) is employed compared to H-ZSM-5 and H-Beta zeolites (pore size of 5.6–7 Å) [86].

With the aim of improving textural properties, Popova et al. modified a mordenite-type zeolite (M) via treatment with HF and NH_4F, managing to increase the pore size from 9 Å to 19 Å. This modification allowed for the conversion to be increased from 68.2% to 89.3% and the selectivity towards TAG to be brough to 63.7%. Furthermore, by impregnating Zr on both solids, it was possible to increase the strength of the acid sites and, as a consequence, to obtain an improvement in the performance of the catalysts, reaching a selectivity towards TAG of 69.2% for the Zr-treated and modified solid (Zr/M1) [87].

Table 7 summarizes the zeolites used in the esterification reaction of glycerol with acetic acid according to their activity.

Table 7. Zeolites employed in glycerol esterification reaction with acetic acid.

Catalyst	T (°C)	AA/G	t (h)	m_c/m_{gly}	X (%)	S_{MAG} (%)	S_{DAG} (%)	S_{TAG} (%)	Ref.
H-Beta	110	3.0	0.5	0.55	14.0	79.0	14.0	0.0	[85]
H-ZSM-5	110	3.0	0.5	0.80	30.0	83.0	10.0	0.0	[85]
H-ZSM-5	120	6.0	4.5	0.04	90.0	45.0	45.0	10.0	[86]

Table 7. *Cont.*

Catalyst	T (°C)	AA/G	t (h)	m_c/m_{gly}	X (%)	S_{MAG} (%)	S_{DAG} (%)	S_{TAG} (%)	Ref.
H-Beta	120	6.0	4.5	0.04	90.0	20.0	60.0	20.0	[86]
Zr/M1	100	10.0	3.0	0.05	94.0	18.4	12.4	69.2	[87]

AA/G, acetic acid/glycerol molar ratio; m_c/m_{gly}, catalyst/glycerol mass ratio; X, glycerol conversion; $S_{MAG/DAG/TAG}$, selectivity towards MAG/DAG/TAG.

3.4. Exchange Resins and Synthetic Polymers

In general, ion exchange resins are made of high-molecular-weight polymers containing functional groups that are capable of exchanging ions with a solution such as H^+ or OH^-.

According to their structure, resins can be divided into two main groups: gel-type resins and macroreticular resins. The former is constituted by a microporous and homogeneous polymeric matrix. The microporosity of these materials once limited their use in catalysis due to matter transport problems, a disadvantage that was solved with the development of macroreticular resins, which consist of agglomerates of small macroporous microspheres; they have been widely used ever since [88].

The presence of exchangeable protons in the structure of cationic resins makes them active catalysts in reactions requiring strong acidity. Cation-exchange macroreticular resins with strong acidity have been commercially used as acid catalysts in different reactions, such as the etherification of olefins with alcohols (e.g., MTBE and TAME production), dehydration of alcohols to olefins or ethers, condensation reactions and hydrolysis of esters, among others [89]. Particularly, due to their insolubility in water, they have been shown to be active in the reactions of ketalization and esterification of glycerol.

3.4.1. Glycerol Ketalization with Acetone

Most of the resins used in solketal synthesis, such as Amberlyst® [73,80,90–93] and Purolite® [91], are made of sulfonated polystyrene (Figure 9) crosslinked with divinylbenzene, at a certain percentage. The presence of the sulfonic group gives them the Brønsted acidity necessary for acetal synthesis.

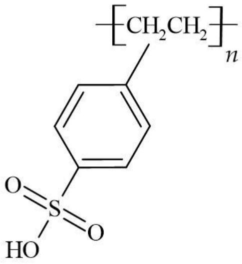

Figure 9. Sulfonated polystyrene schematic.

Exchange resins have been shown to exhibit very good activity in solketal synthesis due to their high density of Brønsted-type acid sites. In addition, it has been shown that the larger the pore size of the resin, the higher the activity, because the transport of reactant and product matter is favored. Some authors have used commercial resins, while others have synthesized different types of polymers, which have intrinsic acidity or can be functionalized to give them acidity. The most relevant results of these publications are summarized in Table 8.

Table 8. Exchange resins used as catalysts in the reaction of glycerol ketalization with acetone.

Catalyst	T (°C)	A/G	t (h)	m_c/m_{gly}	X (%)	S_S (%)	Y_S (%)	Ref.
CT 276 DR	40	4.5	6.0	0.005	NR	NR	32.0	[91]
Amberlyst-35dry	40	4.5	6.0	0.005	NR	NR	37.0	[91]
Amberlyst-36dry	40	4.5	6.0	0.005	NR	NR	37.0	[91]
CT 275 DR	40	4.5	6.0	0.005	NR	NR	40.0	[91]
Lewatit-GF1010	40	4.5	6.0	0.005	NR	NR	45.0	[91]
UAV-63	55	10.0	6.0	0.005	84.0	96.0	80.6	[94]
Amberlyst-46	60	6.0	0.5	0.001	NR	NR	84.0	[93]
PVA40	80	6.0	4.0	0.05	90.0	98.0	88.2	[95]
MP-SO_3H-24	30	5.0	0.5	0.005	94.0	98.5	92.6	[96]
EDGA-co-AMPS	50	20.0	6.0	0.005	NR	NR	95.0	[97]
Synthetic polymer	60	5.0	5.0	0.08	97.0	100	97.0	[98]
Amberlyst-15	70	1.2	0.3	0.07	98.0	100	98.0	[80]
DT-851	58	20.0	2.0	0.05	NR	NR	95.0	[99]

A/G, acetone/glycerol molar ratio; m_c/m_{gly}, catalyst/glycerol molar ratio; X, glycerol conversion; S_s, selectivity towards solketal; Y_s, yield of solketal; NR, not reported.

Among the authors who have synthesized polymers, Lopes et al. functionalized polyvinyl alcohol (PVA) by treatment with sulfosuccinic acid. The synthesized catalysts were named PVAx, where x represents the polymeric matrix, with x% of its -OH groups esterified, representing the degree of crosslinking. The unmodified PVA catalyst showed no activity in the solketal synthesis reaction, while the treated catalysts were active. The results showed that the catalytic activity increases when the degree of crosslinking increases from 5 to 40% due to the increased presence of sulfonic groups. However, when the degree of crosslinking is between 40% and 60%, the activity decreases due to the diffusional limitations of the reagents [95].

Churipard et al. synthesized a polyvinylbenzene polymer and subsequently functionalized it via sulfuric acid treatment. The synthesized catalysts were denoted MP-SO_3H-x, where x represents the amount of time that the polymer was kept with H_2SO_4 under stirring. Under the same reaction conditions, the order of activity was as follows: MP-SO_3H-24 > MP-SO_3H-12 > MP-SO_3H-8 > MP-SO_3H-4. The glycerol conversion increased from 72% to 85.6% and the selectivity towards solketal was 98.5% for all catalysts. The observed behavior is due to an increase in the acidity of the solids with the increasing contact time between the polymer and sulfuric acid [96].

Laskar et al. synthesized a phenol-formaldehyde resin with acidic character, which was evaluated in the solketal synthesis reaction. The effect of the amount of catalyst, molar ratio of reagents, temperature and reaction time was tested. For the best condition, 97% conversion was achieved with 100% selectivity towards solketal, activity that was attributed to the presence of a large number of Brønsted-type acid sites [98].

In turn, Santos-Vieira et al. synthesized polymeric materials obtained by the reaction of trimethylenphosphoric nitrile acid with Ln^{+3} (UAV-63) and with Eu^{+3} (UAV-20). The former is a 3D coordination polymer, while the latter is a 1D coordination polymer. The UAV-63 solid proved to be more active in the solketal synthesis reaction than the UAV-20 solid (84% conversion at 55 °C and 6 h versus 56% conversion under the same conditions). However, the latter proved to be more stable due to the fact that the former modifies its structure with the presence of water [94].

Hideaki Tokuyama et al. synthesized copolymers by the free-radical route, starting from different esters and a sulfonated amide (AMPS) as monomers. The results for the solketal synthesis showed that the copolymers exhibited more activity than the amide alone, and this result was attributed to the higher hydrophobicity contributed by the esters in the polymer. After 6 h and at 50 °C, a solketal yield of about 95% was achieved with the solid named EDGA-co-AMPS [97].

3.4.2. Glycerol Esterification with Acetic Acid

Exchange resins are one of the most widely used catalysts in the esterification of glycerol with acetic acid due to their high acid site density and pore sizes. Within the group of commercial resins, the most commonly used ones were Amberlyst® type 15 [85,100,101] 35 [102,103] and 36 [100,104,105]; and the resins Dowex 650C [106], Purolite® CT-275 [102] and Lewatit® [107,108]. All of these materials were found to be active and selective in the esterification reaction; the best results are presented in Table 9.

Table 9. Exchange resins used as catalysts in the esterification reaction of glycerol with acetic acid.

Catalyst	T (°C)	AA/G	t (h)	m_c/m_{gly}	X (%)	S_{MAG} (%)	S_{DAG} (%)	S_{TAG} (%)	Ref.
PSPF-3	70	3.0	8.0	0.01	81.7	67.1	31.7	1.2	[109]
Amberlyst 36	140	6.0	4.0	0.05	93.0	42.6	49.6	7.8	[105]
Amberlyst 15	110	9.0	2.0	NR	97.0	10.0	45.0	45.0	[101]
PDS-THF	110	6.0	3.0	0.05	97.8	11.4	54.0	34.6	[110]
CT-275	110	6.0	6.0	0.06	99.0	22.0	60.0	18.0	[102]
Amberlyst 36	105	9.0	4.0	0.05	99.0	45.0	15.0	40.0	[104]
Amberlyst 35	88	9.0	50	NR	99.0	10.0	45.0	45.0	[103]
Dowex 650C	120	9.0	4.0	0.04	99.6	16.0	50.0	34.0	[106]

AA/G, acetic acid/glycerol molar ratio; m_c/m_{gly}, catalyst/glycerol mass ratio; X, glycerol conversion; $S_{MAG/DAG/TAG}$, selectivity towards MAG/DAG/TAG; NR, not reported.

In addition to commercial resins, functionalized polymers that were active in the esterification reaction have been synthesized (Table 9). In this regard, Jiang et al. synthesized a phenolic resin by polycondensation from phenol sulfonic acid, phenol and paraformaldehyde, modifying the phenol sulfonic acid/phenol molar ratio at the beginning. The best results were obtained for a molar ratio of 3 (solid PSPF-3), reaching a glycerol conversion of 81.6% after 7 h of reaction at 70 °C, with a selectivity towards the set (MAG + TAG) of 98.9% [54]. In the same vein, Mou et al. synthesized polymers based on polydivinylbenzene (PDVB) and sodium p-styrene sulfonate (SPSS) via hydrothermal synthesis, with subsequent a cation exchange with H_2SO_4 solution. These catalysts achieved a glycerol conversion of 97.8%, with a selectivity towards the set (DAG + TAG) of 88.6%, after 3 h of reaction at 110 °C and a molar ratio AA/G = 6 [110].

3.5. Carbonaceous Materials

In heterogeneous catalysis, carbons are generally used as supports and adsorbents due to their high specific surface area and porosity. However, the incorporation of surface groups introduced by thermal or chemical treatment represents potential active sites, turning carbons into catalysts in themselves and, thus, expanding their application in catalysis [111].

It is known that the acidic surface groups formed by the action of oxygen on carbons at 400 °C can be classified into four groups: carboxylic, phenolic, carbonyl and lactones (formed by combination of a carboxylic group with a carbonyl) [112]. Carboxylic groups are the most acidic ones and can be generated via the oxidation of all surface groups by treatment with HNO_3 and temperature. Another way to generate acidic surface groups on carbons is the incorporation of sulfonic groups -SO_3H via treatment with H_2SO_4. Both treatments have been reported to generate acidity in coals for use in different reactions [113].

The main sources of coal currently are wood, hard coal (anthracite) and coconut shells. Due to its use as an energy source, the worldwide demand for coal is high, and it is estimated to increase even more in the coming years [114]. This situation, added to the large amount of biomass residues available, has generated that the synthesis of charcoal from biomass has become relevant in recent years [115]. Table 10 summarizes the reported sources and processes for the synthesis of catalysts from carbons used in glycerol esterification and ketalization reactions.

Table 10. Biomass sources used for carbon synthesis as a catalyst in the esterification reaction of glycerol with acetic acid.

Biomass Source	**Preparation Method**	**References**
Sucrose	Carbonization + functionalization with H_2SO_4	[116,117]
Rice husk	Carbonization + functionalization with H2SO$_4$	[118]
Glycerol	Carbonization with H_2SO_4	[119,120]
Glucose	Hydrothermal treatment + H_2SO_4	[90,121]
Cellulose	Hydrothermal treatment + H_2SO_4	[121]
Glucose	Treatment with H_2SO_4	[122]
Olive stone	H_2SO_4 + H_3PO_4 treatment	[120]
Sodium lignosulfonate	Pyrolysis + H_2SO_4 treatment	[123]
Bio-oil	Treatment with H_2SO_4	[124]
Mauritia Flexuosa Linnaeus filius	Hydrothermal treatment + H_3PO_4	[125]
Orange kernels	Pyrolysis	[126]
Willow willows	Pyrolysis	[127]
Wastewater	Hydrolysis	[128]
Palm kernel shells	Carbonization + H_2SO_4 functionalization	[129]
Carbohydrates (sucrose, glucose and starch)	Treatment with H_2SO_4	[130]

The wide variety of carbon sources, added to the different strategies to confer acid sites to them, generates a wide variety of synthesized catalysts, which are detailed below for both reactions.

3.5.1. Glycerol Ketalization with Acetone

Carbons from glucose, cellulose, glycerol, sodium lignosulfonate and bio-oils, using strong inorganic acids (HNO_3, H_2SO_4 and HCl) through different functionalization treatments, or the eventual modification of the carbons by impregnation with metals (Ni, Zr), were used for the glycerol ketalization with acetone (Table 11).

Table 11. Carbonaceous materials used as catalysts in the reaction of glycerol ketalization with acetone.

Catalyst	**T (°C)**	**A/G**	**t (h)**	**m_c/m_{gly}**	**X (%)**	**S_S (%)**	**Y_S (%)**	**Ref.**
Ni(1.8)/MWCNTs	40	6.0	3.0	0.06	96.0	72.0	69.0	[131]
CG-1:3	RT	4.0	0.5	0.03	84.0	90.0	75.6	[132]
HSCS/2	70	6.0	0.5	0.05	82.0	99.0	81.2	[90]
$BS_{9.2}$	25	10.0	2.0	0.006	90.0	98.0	88.2	[124]
$80LS20PS450H^+$	40	6.0	2.0	0.05	94.0	99.5	93.5	[133]
AC-S-18M	RT	4.0	6.0	0.027	97.0	98.0	95.0	[120]
$C\text{-}SO_3H$	70	5.0	0.2	0.07	97.0	100.0	97.0	[134]
5%Ni–1%Zr/AC	55	8.0	3.0	0.04	100.0	100.0	100.0	[135]
AC-PMf-80	55	4.0	5.0	0.05	81.0	98.0	79.4	[125]
SAFACAM	70	5.0	0.17	0.08	98	100	98	[122]
G-ASA	RT	4.0	1	0.005	97	97	95	[136]

RT, room temperature; A/G, acetone/glycerol molar ratio; m_c/m_{gly}, catalyst/glycerol molar ratio; X, glycerol conversion; S_s, selectivity towards solketal; Y_s, yield of solketal; NR, not reported.

Regarding the carbon source, Fernandez et al. compared the performance of carbons prepared via hydrothermal treatment from glucose (Glu) and cellulose (Cel), which were subsequently treated with concentrated H_2SO_4. Different preparation variables were evaluated, such as the origin of the materials (Glu or Cel), the temperature (195 °C or 215 °C), HCl concentration used to favor the pre-hydrolysis of the materials (2 M or 5 M) and the hydrothermal treatment time (20 h or 40 h). The catalyst that presented the highest activity was the so-called Cel-215-2 M-20 h-S; however, it was not possible to establish a direct relationship between the number of sulfonic groups and the activity [121]. Employing this same method, Ao et al. synthesized a catalyst from glucose with H_2SO_4

(SAFACAM) and evaluated it by using a microwave-assisted solketal synthesis, achieving almost complete conversion of glycerol, with 100% selectivity towards solketal [122].

In turn, Maraísa Gonçalves et al. synthesized acid carbons via the hydrothermal carbonization of glycerol with H_2SO_4 at 150 °C for 24 h. The catalysts were named CG-X, where X is the glycerol:H_2SO_4 mass ratio used (3:1, 2:1, 1:1, 1:1, 1:2 and 1:3). The CG-3:1 catalyst showed no activity (<5% conversion) due to the scarcity of carboxylic groups and the absence of -SO_3H groups. The rest of the catalysts presented the following order of activity: CG-1:3 > CG-1:2 > CG-1:1 > CG-2:1. This behavior was attributed to the increase in the number of total sites with the acid treatment, mainly due to the increase in -SO_3H groups, since the number of carboxylic groups did not increase significantly. All carbons presented a BET surface area of approximately 10 m^2 g^{-1}, indicating the low influence of textural properties on the activity in these catalysts [132].

Konwar et al. synthesized a macro/mesoporous solid via the pyrolysis of sodium lignosulfonate (LS) monoliths, a by-product of the paper industry, with a certain percentage of sodium polystyrene sulfonate (PS). The pyrolysis solid was treated with H_2SO_4. The catalysts were denoted xLS and PSzH^+, where x represents the percentage of LS (80–100), y the percentage of PS (0–20) and z the treatment temperature (350–450 °C). The 80LS20PS450H^+ catalyst was found to be the most active one, a result attributed to its higher porosity and density of -SO_3H sites than the rest of the solids [133].

Recently, Ballotin et al. synthesized a carbon-based catalyst by treating bio-oil with H_2SO_4 for 2 h at 120 °C, with a H_2SO_4/bio-oil mass ratio of 9.2. In this way, through the processes of dehydration and condensation, nanostructures were formed, which formed an amorphous sulfonated matrix. After 2 h of reaction at 25 °C, a 93% conversion of glycerol was achieved; the solid was stable after four uses [124].

Balotin et al. prepared catalysts from activated carbon from Mauritia Flexuosa Linnaeus filius, a palm tree native to Amazonia. For this purpose, they carried out a hydrothermal treatment, varying the time (20, 40 and 80 min), and, subsequently, the solids obtained were impregnated with H_3PO_4 at 85 wt.%. The results showed that the solids prepared at 40 and 80 min (AC-PMf-40 and AC-PMf-80) presented higher activity in the reaction, and the researchers attributed this result to the presence of both weak and strong acid sites, which allowed for the selective adsorption of acetone and glycerol on each other, without apparent competition between them [125].

Poulose et al. synthesized a catalyst by functionalizing graphene with taurine in DMF, conferring -HSO_3-type sites. The authors reported the high activity of this catalyst in the solketal synthesis reaction, higher than that of the catalysts reported so far. The authors ascribed this behavior to the covalent bonding of the taurine molecules on graphene, which allowed them to reach a high number of sites in the catalyst (40 wt.%) [136].

It has been reported that the inorganic acid that was employed to functionalize the carbons and its concentration also influences the activity of the reaction. Rodrigues et al. acidified activated carbon with HNO_3 (6 M and 15 M) and H_2SO_4 (6 M and 18 M) by stirring for 3 h. The synthesized catalysts were named AC-N-6M, AC-N-15M, AC-S-6M and AC-S-18M. Under the same reaction conditions, the following order of activity was obtained: AC-S-18M > AC-N-15M > AC-N-6M > AC-S-6M, with conversions of 97% for the AC-S-18 M catalyst and a selectivity towards solketal of 96%. The observed behavior can be explained by the higher contribution of strong acid sites for the AC-S-18M catalyst by the presence of sulfonic groups [120]. Following these results, Saikia et al. synthesized acid catalysts from cellulose by hydrothermal treatment with H_2SO_4 for 18 h at 80 °C. The solid obtained was named C-SO_3H. This solid achieved a glycerol conversion of 97%, with a selectivity towards solketal of 100%, and this result was attributed to its mesoporous nature, high specific surface area and the high density of acid sites it presents [134].

As for the preparation method, Nandan et al. synthesized silica–carbon composites by using glucose as carbon source and functionalized them with sulfonic groups via a heat treatment (SCS) and hydrothermal treatment (HSCS). The synthesized materials were named SCS/x and HSCS/x, where x = 0.3, 1 and 2 and represents the tetraethyl orthosilicate

(TEOS)/glucose ratio. The results showed that the HSCS solids presented higher activity than the SCS solids because the acidity generated in these catalysts was higher; in addition, the hydrothermal treatment also favored the generation of mesopores. The best catalyst was HSCS/2, which allowed for an 82% glycerol conversion and 99% selectivity towards solketal to be achieved [90].

Finally, it has been reported that carbons modified by metal impregnation are also active in the ketalization reaction.

Khayoon et al. synthesized multiwalled carbon nanotubes on which Ni was impregnated. The synthesized catalysts were termed Ni(x)/MWCNTs, where x represents the percentage of supported Ni. The catalyst impregnated with 1.8% Ni was found to be the most active one. The results were attributed to the presence of carboxylic groups generated on the carbon nanotubes and the good dispersion of the Ni metal sites. Higher contents of the metal led to lower dispersions, which resulted in a decrease in activity [131].

The same authors also supported Ni-Zr on activated carbon via impregnation at incipient humidity, using different Ni and Zr ratios. The catalysts that were supported only with Ni presented an increase in glycerol conversion due to the addition of metal, from 65% conversion (with 1% Ni) to 95% (with 5% Ni). This behavior was attributed to the higher number of active sites present in the catalyst. The selectivity towards solketal was 86%, with 10% selectivity towards the six-membered ring and 4% towards undesired products. Zr-only supported catalysts showed an increase in glycerol conversion with the increasing metal content from 54% to 67%, with a selectivity towards solketal of approximately 70% and no undesired products. These results showed that Ni was more active, but Zr was more selective, thus leading to the study of the combination of the two metals to evaluate the catalyst performance. As a result, the incorporation of 5% Ni and 1% Zr led to the best catalyst performance: 100% glycerol conversion with 74% selectivity towards solketal, without the presence of undesired products [135].

3.5.2. Glycerol Esterification with Acetic Acid

For the esterification of glycerol with acetic acid, different biomass sources have been explored for the preparation of carbons, such as sucrose, glucose, starch and biomass residues, among others. Table 12 summarizes the carbon-based catalysts used in the esterification reaction of glycerol with acetic acid.

Table 12. Carbonaceous materials used as catalysts in the glycerol esterification reaction with acetic acid.

Catalyst	T (°C)	AA/G	t (h)	m_c/m_{gly}	X (%)	S_{MAG} (%)	S_{DAG} (%)	S_{TAG} (%)	Ref.
KJ-400	120	5.0	4.0	0.08	90.0	56.0	40.0	4.0	[126]
TC-L	150	5.0	5.0	0.05	90.0	10.0	90.0 (*)		[118]
C-WW	120	6.0	6.0	0.16	90.8	46.9	48.4	6.3	[128]
C-glycerol	110	6.0	2.0	0.10	96.0	26.0	56.0	18.0	[130]
-SO_3H/C-Si-Zr	150	9.0	5.0	NR	97.0	3.0	3.0	94.0	[137]
PT800S	120	6.0	3.0	0.12	97.5	5.75	32.23	58.93	[129]
C_{SBA-15}-BDS	120	6.0	24.0	0.09	98.0	16.0	54.0	30.0	[117]
Willow charcoal	120	5.0	5.0	0.07	98.0	5.0	50.0	45.0	[127]
TAC-673	170	9.0	4.0	0.05	99.0	NR	NR	50.0	[116]
Glycerol carbon	115	4.0	1.0	0.05	100.0	20.0	70.0	10.0	[119]

AA/G, acetic acid/glycerol molar ratio; m_c/m_{gly}, catalyst/glycerol mass ratio; X, glycerol conversion; $S_{MAG/DAG/TAG}$, selectivity towards MAG/DAG/TAG; (*) selectivity towards (DAG + TAG).

Sanchez et al. synthesized carbons from sucrose by using two different methods. The first method consisted of carbonizing sucrose for 15 h in a N_2 atmosphere at 400 °C (DC). The second involved employing a silica temperate (TAC) and stationing it for its polymerization with subsequent carbonization for 3 h in a N_2 atmosphere at 400, 600 and 900 °C. These solids were functionalized by two different methods: with fuming sulfuric acid and with 98% liquid sulfuric acid. The best results were obtained for a low carbonization temperature (400 °C), using silica as a temperate and subsequently acidifying with fuming sulfuric acid. This solid led to a glycerol conversion of 99%, with a selectivity towards TAG of 50%, even surpassing the performance of the commercial resin Amberlyst 15. The authors attributed this behavior to the higher density of acid sites present in the solid [116]. Goscianska et al. synthesized carbon from sucrose by using the template hard method, using a silica template SBA-15, which was immersed in a solution of sucrose, concentrated sulfuric acid and distilled water. This mixture was treated at 160 °C for 6 h, and then the procedure was repeated. Subsequently, carbonization was carried out at 900 °C for 6 h in an argon atmosphere, and, finally, the template was then removed with hydrofluoric acid. To confer strong acid sites, two treatments were used: one with 4-aminobenzenesulfonic acid, sodium nitrate and hydrochloric acid for 20 h, under agitation (CSBA-15-BDS), and the other with concentrated sulfuric acid at 140 °C for 20 h, under agitation (CSBA-15-H_2SO_4). The best results were obtained for the solid CSBA-15-BDS, attributing its good performance to the significant increase in site density [117]. In the same vein, Malaika et al. synthesized carbon from known carbohydrates, such as glucose (C-glucose), sucrose (C-sucrose) and starch (C-starch), in addition to glycerol (C-glycerol). For this purpose, saturated solutions of each precursor were heated at 180 °C, under stirring, and H_2SO_4 was added until the solution turned brown. Then, stirring was continued for another 30 min until no further gas release was observed. The solids obtained were washed with distilled water and dried at 110 °C overnight. Of this group, the best results were obtained using the C-glycerol solid, and the authors attributed this behavior to the higher density of -SO_3H groups [130].

Other biomass sources used for the preparation of charcoal are solid biomass residues, such as husks, grains and tree bunches.

Galhardo et al. synthesized char via the carbonization of rice husk at 400 °C for 4 h, and then it was functionalized by different methods: with 6 M sulfuric acid under reflux (TC-6M), with 96% concentrated sulfuric acid (TC-L) and with 96% concentrated sulfuric acid vapors (TC-V), all at a char: acid ratio of 1:10 for 10 h at 80 °C. The best results were obtained with the TC-L solid, and the authors attributed this behavior to the higher number of acid sites generated compared to the rest of the solids. Moreover, these sites turned out to be mostly carboxylic groups so that, on average, the strength of the sites turned out to be higher [118].

Nda-Umar et al. also prepared charcoal from palm kernel shells, but, in their case, from palm kernels, which were previously washed and ground. The charcoal was generated in three different ways. On the one hand, it was carbonized in a furnace at 400 and 800 °C under a CO_2 atmosphere, without any other treatment. Then, the solid was functionalized with H_2SO_4 at 120 °C for 5 h (solids P400S and P800S). On the other hand, it was prepared by chemical treatment by impregnating the solid with 50% H_3PO_4. Subsequently, this solid was carbonized at 400 and 800 °C under a CO_2 atmosphere. The solid was functionalized with H_2SO_4 at 120 °C for 5 h (solids PC400S and PC800S). In the third method, the solid was mixed with dilute HCl and then with Na_2SiO_3 under vigorous stirring, and then it was allowed to polymerize in an oven. Subsequently, it was carbonized at 400 and 800 °C under CO_2 flow. The solid was then functionalized with H_2SO_4 at 120 °C for 5 h (solids PT400S and PT800S). The best results were obtained with the PT800S solid, and the authors attributed this behavior to the higher density of acid sites [129].

On the other hand, Rafi et al. synthesized char by pyrolysis of Karanja grains at 300–500 °C for 4 h in a N_2 atmosphere. The best results were obtained with the solid prepared at 400 °C due to the higher content of medium/high-strength sites that it presents in relation to the rest [126].

Finally, Tao et al. synthesized char via the pyrolysis of willow catkins at 500 °C for 5 h, under a N_2 flow. Subsequently, this solid was heated in concentrated sulfuric acid for 3 h at 70–100 °C and then treated with fuming sulfuric acid to confer acid sites. The best results were obtained for an acidification temperature of 90 °C since a higher number of acid sites were generated under these conditions due to the higher generation of -SO_3H groups [127].

Although glycerol is the reagent in esterification, it has also been employed as a carbon source due to its wide availability as a by-product in biodiesel synthesis. Thus, Chandrakala et al. synthesized a solid through the carbonization of glycerol with concentrated sulfuric acid (1:3 ratio) at 220 °C for 20 min, under vigorous stirring, with subsequent filtering, washing to neutrality and drying. This solid achieved a glycerol conversion of 100%, with a selectivity towards MAG of 20%, towards DAG of 70% and towards TAG of 10%, after 1 h of reaction at 115 °C, with a molar ratio AA/G = 4 and 5% by weight of catalyst with respect to glycerol [119].

Kumar et al. synthesized carbon from glycerol through a treatment with 18 M sulfuric acid at 100 °C for 24 h, under constant stirring. The temperature was then increased to 180 °C and then to 300 °C with the introduction of N2 to constitute porosity in the solid. The solid was then washed with hot water and calcined at 500 °C for 6 h (solid-SO_3H/C). The same procedure was repeated with the introduction of silica, zirconia and their combination to form solid -SO_3H/C-Si, solid -SO_3H/C-Zr and solid -SO_3H/C-Si-Zr, respectively. The best results were obtained with the -SO_3H/C-Si-Zr solid, which achieved 93.9% selectivity towards TAG. This result was attributed to the combination of a high acid site density (7.1 mmol g^{-1}), probably due to the presence of Zr in the structure, and a large average pore size (11.74 nm) [137].

From a different source than the rest, Bartoli et al. synthesized carbon from the hydrolysis of biosolids from municipal wastewater treatment (C-WW). These solids led to a glycerol conversion of 90.8%, with a selectivity towards MAG of 46.9%, towards DAG of 48.4% and towards TAG of 6.3%, after 4 h, at 120 °C, with an AA/G ratio of 6 and 16 wt.% of catalyst with respect to glycerol [128].

Although the carbon source varies among the different authors, all of them agree that the best results are obtained if solids with a high density of acid sites and a high pore size are used, favoring the diffusion of reactants and products inside them.

3.6. Zirconia-Based Catalysts

Zirconia and its modified variants have played an important role as catalysts in the fine chemical, pharmaceutical and petrochemical industries.

The catalytic and surface properties of pure zirconia can be modified through the incorporation of anions ($SO_4{}^{-2}$) or cations (Al^{+3}, Mo^{+6}). It has been reported that zirconia modified by these ions significantly enhances the acidic properties, increasing its catalytic capacity. This versatility of zirconia has been exploited by several authors to synthesize solids with acidic properties, being active in the reactions of ketalization and esterification of glycerol.

3.6.1. Glycerol Ketalization with Acetone

Regarding the use of ZrO_2 modified with different ions, some authors studied the incorporation of W [138,139], Mo [138,139], V [139] and $SO_4{}^{-2}$ groups [42,138]. Of all of them, it has been shown that $SO_4{}^{-2}$ groups, incorporated through treatment with H_2SO_4, lead to a higher generation of acid sites, thus conferring a higher activity onto the catalysts in the reaction of glycerol ketalization with acetone. Of the remaining ions, the following order of activity has been reported: W > V > Mo, attributed to the generation of a higher number of acid sites [138,139].

In addition to evaluating the incorporation of ions into the supports, the coating of the modified ZrO_2 was also studied. In this regard, Reena et al. impregnated ZrO_2 modified with 5% Mo, W and V into a monolith by coating, generating HM-MZ, HM-WZ and HM-VZ materials, respectively. The results showed that the zirconia catalysts supported on HM-MZ presented the highest activity [139].

Vasantha et al. prepared cordierite (HC) monoliths on which ZrO_2 (HC-Z) and its modified variants, such as ZrO_2-Al_2O_3 and $SO_4{}^{-2}/ZrO_2$, were coated with ZrO_2 (HC-Z) and its modified variants, such as ZrO_2-Al_2O_3 and SO_4^{-2}/ZrO_2. The catalysts prepared by ZrO_2_Al_2O_3 coating were named HC-ZA1 (40%ZrO_2_60%Al_2O_3 and HC-ZA2 (60%ZrO_2_40%Al_2O_3). The catalyst prepared by SO_4^{-2}/ZrO_2 coating was denoted HC-SZ and was prepared by dissolving the Zr precursor in 0.5 M H_2SO_4. Under the same reaction conditions, the following order of activity was obtained: HC-SZ > HC-ZA2 > HC-ZA1 > HC-Z. This result was attributed to the higher number of strong acid sites provided by the addition of sulfonic groups to zirconia, which is evident both in powder catalysts and those prepared by coating on another material [140].

Table 13 summarizes the best results using zirconia-based catalysts, according to the performance obtained at solketal.

Table 13. Zirconia-based catalysts employed in glycerol ketalization with acetone.

Catalyst	T (°C)	A/G	t (h)	m_c/m_{gly}	X (%)	S_S (%)	Y_S (%)	Ref.
Zr-S-400	40	6.0	1.0	0.006	80.0	86.0	69.0	[42]
HC-ZS	60	4.0	1.7	0.11	96.0	90.0	86.4	[140]
SZ	RT	6.0	1.5	0.05	98.0	97.0	95.0	[138]
HM-MZ	60	6.0	0.13	0.01	98.0	98.0	96.0	[139]

RT, room temperature; A/G, acetone/glycerol molar ratio; m_c/m_{gly}, catalyst/glycerol molar ratio; X, glycerol conversion; S_s, selectivity towards solketal; Y_s, yield of solketal.

3.6.2. Glycerol Esterification with Acetic Acid

For the case of the esterification reaction of glycerol with acetic acid, textural and acidity properties are the variables to be taken into account in the synthesis of zirconia-based catalysts. In all cases, the incorporation of SO_4^{-2} ions has been reported to impart strong acidity to the catalysts.

Lei et al. synthesized a WO_3-ZrO_2 mixed oxide via the solvent autoevaporation method with different W/Zr ratios (0.33–3) and then calcined it at different temperatures (500–800 °C). Subsequently, sulfate groups were incorporated by the incipient wetting impregnation method with H_2SO_4. The best results were obtained with the solid presenting W/Zr = 1 ratio and calcined at 500 °C, due to the presence of a high number of acid sites and a good tolerance to the presence of water [141].

In order to synthesize a solid with high specific surface area, Popova et al. prepared a silica-based template, on which they then impregnated $ZrCl_2$, with subsequent calcination in air flow, varying the amount of Zr between 4 and 12 wt.%. Subsequently, this solid was treated with H_2SO_4 to confer acidity through the incorporation of sulfate groups. The best results were obtained for the solid with the highest Zr content due to the presence of a higher number of acid sites. Moreover, these results were better than those obtained employing a commercial sulfated zirconia, attributing this result to the high dispersion of Zr on the silica template surface [87].

Abida et al. synthesized a silica–zirconia matrix by using the sol–gel method, to which they then incorporated sulfate ions by treatment with H_2SO_4 in aqueous solution. This solid, named SSZ-550, was employed in the esterification reaction of glycerol with acetic acid, reaching a glycerol conversion of 100%, with a selectivity towards TAG of 93% after 40 min of reaction, results that were attributed to the presence of strong Brønsted-type sites, coming from the sulfate groups [142].

Table 14 summarizes the results reported using zirconia-based catalysts.

Table 14. Zirconia-based catalysts employed in glycerol esterification with acetic acid.

Catalyst	T (°C)	AA/G	t (h)	m_c/m_{gly}	X (%)	S_{MAG} (%)	S_{DAG} (%)	S_{TAG} (%)	Ref.
SO_4^{2-}/WZr (1:1)-500	120	10.0	4.0	0.01	100.0	37.0	60.0	3.0	[141]
12ZrKIL-2	100	10.0	1.0	0.05	100.0	2.7	77.2	20.1	[87]
SSZ-550	80	9.0	0.7	0.03	100.0	0.0	7.0	93.0	[142]

AA/G, acetic acid/glycerol molar ratio; m_c/m_{gly}, catalyst/glycerol mass ratio; X, glycerol conversion; $S_{MAG/DAG/TAG}$, selectivity towards MAG/DAG/TAG.

3.7. Heteropolyacids

In recent decades, heteropolyacids (HPAs) have attracted much attention as catalysts since they possess very high Brønsted-type acidity and are also efficient oxidizers [94]. These compounds are formed through the condensation of Mo, W, V, Nb or Ta oxoanions in aqueous solution which polymerize at an appropriate pH, forming a polyanion (the heteropolyacid itself) and water [143].

HPAs have been widely used as homogeneous acidic and oxidizing catalysts, but the difficulty of separating them from the reaction medium has led to the study of their use in heterogeneous catalysts. In this sense, variants of these materials have been developed that allow their use as acid solids. The first variant resulted from the synthesis of water-insoluble HPAs via the partial substitution of protons by cations of the type Cs^+, K^+, NH_4^+, etc. Another alternative is the synthesis of HPA catalysts supported on SiO_2, ZrO_2, activated carbon or exchange resins. A third variant is the inclusion of HPAs in mesoporous silica or, recently, in zeolites [144]. All of these alternatives have allowed for the use of heteropolyacids in heterogeneous catalysis, facilitating the separation from the reaction medium.

In particular, it has been shown that the high acidity presented by HPAs makes them efficient catalysts in ketalization and esterification reactions. In this sense, their use has been reported in different variants, as insoluble materials, supported or incorporated into porous matrices.

3.7.1. Glycerol Ketalization with Acetone

Ferreira et al. were among the first authors to report the use of heteropolyacids included in silica for the synthesis of solketal. The synthesized catalysts were named PW-S, SiW-S, PMo-S and SiMo-S, depending on whether tungstophosphoric acid (PW), tungstosilicic acid (SiW), phosphomolybdic acid (PMo) or molybdosilicic acid (SiMo) was used. The results showed that the order of activity was PW-S > SiW-S > PMo-S > SiMO-S, behavior that was attributed to the acidic strength of the sites, obtained by potentiometric titration, which follows that same decreasing order [145].

In the same sense, Chen et al. used $Cs_{2.5}H_{0.5}PW_{12}O_{40}$ (Cs2.5) supported on mesoporous silica as a catalyst in the synthesis of solketal. This HPA is water resistant and exhibits high acidity and specific surface area when compared to other similar compounds (125 $m^2\ g^{-1}$). However, to improve the catalytic activity, it was supported on silica, thus significantly increasing the specific surface area. The salt was prepared by coprecipitation and subsequently supported on KIT-6 (mesoporous silica) via the incipient impregnation method. The results showed higher activity for the supported catalyst due to its high specific surface area (574 $m^2\ g^{-1}$) compared to the unsupported salt, which allowed the reagents to reach the acid sites faster. In addition, the experimental results confirmed the absence of salt leaching [146].

Talebian-Kiakalaieh et al. supported tungstophosphoric acid (HPW) on a Y zeolite synthesized in its protonated form, which was previously subjected to citric acid treatment to partially remove Al^{+3} ions and, thus, increase its porosity. The supported materials were denoted as HR/Y-WX, where x is the percentage of HPW. The results showed that the dealuminated zeolites showed higher activity due to their higher porosity, while the presence of HPW increased the total acidity of the solids contributing with Brønsted acid sites. The best result was obtained with the HR/Y-W20 catalyst after 2 h of reaction, with a solketal yield of 97.87% [147].

Recently, Sadjadi et al. impregnated phosphotungstic acid (HPW) on bentonite modified with an acidic polymer containing carboxylic groups. The authors evaluated the effect of the amount of supported HPW (5–25 wt.%), determining that an increase between 5 and 20% increased the activity of the catalyst, while a higher content decreased the activity, which could be due to the aggregation of the supported HPW [148].

On the other hand, Chansorn et al. synthesized catalysts from the immobilization of phosphotungstic acid (PTA) on a layer of poly(N-methyl-4-vinylpyridinium) (PMVP) grafted onto silica nanoparticles (SNSs-g-PMVP/PTA), with the aim of improving the catalytic activity of PTA. The authors reported the high activity of this catalyst compared to other solids, attributed to the high dispersion of the heteropolyacid on the support. Furthermore, they concluded that PMVP confers a hydrophobic environment, which prevents the deactivation of PTA by the presence of water [149].

Since the exchange of protons by ions of different nature has been shown to be another avenue for the implementation of HPAs in heterogeneous catalysis, Sandesh et al. prepared hybrid materials from different heteropolyacids with ammonium salts. Tungstophosphoric acid (PWA), tungstosilicic acid (SWA) and phosphomolybdic acid (PMoA) were used as HPAs and $(C_3H_7)_4N^+Br$ as salt. The materials were denominated $(C_3H_7)_4N^+$/PWA, $(C_3H_7)_4N^+$/SWA and $(C_3H_7)_4N^+$/PMoA. The materials were insoluble in the reaction medium, presenting the following order of activity: $(C_3H_7)_4N^+$/PWA > $(C_3H_7)_4N^+$/SWA > $(C_3H_7)_4N^+$/PMoA, with a glycerol conversion of 94%, 90% and 87%, respectively. Selectivity towards solketal was 98% in all cases. The similarity in activity and selectivity highlights that the acid sites of all materials are similar. The reaction of untreated PWA led to the 90% conversion of glycerol in 10 min of reaction, indicating that the activity comes mostly from HPA. However, the homogeneous nature of PWA marks the disadvantage of this type of material with respect to the synthesized solids. Moreover, the $(C_3H_7)_4N^+$/PWA catalyst was shown to maintain its activity even in the presence of water [74].

Following these results, Da Silva et al. exchanged the protons of the silicotungstic acid for Sn^{+2} ions, thus allowing for the resulting salt to be insoluble in polar media. Compared to similar HPA and inorganic acids such as H_2SO_4 and HCl, the $Sn_2SiW_{12}O_{40}$ solid was found to be more active. The authors attributed this behavior to the stability conferred by this solid to charged intermediates. In addition, the hydrolysis undergone by Sn^{+2} ions in the presence of their hydration sphere generates protons that constitute active sites themselves [150]. In turn, in another work, the same authors replaced the protons of HPA by Fe^{+3}, Co^{+2}, Cu^{+2}, Ni^{+2} and Al^{+3}, obtaining the best results with the replacement of the protons by Fe^{+3} ions, a result attributed to the higher Lewis-type acidity presented by this salt [151].

Table 15 summarizes the main results of heteropolyacids employed in glycerol ketalization with acetone.

Table 15. Heteropolyacids employed as catalysts in glycerol ketalization with acetone.

Catalyst	T (°C)	A/G	t (h)	m_c/m_{gly}	X (%)	S_S (%)	Y_S (%)	Ref.
$(C_3H_7)_4N^+$/PWA	30	6.0	2.0	0.15	94.0	98.0	92.1	[74]
PW-S	70	6.0	2.0	0.05	95.0	97.0	92.1	[145]
$Sn_2SiW_{12}O_{40}$	25	12.0	1.0	0.03	95.0	98.0	93.0	[150]
30% $Cs_{2.5}$/KIT-6	25	6.0	0.25	0.05	95.0	98.0	93.1	[146]
$Fe_{4/3}SiW_{12}O_{40}$	25	20.0	1.0	0.09	98.0	97.0	95.0	[151]
HR/Y-W_{20}	40	10.0	2.0	0.10	100.0	97.9	97.9	[147]
Bent-P-IL-HPW	55	20.0	2.0	0.10	100.0	99.0	99.0	[148]
SNSs-g-PMVP/PTA	70	8.0	1.0	0.05	94.3	96.7	91.1	[149]

A/G, acetone/glycerol molar ratio; m_c/m_{gly}, catalyst/glycerol molar ratio; X, glycerol conversion; S_s, selectivity towards solketal; Y_s, yield of solketal.

3.7.2. Glycerol Esterification with Acetic Acid

Gonçalves et al. were among the first to employ HPAs as catalysts, directly using $H_3PW_{12}O_{40}$ (HPW or TPA) in the esterification of glycerol with acetic acid. As a result, the solid was able to achieve 95% glycerol conversion, with selectivity towards MAG of 16%, towards DAG of 72% and towards TAG of 22%, after 12 h of reaction, at 60 °C, employing an AA/G ratio of 12 and 0.04 mmoles of HPW [152]. However, the direct use of HPAs as catalysts presents certain drawbacks related to the low specific surface area, low thermal stability and solubility of these in the reaction medium, as indicated for the catalytic reaction. For this reason, several authors have reported their implementation by incorporating HPAs in support of a different nature.

In this sense, several authors impregnated HPW on different supports, such as silica [153–155], Nb_2O_5 [156], zirconia [155] and NaUSY zeolites [157]. All of them observed that the activity of the catalysts increases as the amount of supported HPW increases. However, they also reported that there is an optimum content, depending on the type of support, above which a decrease in the specific surface area could occur, leading to a decrease in the activity of the catalysts. In particular, better activity was observed in those catalysts synthesized from supports with higher specific surface area. For example, Patel et al. supported $H_3PW_{12}O_{40}$ acid on MCM-41 and ZrO_2, observing the best results for the MCM-41 support, due to the higher specific surface area values [155].

In line with what was described above, Neto et al. supported molybdophosphoric acid (MPA) on Si-Al nanotubes, formula $Al_2Si_2O_5(OH)_4 \cdot 2H_2O$ (HNT), by using the wet impregnation method. The authors modified the supported HPA content, generating the solids x-MPA/HNT, where x is the amount of MPA (10, 25 or 50%). As for the HPW, the best results were obtained for the solid with higher MPA content (50-MPA/HNT), since it presents a higher number of MPA ions available to achieve the reaction. In this case, lower MPA loadings lead to the formation of sites preferentially inside the pores, thus hindering the access of the reagents to the sites [158].

For example, Zhu et al. supported $H_4SiW_{12}O_{40}$ (HSiW or STA), $H_3PW_{12}O_{40}$ (HPW) and $H_3PMo_{12}O_{40}$ (HPMo) on ZrO_2 by using the incipient wetting impregnation method. The best results were obtained for the HSiW/ZrO_2 solid due to a higher contribution of Brønsted sites and the good hydrothermal stability of the catalyst [105]. In the same sense, Magar et al. synthesized catalysts via the impregnation of silicotungstic acid (HSiW), dodecanotungstophosphoric acid (DTP) and phosphomolybdic acid (PMA), on polyvinylpyrrolidone (PVP) as support. Of these solids, PVP-DTP presented higher activity, and this behavior was attributed to the higher generation of acid sites and better incorporation of DTP on PVP [159].

Kale et al. synthesized different catalysts by combining different HPAs on different supports, with the aim of finding an optimal combination. These authors supported silicotungstic acid (HSiW or STA), tungstophosphoric acid (HPW or TPA) and phosphomolybdic acid (PMA) on different supports, such as SiO_2, Al_2O_3 and SiO_2-Al_2O_3. Of all the combinations evaluated, STA/SiO_2 and TPA/SiO_2 solids led to the best results, both presenting similar activity. The authors attributed this behavior to the high density of Brønsted sites generated in the solids, combined with the higher retention of the HPA structure on the SiO_2 supports. In contrast, the PMA/SiO_2 solid presented a good density of Brønsted sites but was less stable, making this HPA unsuitable as an active site in the reaction. Moreover, the use of Al_2O_3 and SiO_2-Al_2O_3 supports led to a higher number of Lewis sites, which made its activity in the reaction lower [160]. It is worth clarifying that, in their study, the authors employed toluene as an entrainer, which favored the removal of water from the reaction medium and led to a higher progress of the reaction.

Another alternative for the use of HPAs as heterogeneous catalysts is the exchange of their protons for ions of different nature. In particular, in the esterification reaction of glycerol with acetic acid, exchanges with Cs [74,161], Ag [162], metal cations of hydrated nitrate salts [163] and In [164] have been studied. All of them used heteropolyacids of the type $H_3PW_{12}O_{40}$ (HPW or TPA). Regardless of the nature of the ions exchanged, all authors have observed that total proton substitution leads to a decrease in catalyst activity, which is attributed to the presence of residual protons enhancing the activity since they act as higher-strength Brønsted-type acid sites.

In this sense, Sandesh et al. synthesized a catalyst from the partial proton exchange of TPA for Cs^+ ions, whose final molecular formula is $Cs_{2.5}H_{0.5}PW_{12}O_{40}$. The authors compared the activity of this catalyst with other solids, such as sulfated zirconia, activated clay and beta zeolite, showing that the synthesized solid presented higher activity than the rest. The authors attributed this behavior to the higher ratio of Brønsted/Lewis acid sites, attributed to the presence of both Cs+ ions and residual protons [74]. Jagadeeswaraiah et al. supported $H_3PW_{12}O_{40}$ (TPA) on a zirconia doped with Cs. The authors varied the Cs content present in the zirconia, so that they were able to replace 1, 2 or 3 protons of the HPA, keeping the amount of TPA present in the catalysts constant and equal to 20 wt.%. The best results were obtained for the TPA/Cs_2-ZrO_2 catalyst, since the addition of Cs replacing 2 protons of the HPA improved the number of acid sites available, leaving residual protons in the catalyst. However, if all of the HPA protons are exchanged for Cs, no residual protons are left and the acidity decreases significantly, leading to low catalyst activity [161].

Regarding the exchange with Ag, Zhu et al. studied the proton exchange of the $H_3PW_{12}O_{40}$ (HPW) acid for Ag ions by modifying the number of substituted ions. In this regard, the synthesized solids were named Ag1PW, Ag2PW and Ag3PW, depending on whether 1, 2 or 3 protons of the acid were substituted, respectively. The order of activity obtained was Ag1PW > Ag2PW > Ag3PW > HPW, and the authors attributed this behavior to the higher number of total acid sites generated in each of them [162].

On the other hand, Sun et al. synthesized proton exchange catalysts of $H_3PW_{12}O_{40}$ (HPW) for In^{+3} ions in different ratios, forming In_3/xH_1-xPW solids, where x = 1.5, 1.8, 2.4 and 2.7. The results showed that the activity of the solid increased upon an increase in In content from 0.5 to 0.8, while an increase from 0.8 to 1 led to a decrease in the activity of the solid. Therefore, the most active catalyst turned out to be $In_{0.8}H_{0.6}PW$. The authors attributed this behavior to the generation of Lewis-type sites by adding In but maintaining a remnant of Brønsted sites. For this reason, by replacing all the protons by In^{+3}, the activity of the solid decreased, a result that agrees with that reported by other previously mentioned authors [164].

On the other hand, da Silva et al. synthesized catalysts by totally replacing the protons of some HPAs, such as $H_3PW_{12}O_{40}$, $H_3PMo_{12}O_{40}$ and $H_4SiW_{12}O_{40}$, with metal cations of hydrated nitrate salts, such as $Fe(NO_3)_3$, $Co(NO_3)_2$, $Mn(NO_3)_2$ and $Cu(NO_3)_2$. According to these authors, this procedure generates the compounds $M_3/nPW_{12}O_{40}$, $M_3/nPMo_{12}O_{40}$ and $M_4/2SiW_{12}O_{40}$, where M is the M^{n+} ion (M = Fe^{3+}, Co^{3+}, Cu^{2+} and Mn^{2+}). Thus, the activity of HPA salts containing these metal ions was Fe^{3+}> Cu^{2+}> Mn^{2+}> Co^{3+}, and the researchers attributed this behavior to the fact that the acidic protons of HPA could be successfully exchanged only with Fe^{+3} cations, forming the corresponding salt [163].

Table 16 summarizes the results reported by the different authors.

Table 16. Heteropolyacids employed as catalysts in glycerol esterification with acetic acid.

Catalyst	T (°C)	AA/G	t (h)	m_c/m_{gly}	X (%)	S_{MAG} (%)	S_{DAG} (%)	S_{TAG} (%)	Ref.
50-HPA/HNT	80	9.0	5.0	NR	38.0	NR	NR	98.0	[158]
PMo3-NaUSY	NR	16.0	3.0	0.10	68.0	37.0	59.0	2.0	[157]
PW-on-S2	120	16.0	7.0	0.10	87.0	36.0	60.0	4.0	[153]
TPA/Cs_2-ZrO_2	120	5.0	4.0	NR	90.0	42.0	50.0	8.0	[161]
TPA_3/MCM-41	100	6.0	6.0	NR	92.0	20.0	70.0	10.0	[155]
HPW	60	12.0	12.0	0.026	95.0	16.0	72.0	22.0	[152]
25%TPA/Nb_2O_5	120	5.0	4.0	0.04	98.0	22.0	58.0	20.0	[156]
CsPWA	85	8.0	2.0	0.07	98.1	25.0	59.0	16.0	[74]
$Fe_4(SiW_{12}O_{40})_3$	60	3.0	4.0	0.058	100.0	24.0	69.0	7.0	[163]
$In_{0.8}H_{0.6}PW$	120	4.0	3.0	0.052	100.0	20.0	65.0	15.0	[164]
SBAH-15(15)	110	6.0	3.0	0.02	100.0	18.0	64.0	18.0	[154]
Ag_1PW	120	10.0	4.0	0.01	100.0	10.0	60.0	30.0	[162]
HSiW/ZrO_2	120	10.0	4.0	0.06	100.0	6.4	61.3	32.3	[55]
PVP-DTP	110	20.0	6.0	0.22	100.0	13.0	54.0	34.0	[159]
STA/SiO_2	105	6.0	24.0	0.05	100.0	0.0	20.0	70.0	[160]

AA/G, acetic acid/glycerol molar ratio; m_c/m_{gly}, catalyst/glycerol mass ratio; X, glycerol conversion; $S_{MAG/DAG/TAG}$, selectivity towards MAG/DAG/TAG; NR, not reported.

3.8. Silica-Based Catalysts

Silica (SiO_2) is one of the most widely used supports in catalysis. Several authors have synthesized different silica-based catalysts in different forms, such as SBA-15, KIT-6 and

MCM-41, modifying them with different metals to improve their catalytic properties, and have applied them to glycerol acetylation and esterification reactions.

3.8.1. Glycerol Ketalization with Acetone

The MCM-41 support has been the one most employed in the synthesis of catalysts for the reaction of glycerol ketalization with acetone, supporting different types of compounds and elements, such as Al [165], V [166], Zr [167], Hf [167], Sn [167], Ga [167] and W [168].

Tayade et al. incorporated aluminum triflate on MCM-41 (MS) with the aim of preparing a water-resistant solid with high acidity. An aluminum-incorporated material was synthesized via the sol–gel method (Al-MS) and a supported variant (Al (TF)-MS). In addition, the MS and Al-MS solids were treated with trifluoromethanesulfonic acid (TFA). The resulting catalysts were named TFA/MS and TFA/Al-MS, respectively. While the MS and Al-MS solids showed no activity, the order of activity for the rest of the catalysts was as follows: TFA/Al-MS > Al (TF)-MS > TFA/MS. This behavior was attributed to the generation of more acid sites in the more active catalysts. However, the only catalyst that proved to be reusable was Al (TF)-MS, which achieved 93% glycerol conversion, with 100% selectivity towards solketal [165].

Also employing MCM-41, Abreu et al. supported V at different percentages (0.4–6.8 wt.%). The solids activity increased as more V was added, reaching a maximum glycerol conversion of 92%, with a selectivity towards solketal of 98%. This behavior was attributed to the increase in the number of sites available for the reaction [166].

Li et al. also used MCM-41 and TUD-1 substituted with different metals, such as Zr, Hf and Sn, conferring Lewis-type acidity. The synthesized solids were named Zr-TUD-1, Hf-TUD-1 and Sn-MCM-41, respectively. The order of activity obtained was as follows: Hf-TUD-1 > Zr-TUD-1 > Sn-MCM-41. This behavior was attributed to the high specific surface area, the relative hydrophobicity of the surface and the higher number of accessible sites in the most active solids. Thus, the Hf-TUD-1 catalyst achieved 52% glycerol conversion, with 100% selectivity towards solketal [44]. Subsequently, the same authors synthesized Ga-MCM-41 in the form of nanoparticles (<150 nm) with different levels of Ga content. The solids with a higher content of the metal were named XS-Ga-MCM-41-H, and those with lower content were subjected to ion exchange with NH_4OH and calcined to transform them into their protonated form (XS-Ga-MCM-41-L). The results showed that both catalysts led to the same conversion; however, the solid XS-Ga-MCM-41-L presented higher TON value, which was due to the presence of Brønsted sites mostly [167].

Recently, Huang et al. synthesized tungsten oxide catalysts on MCM-41 via high-temperature impregnation. The catalysts thus synthesized were named WO_x/MCM-41-Y-Y-H (L), where Y is the mass ratio of precursor $(NH_4)_{10}[H_2W_{12}O_{42}]\cdot 4H_2O$ with respect to the support, while H corresponds to calcination at 550 °C and L at 350 °C. The best results were obtained for the solid impregnated with 20 wt.% and calcined at 350 °C, reaching a glycerol conversion of 88% after 2 h of reaction at 50 °C [168].

On the other hand, SBA-15 silica has also been used as a support, on which different metals, such as Mo, Al, Zr, Ti and Nb, have been supported.

Gadamsetti et al. synthesized molybdenum phosphate catalysts supported on SBA-15 (xMoPO/SBA-15) via the incipient wetting impregnation method. The authors evaluated the effect of MoPO percentage (x) on catalyst activity (0–50%) and found that, for x = 40% MoPO, a complete conversion of glycerol, along with high selectivity towards solketal (98%), could be achieved. The results indicated that this behavior was due to the generated surface acidity and good dispersion of molybdenum phosphate on the silica matrix [169].

Similar results were obtained by Ammaji et al., who incorporated various metals into the SBA-15 structure, such as Al, Zr, Ti and Nb, at a Si/M = 20 ratio [170]. The Nb-SBA-15 and Zr-SBA-15 catalysts presented higher activity than the Ti-SBA-15 and Al-SBA-15 solids, and this result was attributed to the higher acidity and specific surface area of the catalysts, with Nb-SBA-15 being the most active and selective solid.

SBA-15 supports can also be functionalized to confer acidic sites, as reported by Vicente et al., who incorporated propyl sulfonic (Pr-SBA-15) and arenesulfonic (Ar-SBA-15) groups to evaluate their effect on the activity of the solids. In addition, they modified the hydrophobicity of the materials by silylation of free silanol (Si-OH) groups through a reaction with trimethylmethoxysilane. The obtainment of hydrophobic materials is useful for glycerol ketalization with acetone due to the formation of water as a reaction product, which could deactivate the active sites. However, the authors reported that this treatment is not suitable for the synthesis of catalysts for this reaction because the specific surface area of the solids is significantly reduced, and the pores with silyl groups limit the access of the reagents. For this reason, the functionalized SBA-15 resulted in being more active, and, in turn, the solid Ar-SBA-15 turned out to be more active due to the generation of higher acidic strength through the incorporation of arenesulfonic groups [171].

On the other hand, Li et al. incorporated metals (Zr and Mo) on a mesoporous silica KIT-6. The synthesized catalysts were named ZrMo/KIT-6(X), where X (X = 1, 3, 5, 7, 9%) is the Zr-Mo/Si ratio. The KIT-6 support did not present catalytic activity, but the incorporation of Zr and Mo species gradually increased the activity of the solids, with ZrMo/KIT-6(5) being the one that presented higher glycerol conversion and selectivity towards solketal, which was due to a better dispersion of the metals in the support. However, the incorporation of Zr and Mo at 7 and 9% led to a decrease in activity due to the generation of metal aggregates and the consequent formation of crystalline ZrO_2 and MoO_3, leading to a decrease in active sites [172].

In addition to ordered mesoporous silicas, commercial silica and its modified variants have also been employed.

In this regard, Kao et al. impregnated niobium oxide on commercial SiO_2 in the range of 0.5–20 wt.%. The best results were obtained for the solid with 15 wt.% Nb (Si-15%Nb), which led to 45.6% glycerol conversion and 97% selectivity towards solketal. Above this amount of Nb, the conversion decreased as a result of Nb overloading on the support, partially covering the active sites [173].

On the other hand, Vivian et al. synthesized SiO_2 catalysts with Ga as the active material, prepared by using the sol–gel technique (solids named Ga-X, where X is the Si/Ga ratio) and dropwise impregnation (solid named Ga-impregnated). The best results were obtained for the Ga-74 solid due to the efficient insertion of Ga into the SiO_2 matrix, with yields of solketal of 55% after 10 h of reaction [174].

Nowadays, the discovery of silicon sponges (MCF) has allowed researchers to significantly reduce the limitations of matter transport and the limit of metal incorporation into the supports due to the fact that these materials present a higher porosity than SBA-15 and MCM-41 and allow high contents of active sites to be supported [175].

Calvino-Casilda et al. modified MCFs with (3-mercaptopropyl) trimethoxysilane (MP-MCF) and through the addition of certain metals such as Nb (MP-NbMCF), Ta (MP-TaMCF) and Ta with P (MP-PTaMCF). Their results showed that the incorporation of Nb and Ta increased the number of Brønsted sites generated by the oxidation of SH groups from (3-mercaptopropyl) trimethoxysilane. The addition of Ta, in addition, increased the cell size, leading to higher glycerol conversions. The addition of P increased the acidity but significantly decreased the porous structure. The MP-TaMCF catalyst allowed the researchers to achieve 80% glycerol conversion, along with 97% selectivity towards solketal [176].

Stawicka et al. modified MCFs with (3-mercaptopropyl) trimethoxysilane (MP-MCF), with (4-chlorosulfonylphenyl) ethyltrimethoxysilane (CS-MCF) and with Nb (NbMCF), Ta (TaMCF) and Mo (MoMCF), with the aim of studying the effect of the presence of Lewis or Brønsted sites on the solketal activity. Under the same reaction conditions, the following order of activity was obtained: CS-MCF > MP-MCF > TaMCF > MoMCF > NbMCF. This behavior was attributed to the presence of Brønsted-type sites exclusively, since those catalysts containing both types of sites or those possessing only Lewis-type sites presented a lower activity in the reaction. Under optimal reaction conditions, the CS-MCF catalyst led to 87% glycerol conversion, with a selectivity towards solketal of 99% [177].

Other authors, such as Bivona et al., synthesized 1D silica-based tubular nanostructures, in which Sn particles were inserted in a controlled manner. The activity of silica nanotubes without Sn and with Sn was evaluated, with the solids being denoted Si-NTs and Sn-NTs-B, respectively. The Si-NTs catalyst achieved 8% glycerol conversion, while the Sn-NTs-B solid achieved 60% glycerol conversion. This result was attributed to the high specific surface area, high number of sites and good pore accessibility of the latter material with respect to the former [178].

Table 17 summarizes the best results obtained for silica-based catalysts employed in glycerol cycloaddition with acetone.

Table 17. Silica-based catalysts employed in glycerol ketalization with acetone.

Catalyst	T (°C)	A/G	t (h)	m_c/m_{gly}	X (%)	S_S (%)	Y_S (%)	Ref.
Ar-SBA-15	70	6.0	0.5	0.05	89.5	NR	NR	[171]
XS-Ga-MCM-41-L	80	1.0	6.0	0.03	25.0	99.0	24.7	[167]
Si-15%Nb	NR	2.0	NR	0.02	45.6	97.0	44.2	[173]
Hf-TUD-1	80	1.0	6.0	0.03	52.0	100.0	52.0	[44]
Ga-74	50	4.0	10.0	0.01	NR	NR	55.0	[174]
Sn-NTs-B	50	4.0	6.0	0.11	63.0	99.0	63.0	[178]
MP-TaMCF	40	2.0	3.0	0.02	80.0	97.0	78.0	[176]
ZrMo/KIT-6(5–700)	50	8.0	4.0	0.01	85.8	97.8	84.0	[172]
CS-MCF	40	2.0	3.0	0.02	87.0	99.0	86.0	[177]
WO_X/MCM-41–20%-L	50	6.0	2.0	0.10	NR	NR	87.7	[168]
6.8 V	60	6.5	1.0	0.11	92.0	98.0	91.0	[166]
Al (TF)-MS	50	7.5	4.0	0.10	93.0	100.0	93.0	[165]
Nb-SBA-15	RT	3.0	1.0	0.11	95.0	100.0	95.0	[170]
40MoPO/SBA-15	RT	3.0	1.0	0.05	100.0	98.0	98.0	[169]

RT, room temperature; A/G, acetone/glycerol molar ratio; m_c/m_{gly}, catalyst/glycerol molar ratio; X, glycerol conversion; S_s, selectivity towards solketal; Y_s, yield of solketal.

3.8.2. Glycerol Esterification with Acetic Acid

The incorporation of acid groups into a silica matrix has been shown to generate solids with high acidic strength, high specific surface area and narrow pore size distribution with high accessibility to the active sites. Therefore, this method has become the most widely employed technique for the synthesis of active solids in the esterification reaction of glycerol with acetic acid.

In this sense, Melero et al. functionalized an SBA-15 silica support with different acids: propyl sulfonic acid (Pr-SBA-15), arenesulfonic acid (Ar-SBA-15) and 1,2,2-trifluoro-2-hydroxy-1-trifluoromethylethane-sulfonic acid (F-SBA-15). The best results were obtained for the solid Ar-SBA-15, and the authors attributed this behavior to the higher acid strength presented by this catalyst with respect to the others [179].

In turn, using the sol–gel method, Dalla Costa et al. synthesized a mesoporous propylmercapto silica (Pr-SH-SBA-15), which was then acidified with a 1 M H_2SO_4 solution for 2 h. When this solid was compared with commercial zeolites (H-ZSM-5 and H-Beta), the authors reported that the silica presented a better performance, attributing these results to the higher density and strength of the acid sites of the synthesized solid [86].

Popova et al. synthesized SBA-15 and SBA-16, which were functionalized by employing 3-mercaptopropyl trimethoxysilane dispersed in toluene and subsequently oxidized with H_2O_2 to generate -SO_3H groups (solids SBA-15SO_3H and SBA-16SO_3H). The best results were obtained for the SBA-15SO_3H solid, and the researchers attributed these results to the higher availability of pores with accessible channels for the reagents and a good site density [180].

Similarly, Tonutti et al. synthesized various silica-based solids by mixing TEOS with 3-mercaptopropyl trimethoxysilane in different proportions and subsequently oxidized them with H_2O_2 to generate -SO_3H groups (solids SBA-15, SBA-16, MCM-41 and MCM-48).

Solid SBA-15 was the most active one, and the authors attributed this behavior to the high density of acid sites generated in this solid [181].

Alternatively, Manurung et al. synthesized a solid from bamboo leaves, which were calcined and subjected to a process of silicon extraction from the ashes with NaOH. Subsequently, HCl was added dropwise to generate a hydrogel. The solid thus obtained was functionalized with H_3PO_4, with a SiO_2-H_3PO_4 molar ratio of 1:2, 1:3 and 1:4. The best results were obtained for the solid prepared with a SiO_2/H_3PO_4 molar ratio of 2, reaching a glycerol conversion of 100%, with a selectivity towards TAG of 22.8%, after 4 h of reaction, with an AA/G molar ratio of 9 and using 5 wt.% of the catalyst with respect to glycerol [182].

With the aim of favoring the oxidation of the thiol groups to sulfonic groups, Trejda synthesized SBA-15 with the incorporation of Nb as ammonium niobate (V) oxalate during the preparation of the solid, with TEOS/Nb molar ratios of 64 and 32. Subsequently, these solids were functionalized with 3-mercaptopropyl trimethoxysilane (MPTMS) with Si/MPTMS ratios of 1, 5 and 10 and then oxidized via treatment with H_2O_2. The authors reported that an excess of MPTMS during the synthesis failed to increase the number of acid sites, but that the incorporation of Nb allowed them to favor the oxidation of the existing groups towards sulfonic groups, compared to SBA-15 without Nb incorporated. In any case, the variation in the amount of Nb also failed to significantly improve the activity of the solid, so that, with a Si/MPTMS and TEOS/Nb ratio of 1 and 32 (MP(1)/NbSBA-15-32), respectively, a glycerol conversion of 94% was achieved, with a selectivity towards MAG of 11%, towards DAG of 52% and towards TAG of 37%, after 4 h of reaction, at 150 °C, a ratio AA/G = 9 and an amount of catalyst of 4 wt.% with respect to glycerol [183].

On the other hand, Khayoon et al. synthesized a Y-incorporated SBA-3 by adding $Y(NO_3)_3 \cdot 6H_2O$ during the preparation of the material, at a Y/SBA-3 mass ratio of between 1 and 3.5 wt.%. The best results were obtained for the 3%Y/SBA-3 solid, achieving 100% glycerol conversion, with a selectivity towards MAG of 11%, towards DAG of 34% and towards TAG of 55%, after 2.5 h, at 110 °C, with a molar ratio AA/G = 4 and a 4 wt.% of catalyst with respect to glycerol. The authors attributed these results to the high acid strength and high specific surface area of the catalyst, combined with a large pore size that facilitated the accessibility of reactants and products to the active sites [184].

Table 18 summarizes the best results obtained with silica-based solids in the esterification reaction of glycerol with acetic acid.

Table 18. Silica-based solids used as catalysts in glycerol esterification with acetic acid.

Catalyst	T (°C)	AA/G	t (h)	m_c/m_{gly}	X (%)	S_{MAG} (%)	S_{DAG} (%)	S_{TAG} (%)	Ref.
Ar-SBA-15	125	9.0	4.0	0.04	90.0	15.0	45.0	40.0	[179]
MP(1)/NbSBA-15-32	150	9.0	4.0	0.04	94.0	11.0	52.0	37.0	[183]
Pr-SH-SBA-15	120	6.0	2.5	0.04	98.0	13.0	55.0	32.0	[86]
SBA-15	120	6.0	6.5	0.05	100.0	21.0	60.0	19.0	[181]
SBA-15SO_3H	130	5.0	3.0	0.025	100.0	21.3	57.2	21.5	[180]
SiO_2-H_3PO_4 1:2	NR	9.0	4.0	0.05	100.0	NR	NR	22.8	[182]
3%Y/SBA-3	110	4.0	2.5	0.04	100.0	11.0	34.0	55.0	[184]

AA/G, acetic acid/glycerol molar ratio; m_c/m_{gly}, catalyst/glycerol mass ratio; X, glycerol conversion; $S_{MAG/DAG/TAG}$, selectivity towards MAG/DAG/TAG; NR, not reported.

3.9. Clays

Many of the clay minerals exhibit a high ion exchange capacity, making them versatile materials that can be modified to acquire specific catalytic properties. In particular, the cation exchange of interlaminar ions (Na^+, Ca^{+2}, K^+, etc.) for protons (H^+) gives them acidic properties that make them capable of catalyzing glycerol esterification and ketalization reactions, as discussed in this section.

3.9.1. Glycerol Ketalization with Acetone

Most authors have used commercial montmorillonite K-10 in the synthesis of solketal, which is industrially synthesized using a calcination process and a subsequent treatment with mineral acid [73,74,80]. The best results were reported by da Silva et al., who obtained a solketal yield of 80% after 40 min of reaction at 70 °C, using a molar ratio A/G = 1.2 and 60 wt.% catalyst with respect to glycerol [80].

Other authors modified montmorillonite via treatment with nitric acid, with the aim of conferring acidity through the exchange of interlamellar ions for acid protons. Following this idea, Timofeeva et al. studied the effect of HNO_3 concentration (0.125–3 M) on the activity of clays modified to obtain solketal. Catalysts treated with HNO_3 from 0.125 to 1 M presented a glycerol conversion in the range of 39–57% due to the Brønsted sites generated by the acid treatment. Higher concentrations of HNO_3 did not allow for the catalyst activity to be increased, and this result was attributed to the leaching of aluminum from the clay structure and the lack of generation of new sites. In all cases, the selectivity towards solketal was higher than 97% [185].

As an alternative to the use of HNO_3, Alali et al. acidified montmorillonites with HCl to impart acidic properties. In their study, the effect of the acid concentration and acidification time on the catalytic properties of the materials was evaluated. The synthesized solids were named AL1 (0.5 M, 2 h), AL2 (0.5 M, 6 h), AL3 (3 M, 2 h) and AL4 (3 M, 6 h). After 48 h of reaction, the order of activity with respect to the yield of solketal was as follows: AL1 > AL2 > AL3 > AL4, which was attributed to the loss of the structure of the clays through treatment at for long amounts of time and at high HCl concentrations [186].

The use of acidified clays as catalysts presents certain operational drawbacks associated with the presence of water in the reaction medium since montmorillonites generate colloidal suspensions in aqueous media, thus making their separation difficult. For this reason, the synthesis of composite materials, including montmorillonite, has been reported in order to facilitate the activation process and the subsequent separation from the reaction medium. In this sense, Perez et al. synthesized a silica–resin–bentonite composite, which was subsequently activated with HNO_3 of varying concentrations (0.15–0.5 M) and at different temperatures (30–90 °C). The authors reported that the incorporation of montmorillonite into the silica–resin matrix substantially improves the separation capacity in aqueous media, avoiding the formation of colloidal suspensions without modifying the clay properties. In addition, increasing the acidification temperature and acid concentration generates a higher number of sites, reaching values similar to those of natural clay [18,187].

Table 19 summarizes the results obtained by the different authors.

Table 19. Clays used as catalysts in glycerol ketalization with acetone.

Catalyst	T (°C)	A/G	t (h)	m_c/m_{gly}	X (%)	S_S (%)	Y_S (%)	Ref.
0.5 M MM	50	2.5	0.5	0.03	57.0	97.7	56.0	[185]
Montmorillonite K-10	70	1.2	0.6	0.60	80.0	100.0	80.0	[80]
AL1	40	4.0	48.0	0.04	NR	NR	92.0	[186]
CB-0.5-90	60	6.0	4.0	0.0025	80.0	98.0	78.4	[18]

RT, room temperature; A/G, acetone/glycerol molar ratio; mc/mgly, catalyst/glycerol molar ratio; X, glycerol conversion; Ss, selectivity towards solketal; Ys, yield of solketal; NR, not reported.

3.9.2. Glycerol Esterification with Acetic Acid

Venkatesha et al. were among the first authors to report the use of activated clays as catalysts in the esterification reaction of glycerol with acetic acid. In their work, montmorillonite-type clays were treated with 1 M solutions of methanesulfonic acid (MSA), p-toluenesulfonic acid (p-TSA) and peroxydisulfuric acid (PDSA). The treatment of the clays with organic acids modified their acidic and textural properties due to the partial removal of octahedral cations and the formation of soluble complexes, which hydrolyze in the interlaminar space. In this way, the authors observed better yields to TAG if the clays were treated with PDSA and observed that, as the acid concentration increased, the volumetric parameter of accessibility increased (calculated as the product between the volume of micropores and the pore size) due to the removal of Al^{+3} ions, which favored TAG formation [52].

For their part, Tangestanifard et al. treated a bentonite-type clay with HCl, then with benzyl alcohol and finally with chlorosulfonic acid, with the aim of forming acidic arenesulfonic groups. The authors studied the reaction variables by using toluene as the solvent, achieving a glycerol conversion of 100%, with a selectivity towards DAG of 26% and towards TAG of 74% [188].

Table 20 summarizes the best results using clays in the esterification of glycerol with acetic acid.

Table 20. Clays used as catalysts in glycerol esterification with acetic acid.

Catalyst	T (°C)	AA/G	t (h)	m_c/m_{gly}	X (%)	S_{MAG} (%)	S_{DAG} (%)	S_{TAG} (%)	Ref.
PDSA-Clay	120	3.0	1.0	0.54	96.0	14.0	26.0	56.0	[52]
AS-BEN	100	7.0	3.0	0.074	100.0	0.0	26.0	74.0	[188]

AA/G, acetic acid/glycerol molar ratio; m_c/m_{gly}, catalyst/glycerol mass ratio; X, glycerol conversion; $S_{MAG/DAG/TAG}$, selectivity towards MAG/DAG/TAG.

3.10. Other Catalysts

This section describes some solids used as catalysts in glycerol ketalization and esterification reactions which do not fall into any of the above categories.

3.10.1. Glycerol Ketalization with Acetone

Other solids employed in the acetone-based ketalization of glycerol are based on mixed oxides [189–193], spinels [194], transition metal nanotubes [195,196], metal–organic frameworks (MOFs) [197,198] and aluminum-borate solids [199].

As for mixed oxides, it has been reported that pure TiO_2 or pure SiO_2 present only Lewis sites, but the combination of both generates Ti-O-Si bonds, leading to the formation of Brønsted sites, so this type of solid can provide Lewis and Brønsted sites simultaneously. They have been reported to be used in reactions requiring acid sites, such as dehydration and isomerization reactions. Following this idea, Chun-Ni Fan et al. synthesized TiO_2-ySiO_2 type sol–gel solids, where y represents the Si/Ti molar ratio. For the same calcination temperature, increasing y from 0.33 to 1 led to an increase in acid sites due to the increase in the number of Ti-O-Si bonds. A higher ratio of y decreased the number of sites. The TiO_2-1SiO_2 solid was calcined at different temperatures and evaluated in the solketal synthesis reaction, finding that, at a temperature of 550 °C, the highest number of sites and, consequently, the highest glycerol conversion were obtained [189].

Mallesham et al. synthesized MoO_3-SnO_2- and WO_3-SnO_2-type solids by using the incipient wetting impregnation method. The addition of MoO_3 and WO_3 to SnO_2 oxide led to higher glycerol conversions due to an increase in the specific surface area and the number of acid sites in the solids. The most active catalyst proved to be MoO_3 [191]. Similar results were obtained by Souza et al., who synthesized catalysts from $NbCl_5$ as the precursor, modifying the surface with surfactant groups to achieve hydrophobicity. By adding NH_4OH for 12 h (S4 catalyst) or 48 h (S4-2D catalyst), they were able to precipitate solids that were contrasted with a catalyst without the addition of surfactants (S4-SS catalyst). Of all the materials, the S4-2D catalyst presented the highest activity due to its high specific surface area and number of sites [190].

Similar solids based on Nb_2O_5/Al_2O_3 were synthesized by Rodrigues et al., using the sol–gel method, varying the Al/Nb ratio (1, 0.6, 0.3, 0.1 and 0.05). These catalysts presented Lewis acidity due to the strong polarization of the Nb=O bond and Brønsted acidity due to the polarization of the surface -OH groups in the O-Nb-OH bonds. In addition, the Nb-OH-Al bonds of the mixed oxide contributed to the Brønsted acidity. The catalysts containing a higher amount of aluminum presented a higher specific surface area and higher number of acid sites. However, their activity was lower than the rest of the catalysts. This behavior was attributed to the higher water adsorption capacity of the solids due to the high aluminum content, which decreased their performance. On the contrary, those catalysts with low aluminum content presented better activity in solketal synthesis due to the higher hydrophobicity and water resistance. In addition, the Nb_2O_5 solid without an aluminum addition presented lower activity than the Al-containing solids. The 1Nb:0.05Al catalyst achieved 84% glycerol conversion and 98% selectivity towards solketal [192].

Recently, Shen et al. synthesized catalysts formed by a highly ordered mesoporous SnO_2 support with supported WO_x. The authors showed that the catalyst containing 20 wt.% WO_x proved to be the most active one (WO_x/SnO_2), attributing this result to the high dispersion of WO_x, leading to a higher acidity of the catalyst [193].

Regarding the use of spinels, Li et al. synthesized Co-Al structures of the $Co[II](Co[III]_x Al_{2-x})O_4$ type with different Co/Al contents, yielding the following catalysts: $Co[II](Co[III]_{0.5} Al_{1.5})O_4$, $Co[II](Co[III]_1 Al_1)O_4$, $Co[II](Co[III]_{1.25} Al_{0.75})O_4$ and $Co[II](Co[III]_{1.4} Al_{0.6})O_4$. The results showed that increasing the Co/Al ratio up to 1.25/0.75 increased the glycerol conversion due to the increase in the number of strong acid sites. However, further increasing the Co/Al ratio led to a decrease in conversion due to a decrease in the number of strong acid sites. The best results were obtained with the $Co[II](Co[III]_{1.25} Al_{0.75})O_4$ catalyst, which achieved 69.2% glycerol conversion, with 98.6% selectivity towards solketal [194].

The use of transition metal nanotubes has also been explored in the literature. Carvalho et al. synthesized titanate nanotubes (TNTs) from TiO_2 in its anatase form, varying the hydrothermal treatment time (24, 48 or 72 h). These solids were named NaTNT24, NaTNT48 and NaTNT72 and showed no activity, a result that was attributed to the weak site strength and low structure stability of the solids. Subsequently, these materials were acidified with HCl. The solids thus treated were named HTNT24, HTNT48 and HTNT72. Of these, HTNT72 proved to be the most active one due to a larger mesopore diameter and the presence of a higher density of acid sites [200]. Following their study, the same authors incorporated Co, Ni and Pt into the NaTNT24 material. The synthesized solids were named CTNT, NTNT and PTNT, obtaining the following reaction order: PTNT > NTNT > CTNT. This behavior was attributed to the higher number of acid sites present in the PTNT solid and its higher accessibility [195].

Pinheiro et al. synthesized vanadium nanotubes (VOx-NTs) in which they incorporated different metals (MVOx-NTs, M = Ni, Co and Pt). The results showed that, at 50 °C, the VOx-NTs and NiVOx-NTs catalysts presented higher activity due to the higher stability of the structure. The low activity of CoVOx-NTs and PtVOx-NTs catalysts was attributed to the high percentage of micropores and the phenomenon of metal leaching during the reaction. At 110 °C, all catalysts showed low activity due to the collapse of the porous structure. The VOx-NT catalyst achieved 76.2% glycerol conversion, along with a selectivity towards solketal of 46.2% [196].

Regarding MOFs, Bakuru et al. synthesized organic structures with Zr, Ce and Hf as metals, solids named UiO-66 (Zr), UiO-66 (Ce) and UiO-66 (Hf), respectively. The UiO-66 family of MOFs presented a high specific surface area and large pore size, in addition to Brønsted acidity, obtaining the following order of activity: UiO-66 (Hf) > UiO-66 (Ce) > UiO-66 (Zr). This trend was attributed to the higher acidity of the more active solids due to a higher dissociation energy of the M-O bond for Hf than for the rest of the metals, resulting in a higher Brønsted acidity. The solid UiO-66 (Hf) achieved a glycerol conversion of 94.5%, with a solketal selectivity of 97.2% [197].

Furthermore, Timofeeva et al. synthesized MIL-type MOFs (100, 53 and 47) to which a metal was incorporated (M = V^{+3}, Al^{+3}, Fe^{+3}, Cr^{+3} and V/Al) and evaluated in the synthesis of solketal, using acetonitrile as the solvent. The results showed a decrease in glycerol conversion according to the following trend: $V^{+3} > Al^{+3} > Fe^{+3} > Cr^{+3}$. This behavior was attributed to the difference in surface acidity conferred by each metal and the interaction of the ions with the water molecules formed as a reaction product. Under optimum reaction conditions, the MIL-100-(V) solid led to 85.4% glycerol conversion with 97.7% selectivity [198].

Recently, Wang et al. synthesized Fe-promoted aluminum-borate solids (Fe-PKU-1). Boron is an element that has been reported as a spectator, but recently its catalytic activity in certain reactions, such as the hydrogenation of propane, was discovered [199]. Moreover, the incorporation of metals and nonmetals into catalysts can modify the electronic structure of boron, conf it with particular catalytic properties. In this sense, the authors synthesized solids with different crystalline structure by modifying the temperature and acidity of the preparation medium. The results showed that, if the surface boron composition is increased, the Fe-Bo bond is favored, facilitating the loss of electrons from Bo and increasing the Lewis-type acidity [199].

Table 21 summarizes the best results employing different acid solids in the reaction of glycerol ketalization with acetone.

Table 21. Other solids used as catalysts in glycerol ketalization with acetone.

Catalyst	T (°C)	A/G	t (h)	m_c/m_{gly}	X (%)	S_S (%)	Y_S (%)	Ref.
CO_2	115	2.0	4.2	NR	60.6	NR	NR	[63]
PTNT	50	4.0	6.0	NR	86.5	22.0	19.0	[195]
VO_x-NT	50	8.0	6.0	NR	76.2	46.2	35.2	[196]
HTNT72	50	1.0	6.0	NR	45.5	98.0	44.6	[200]
$Co[II](Co[III]_{1.25}Al_{0.75})O_4$	130	10.0	4.0	0.05	69.2	98.6	68.2	[194]
$MoSO_3$	RT	1.0	2.5	0.05	70.0	98.0	68.6	[191]
1Nb:0.05Al	50	4.0	6.0	0.027	84.0	98.0	82.0	[192]
MIL-100-(V)	25	4.0	1.5	0.002	85.0	98.0	83.0	[198]
S4-2D	70	4.0	1.0	NR	70.0	NR	85.0	[190]
TiO_2-1SiO_2	90	4.0	3.0	0.022	95.0	90.0	85.5	[189]
UiO-66 (Hf)	RT	4.0	1.0	0.1	94.5	97.2	92.0	[197]
WO_x/ SnO_2	20	30.0	2.0	0.05	100.0	97.4	97.4	[193]
Fe-PKU-1-(3)	45	8.0	3.0	0.05	97.0	99.0	96.0	[199]

RT, room temperature; A/G, acetone/glycerol molar ratio; m_c/m_{gly}, catalyst/glycerol molar ratio; X, glycerol conversion; S_s, selectivity towards solketal; Y_s, yield of solketal, NR, not reported.

3.10.2. Glycerol Esterification with Acetic Acid

In the case of glycerol esterification, mainly salts [48], mixed oxides [56,191,201] and coordination complexes [202,203] have been employed.

Regarding the use of salts, Troncea et al. synthesized partially hydrolyzed MgF_2 by employing a solution of HF and Mg solutions in methanol in the range 40–87 wt.%. The solids, named MgF_2-x, where x represents the percentage of HF, presented a number of interesting properties for application in catalysis, such as high specific surface area with mesoporosity, low solubility in polar solvents, and Lewis and Brønsted acid sites of medium acidity. In this case, the authors concluded that, as the HF concentration increases, the Lewis/ Brønsted ratio increases, leading to higher levels of conversion and selectivity towards the most substituted products so that the most active catalyst turned out to be the so-called MgF_2-87 [48].

Regarding the use of oxides, Hu et al. evaluated the catalytic activity of Bi_2O_3, Sb_2O_3, SnO_2, TiO_2, Nb_2O_5 and Sb_2O_5 in the glycerol esterification reaction. Of all of them, Sb_2O_5 presented a remarkable activity compared to the rest, and the researchers attributed this behavior to the presence of strong Lewis and Brønsted acid sites, which were detected through pyridine FTIR analysis. The Sb_2O_5 sample presented sites capable of adsorbing pyridine, while the Sb_2O_3, SnO_2, TiO_2 and Nb_2O_5 oxides presented sites capable only of coordinating to pyridine. In contrast, the Bi_2O_3 oxide did not present any signal indicating the presence of pyridine adsorbed or coordinated on acid sites [201].

Alves et al. also synthesized binary oxides of different natures by using the coprecipitation method, using Ti, Zr, Si and Al (ZrAlA, TiAlA, ZrSiA, TiSiA and SiAlA). Then, these solids were calcined (ZrAlC, TiAlC, ZrSiC, TiSiC and SiAlC solids), and the SiAlA solid underwent an extraction process to remove the surfactant CTAB (cetyltrimethylammonium bromide) used in the synthesis process (SiAlE solid). Finally, the above process was repeated under reflux (solid SiAlR). The best results were obtained for the SiAlR solid, reaching high selectivity towards TAG. These results were attributed to the combination of pores accessible to reagents and products, the stability of the structure and the high acidity [56].

In turn, Mallesham et al. synthesized SnO_2-based catalysts, incorporating into this oxide different promoters, such as WO_3 (WO_3/SnO_2), MoO_3 (MoO_3/SnO_2) and SO_4^{2-} (SO_4^{2-}/SnO_2). Of all of them, the solid SO_4^{2-}/SnO_2 presented higher activity than the rest due to the presence of a higher number and strength of acid sites [191].

Recently, Abida et al. synthesized catalysts with magnetic properties by coating Fe_2O_3 nanoparticles on silica by using the sol–gel method. Subsequently, the solid obtained was functionalized by wet impregnation with H_2SO_4, which generated SO_4^{2-} (solid $Fe_2O_3@SiO_2@SO_4^{2-}$) groups. The authors reported 100% selectivity towards TAG, and this result was attributed to the combination of high acidity with large pore size [203].

Regarding the use of coordination complexes, da Silva et al. employed a series of commercial catalysts based on Sn (IV) complexes, such as Bu_2SnCl_2, Me_2SnCl_2, $BuSnCl_3$, Bu_2SnLau_2, BuSnO(OH) and Bu_2SnO. Of all of them, the $BuSnCl_3$ catalyst led to the best results because, when the complex contains more alkyl ligands, the Lewis acidity decreases. For this reason, the other catalysts presented lower activity [202].

Similar results were obtained by Altino et al. when using commercial Sb complexes ($SbCl_5$ and $SbCl_3$). The best results were obtained using the $SbCl_5$ catalyst, due to its higher Lewis acidity. This is due to the fact that when the complex contains more Cl^- groups, the Sb center will have higher Lewis-type acidity, given the electronegativity of these substituents [204].

Table 22 shows the best results of the solids used for the esterification of glycerol with acetic acid discussed in this section.

Table 22. Other solids used as catalysts in glycerol esterification with acetic acid.

Catalyst	T (°C)	AA/G	t (h)	m_c/m_{gly}	X (%)	S_{MAG} (%)	S_{DAG} (%)	S_{TAG} (%)	Ref.
SiAlR	80	3.0	20.0	NR	35.0	0.0	0.0	100.0	[56]
$Fe_2O_3@SiO_2@SO_4^{2-}$	80	6.0	1.0	0.05	90.0	0.0	0.0	100.0	[203]
MgF_2-87	100	3.0	22.0	0.028	94.2	0.0	94.3 *		[48]
Sb_2O_5	120	6.0	6.0	0.022	99.0	30.0	55.0	15.0	[201]
$SbCl_5$	40	5.0	3.0	0.042	100.0	50.0	30.0	20.0	[204]
$BuSnCl_3$	80	4.0	3.0	NR	100.0	25.7	43.5	30.8	[202]
SO_4^{2-}/SnO_2	100	9.0	10.0	0.05	100.0	20.0	25.0	55.0	[191]

AA/G, acetic acid/glycerol molar ratio; m_c/m_{gly}, catalyst/glycerol mass ratio; X, glycerol conversion; $S_{MAG/DAG/TAG}$, selectivity towards MAG/DAG/TAG; (*) selectivity towards (DAG + TAG).

The general characteristics of solid catalysts necessary to achieve good yields for the desired products in both reactions (solketal and acetylglycerols) result from the combination of a high density of acid sites with large pore sizes. The high density of acid sites should combine a high number of acid sites and a high specific surface area.

Of all the heterogeneous catalysts studied in glycerol ketalization with acetone, the ones with the highest activity are zeolites, exchange resins and functionalized carbons, achieving glycerol conversions higher than 90%, with selectivity towards solketal higher than 95% in most cases.

In the case of glycerol esterification with acetic acid, the heterogeneous catalysts that showed the highest activity and selectivity towards the most substituted products (DAG and TAG) were functionalized carbons, clays and sulfonated zirconia, allowing complete glycerol conversions with TAG selectivity values higher than 90%.

4. Stability and Reuse of Catalysts

The study of the stability of catalysts is of utmost importance to evaluate their possible technological application at industrial level. There are different mechanisms through which catalysts can lose activity, such as adsorption of reactants and/or products on the active sites, leaching of the active phase, loss of specific surface area, etc.

Most authors have carried out the reactions in batch reactors, so that they have evaluated the reusability of the catalysts by subjecting them to successive reaction cycles, separating the solid from the liquid medium after each use. In some cases, the solids were subjected to solvent washing or heat treatments between each cycle.

The main deactivation mechanisms reported for the different catalysts are briefly described below.

4.1. Glycerol Ketalization with Acetone

With respect to the reaction of glycerol ketalization with acetone, various solids have been shown to be stable after several reaction cycles. Table 23 summarizes the catalysts that have been stable and the number of reaction cycles at which they have been evaluated.

Table 23. Catalysts that were stable in the glycerol ketalization reaction with acetone.

Catalyst	**RC**	**T (°C)**	**A/G**	**t (h)**	**m_c/m_{gly}**	**X (%)**	**S_S (%)**	**Y_S (%)**	**Ref.**
0.5 M MM	3	50	2.5	0.5	0.03	57.0	97.7	56.0	[185]
Co[II](Co[III]$_{1.25}$Al$_{0.75}$)O$_4$	5	130	10.0	4.0	0.05	69.2	98.6	68.2	[194]
1Nb:0.05Al	4	50	4.0	6.0	0.027	84.0	98.0	82.0	[192]
ZrMo/KIT-6(5-700)	5	50	8.0	4.0	0.01	85.8	97.8	84.0	[172]
S4-2D	3	70	4.0	1.0	NR	70.0	NR	85.0	[190]
UiO-66 (Hf)	3	RT	4.0	1.0	0.1	94.5	97.2	92.0	[197]
PW-S	4	70	6.0	2.0	0.05	95.0	97.0	92.1	[145]
30% Cs$_{2.5}$/KIT-6	3	70	6.0	25	0.05	95.0	98.0	93.1	[146]
Fe-PKU-1-(3)	5	45	8.0	3.0	0.05	97.0	99.0	96.0	[199]
5%Ni–1%Zr/AC	4	55	8.0	3.0	0.04	100.0	100.0	100.0	[135]

NR, not reported; A/G, acetone/glycerol molar ratio; m_c/m_{gly}, catalyst/glycerol mass ratio; X, glycerol conversion; S_S, selectivity towards solketal; Y_S, yield of solketal; RC, number of reaction cycles.

For other catalytic systems, however, the loss of activity due to different deactivation mechanisms has been reported.

In this sense, the loss of activity due to adsorption of reactants and/or products on the catalyst surface has been reported. Solids that have experienced this type of deactivation are BEA-type zeolites [205], transition-metal-ion-promoted mordenite [46], Amberlyst-46 resin [93], Sn embedded in 1D silica-based tubular nanostructures [178], mesoporous molybdenum dioxide [206] and functionalized carbons [120,121,132]. With respect to the functionalized carbons, the loss of activity has been attributed to the formation of bonds between the -OH group of the glycerol and the -COOH and -SO$_3$H groups present on the carbonaceous supports [120,121,132].

In some cases, the loss of activity has been attributed to the adsorption of water formed during the reaction onto the active sites. The catalysts shown to be affected by water are the commercial catalyst Polymax 845 [207], Montmorillonite K-10 [74], zeolite H-BETA [74] and V supported on MCM-41 [166].

Other authors have reported loss of activity due to modifications of the specific surface area and pore size of the solids, as in the case of titanate nanotubes [200].

Finally, the leaching of active sites has also been reported as a deactivation mechanism, as is the case of $(MoO_2)_2P_2O_7$ supported on SBA-15 [169], synthetic polymers functionalized with -SO$_3$H groups [98] and vanadium catalysts supported on MCM-41 [166].

4.2. Glycerol Esterification with Acetic Acid

With respect to the esterification reaction of glycerol with acetic acid, the solids that have been shown to be stable after several reaction cycles are shown in Table 24.

Table 24. Catalysts that were stable in the glycerol esterification reaction with acetic acid.

Catalyst	RC	T (°C)	AA/G	t (h)	m_c/m_{gly}	X (%)	S_{MAG} (%)	S_{DAG} (%)	S_{TAG} (%)	Ref.
SO_4^{2-}/WZr (1:1)-500	5	120	10.0	4.0	0.01	100.0	37.0	60.0	3.0	[141]
KJ-400	5	120	5.0	4.0	0.08	90.0	56.0	40.0	4.0	[126]
Wastewater	5	120	6.0	6.0	0.16	90.8	46.9	48.4	6.3	[128]
TPA_3/MCM-41	4	100	6.0	6.0	NR	92.0	20.0	70.0	10.0	[155]
Glycerol carbon	5	115	4.0	1.0	0.05	100.0	20.0	70.0	10.0	[119]
Sb_2O_5	6	120	6.0	2.0	0.022	99.0	30.0	55.0	15.0	[201]
$[(HSO_3\text{-p})_2\text{im}][HSO_4]$	5	100	5.0	1.0	0.002	95.7	32.8	52.1	15.1	[69]
C-glycerol	6	110	6.0	24.0	0.10	96.0	26.0	56.0	18.0	[130]
12ZrKIL-2	3	100	10.0	1.0	0.05	100.0	2.7	77.2	20.1	[87]
$C_{SBA\text{-}15}$-BDS	4	110	6.0	24.0	0.09	98.0	16.0	54.0	30.0	[117]
[H-NMP][HSO_4]	4	100	6.0	0.5	0.106	99.0	12.0	58.0	30.0	[70]
Ag_1PW	5	120	10.0	0.15	0.01	100.0	10.0	60.0	30.0	[162]
HSiW/ZrO_2	4	120	10.0	4.0	0.06	100.0	6.4	61.3	32.3	[55]
Dowex 650C	5	120	9.0	4.0	0.04	99.6	16.0	50.0	34.0	[106]
PDS-THF	5	110	6.0	3.0	0.05	97.8	11.4	54.0	34.6	[110]
Willow charcoal	6	120	5.0	5.0	0.07	98.0	5.0	50.0	45.0	[127]
$[BS_2TMEDA]HPW_{12}O_{40}$	4	120	7	8	0.06	100	1	28.1	70.9	[71]
AS-BEN	5	100	7.0	3.0	0.074	100.0	0.0	26.0	74.0	[188]
50-HPA/HNT	3	80	9.0	5.0	NR	38.0	NR	NR	98.0	[158]

AA/G, acetic acid/glycerol molar ratio; m_c/m_{gly}, catalyst/glycerol mass ratio; X, glycerol conversion; $S_{MAG/DAG/TAG}$, selectivity towards MAG/DAG/TAG; RC, number of reaction cycles.

Regarding the loss of activity observed in solids, some authors associated the deactivation with the blocking of active sites by the adsorption of reagents and/or products, as is the case of carbons functionalized with H_2SO_4 [154], sulfated γ-Al_2O_3 [208], Amberlyst-70 and -15 resins [49] and silica functionalized with propylsulfonic groups [86].

Other authors have attributed the loss of activity to the low thermal stability of some solids, such as Amberlyst-70 and 15 resins [49]. Since the esterification reaction of glycerol with acetic acid is generally carried out at temperatures above 100 °C, thermal stability turns out to be an important property when synthesizing stable catalysts.

Some solids have suffered attrition as a result of mechanical wear due to agitation during the reaction, such as Amberlyst-70 and -15 resins [49] and phenolic resins functionalized with sulfonic groups [109].

For their part, catalysts based on heteropolyacids immobilized on SBA-15 have undergone modifications of their textural properties with consecutive reaction cycles, leading to the loss of activity [154]

Finally, some authors have attributed the loss of activity to the leaching of active sites, as is the case of silica-supported heteropolyacids [160], sulfated zirconia [142], H_2SO_4-functionalized carbons [209] and Fe_3O_4-SiO_2 nanoparticles functionalized with sulfonic groups [203].

5. Kinetic Models

The development of kinetic expressions is especially important for the design of chemical reactors that are capable of carrying out the reactions of glycerol esterification and ketalization. In this sense, several authors have carried out kinetic studies by using a wide variety of acid catalysts, such as exchange resins, heteropolyacids supported on different supports, sulfated zirconia, etc.

5.1. Glycerol Ketalization with Acetone

Regarding the reaction of glycerol ketalization with acetone, several kinetic models have been proposed, such as the power law (PL) [66,76,210], pseudo-homogeneous model (PH) [42], Eley–Rideal (ER) model [91] and Langmuir–Hinshelwood–Hougen–Watson (LHHW) model [18,38,39].

Some authors have considered the power law to describe the reaction rate, employing various catalysts, such as zeolites [76], sulfuric acid [210] or ionic liquids [66].

Other authors, such as Vannucci et al., have proposed a pseudo-homogeneous model for the overall reaction rate, neglecting the adsorption of all species involved in the reaction, employing a sulfated zirconia [42].

Esteban et al. employed the Eley–Rideal model, using a Lewatit GF101 resin as the catalyst. In the model, they considered that acetone participates from the reaction medium, without adsorbing on the active sites of the catalyst [91].

As for the LHHW and ER models, different simplifications have been put forward with respect to the inhibitory term of the overall kinetic expression, depending on the catalyst employed. For example, Nanda et al. and Moreira et al. used Amberlyst-35 resin as a catalyst, for which they considered that water adsorbs preferentially on the solid due to the high adsorption capacity of the exchange resins [38,39]. On the other hand, Perez et al. used a silica–resin–bentonite composite material with a high affinity for polar compounds, so they proposed a kinetic model of LHHW where only the glycerol adsorption constant appears in the inhibitory term [18].

Table 25 summarizes the reported kinetic expressions and the catalysts used.

Table 25. Kinetic expressions reported in the glycerol ketalization reaction with acetone.

Model	Catalyst	Kinetic Expression	Reference
PL	HBEA	$r = k\,(C_G\,C_A – C_S\,C_W)$	[76]
PL	H_2SO_4	$r = k\,(C_G\,C_A - C_S\,C_W)$	[210]
PL	Ionic Liquid	$r = k\left(C_G\,C_A - \frac{C_S\,C_W}{K_{eq}}\right)$	[66]
PH	Sulfated zirconia	$r = k\left(a_G a_A - \frac{a_S a_W}{K_{eq}}\right)$	[42]
ER	Lewatit GF101	$r = \frac{k_1 – k_2\,C_S\,C_W}{1 + K_W C_W}$	[91]
LHHW	Amberlyst-35	$r = k\frac{C_G C_A - \frac{C_S\,C_W}{K_{eq} C_G}}{(1 + K_W C_W)^2}$	[38]
LHHW	Amberlyst-35	$r = k\frac{a_G\,a_A - \frac{a_S\,a_W}{K_{eq}}}{(1 + K_W a_W)^2}$	[39]
LHHW	CBA	$r = k\frac{C_G\,C_A - \frac{C_S\,C_W}{K_{eq}}}{(1 + K_G C_G)^2}$	[18]

5.2. Glycerol Esterification with Acetic Acid

With respect to the esterification reaction of glycerol with acetic acid, the kinetic expressions that have been reported correspond to power law (PL) [155,211,212], Langmuir–Hinshelwood (LHHW) [213,214], Eley–Rideal (ER) [215] and pseudo-homogeneous (PH) models [181].

With respect to the power law, Patel et al. employed heteropolyacids supported on MCM-41 and ZrO_2 as catalysts, concluding that the reaction rate follows a first-order dependence on glycerol [155]. Subsequently, Rane et al. employed a sulfated alumina (2 M $SO_4^{2-}/\gamma\text{-}Al_2O_3$) as catalyst, determining that the reaction rate follows a pseudo-second-order dependence on glycerol [211]. In turn, Veluturla et al. employed a partially Cs-exchanged heteropolyacid (CsPWA), from which they determined that each stage of the esterification reaction can be described by the power law with pseudo-first order for each compound involved [212].

Recently, Tonutti et al. adopted the pseudo-homogeneous model to describe the reaction kinetics, employing different functionalized mesoporous silicas, such as SBA-15, SBA-16, MCM-41 and MCM-48. The authors considered this model to simplify the study to avoid the over-parameterization of the system [181].

Reinoso et al. used a Dowex 650C resin and considered the Eley–Rideal model, in which both reagents diffuse to the catalyst surface, but only acetic acid adsorbs with glycerol participating from the liquid phase. The following reactions occur in the same way, with MAG and DAG participating from the liquid phase without adsorbing on the catalyst surface [215].

With respect to the LHHW model, Banu et al. used a Purolite CT-275 resin, for which they considered that the most strongly adsorbed compounds on the catalyst are water, glycerol and acetic acid, so that only these compounds are part of the inhibitory term of the equation [213]. In contrast, Keogh et al. neglected the adsorption of all compounds and even considered each reaction step to be irreversible due to the presence of excess acetic acid in the reaction medium. In their study, these authors used tungstophosphoric acid partially exchanged with Sn and supported on a K-10 montmorillonite (Sn1DTP/K-10) [214].

Table 26 summarizes the reported expressions and the catalysts used for their study.

Table 26. Kinetic expressions reported in the glycerol esterification reaction with acetic acid.

Kinetic Model	Catalyst	Kinetic Expression	Reference
PL	$TPA_3/MCM\text{-}41$ TPA_3/ZrO_2	$r = k\,C_G$	[155]
PL	$2\ M\ SO_4{}^{2-}/\gamma\text{-}Al_2O_3$	$r = k\,C_G{}^2$	[211]
PL	Amberlyst-35	$r_1 = k_1\,C_G$ $r_2 = k_1\,C_G - k_2\,C_{MAG}$ $r_3 = k_2\,C_{MAG} - k_3\,C_{TAG}$	[212]
PH	Functionalized Mesoporous silicas	$r_1 = k_1\left(C_G\,C_{AA} - \frac{C_{MAG}\,C_W}{K_{eq,1}}\right)$ $r_2 =$ $k_2\left(C_{MAG}\,C_{AA} - \frac{C_{DAG}\,C_W}{K_{eq,2}}\right)$ $r_3 =$ $k_3\left(C_{DAG}\,C_{AA} - \frac{C_{TAG}C_W}{K_{eq,3}}\right)$	[181]
ER	Dowex 650C	$r_1 = k_1\frac{C_G\,C_{AA} - \frac{C_{MAG}\,C_W}{K_{eq,1}}}{1 + K_WC_W + K_GC_G}$ $r_2 = k_2\frac{C_{MAG}\,C_{AA} - \frac{C_{DAG}\,C_W}{K_{eq,2}}}{1 + K_WC_W + K_GC_G}$ $r_3 = k_3\frac{C_{DAG}\,C_{AA} - \frac{C_{TAG}\,C_W}{K_{eq,3}}}{1 + K_WC_W + K_GC_G}$	[215]
LHHW	Purolite CT-275	$r_1 =$ $k_1\frac{a_G\,a_{AA} - \frac{a_{MAG}\,a_W}{K_{a,1}}}{(1 + K_Wa_W + K_Ga_G + K_{AA}a_{AA})^2}$ $r_2 =$ $k_2\frac{a_{MAG}\,a_{AA} - \frac{a_{DAG}\,a_W}{K_{a,2}}}{(1 + K_Wa_W + K_Ga_G + K_{AA}a_{AA})^2}$ $r_3 =$ $k_3\frac{a_{DAG}\,a_{AA} - \frac{a_{TAG}\,a_W}{K_{a,3}}}{(1 + K_Wa_W + K_Ga_G + K_{AA}a_{AA})^2}$	[213]
LHHW	$Sn_1DTP/K\text{-}10$	$r_1 = k_1C_GC_{AA}$ $r_2 = k_2C_{MAG}C_{AA}$ $r_3 = k_3C_{DAG}C_{AA}$	[214]

G, glycerol; AA, acetic acid; W, water; MAG, mono-acetylglycerol; DAG, di-acetylglycerol; TAG, tri-acetylglycerol.

6. Technological Aspects of the Ketalization and Esterification Reactions

From the process-engineering point of view, there are certain aspects to consider in order to carry out the ketalization and esterification reactions of glycerol on an industrial scale.

The first of these is the replacement of batch reactors by flow reactors that allow for the continuous production of solketal or acetylglycerols; this point is of vital importance if they are to be produced on a large scale.

The second aspect to take into account is the immiscibility of the reactive mixture in the case of ketalization, given by the low solubility of glycerol in acetone, which generates the presence of two phases in the reactor feed, hindering the transport phenomena of matter and energy to produce the chemical reaction.

The third and no less important aspect is the presence of water as a by-product of both reactions. Since both the ketalization and esterification reactions are reversible, the generation of water makes both reactions limited by thermodynamic equilibrium.

Finally, the use of crude glycerol as a starting feedstock is of vital importance if the glycerol obtained as a by-product of the biodiesel industry is to be revalued. Its impurities can play a fundamental role in the activity levels and quality of the products obtained in both reactions.

The aspects mentioned above are presented below for both reactions, and then the latest technological developments are discussed.

6.1. Continuous Flow Reactors

Continuous flow reactors are the most suitable reactors to carry out ketalization and esterification reactions in liquid phase if an industrial application is considered. Although different variants for continuous flow reactors have been reported, a general scheme is shown in Figure 10.

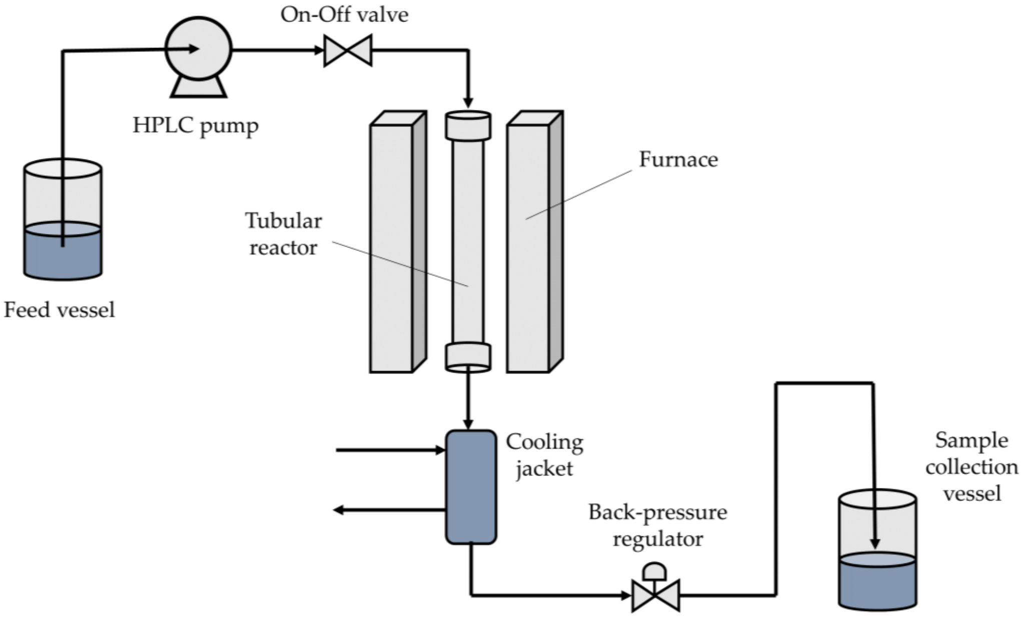

Figure 10. General scheme of the continuous process used in glycerol ketalization with acetone.

The implementation of these reactors allows for increases in the mass and energy transfer efficiency and facilitates scale-up, in addition to ensuring the constant quality of the product obtained [28]. In these reactors, the effect of the temperature, pressure, molar ratio of reagents and space velocity are the main variables to be taken into account, both for design and operation. Regarding the glycerol ketalization with acetone, several studies have been published, mainly using exchange resins and zeolites as catalysts.

Table 27 summarizes the catalysts employed in the glycerol ketalization reaction with acetone and the operating conditions under which they were employed, ordered in increasing order according to the yield obtained to solketal.

Table 27. Results of glycerol ketalization with acetone using continuous flow reactors.

Catalyst	T (°C)	P (MPa)	A/G	SV (h^{-1})	Solvent	X (%)	S_S (%)	Y_S (%)	Ref.
KU-2	70	NR	2.0	0.6	-	NR	NR	70.0	[216]
PD206	20	12	5.0	6.7	Ethanol	95.0	100.0	95.0	[217]
Amberlyst Wet	40	4.1	6.0	4.0	Ethanol	90.0	97.0	88.0	[207]
Amberlyst-15	50	0.1	20.0	6.9	Dimethylformamide	92.0	96.0	88.0	[218]
80LS20PS450H$^+$	30	0.1	8.0	7.2	Ethanol	90.0	99.5	89.6	[133]
PD206	41	4.2	5.0	50.7	Ethanol	NR	NR	NR	[219]
SO_3H-C	57	-	8.0	2.9	-	100.0	99.0	99.0	[220]
Hβ	50	0.1	3.0	11.9	Methanol	90.0	98.0	88.0	[75]

NR, not reported; A/G, acetone/glycerol molar ratio; SV, space velocity based on weight hourly space velocity (WHSV); X, glycerol conversion; S_S, selectivity towards solketal; Y_S, yield of solketal.

Marksimov et al. carried out the solketal synthesis reaction in a continuous process, using different catalysts, such as zeolites Hβ, mordenite and HY, a polymer F-4SF (analogous to the sulfonated polymer Nafion) and the sulfonated resin KU-2. The best results were obtained for the KU-2 catalyst, with a molar ratio A/G = 2, a temperature of 70 °C and a space velocity of 0.6 h^{-1}. However, the characteristics of the reactor used were not detailed [216].

Shirani et al. studied the solketal synthesis reaction in a continuous flow reactor, using a Purolite® PD206 resin as the catalyst. The reactor consisted of a 316 stainless steel tube, into which a mixture of acetone, glycerol and ethanol as cosolvent was fed, driven by an HPLC pump. As reaction variables, the catalyst mass, A/G molar ratio, temperature, pressure and feed flow rate were studied. The best activity results were found at 20 °C, 12 MPa and 6.7 h^{-1} of WHSV. The yield obtained under these conditions was 95%, with 100% selectivity towards solketal [217].

On the other hand, Nanda et al. carried out a study of the activity of different catalysts in the synthesis of solketal, such as Amberlyst 36 Wet and Dry resins, Zeolite beta in its acid form, montmorillonite K10, sulfated zirconia and Polymax 845 (an acid polymer). The experiments were carried out in a continuous 316 stainless steel reactor with downflow, heated by means of an oven. The mixture of glycerol, acetone and ethanol as solvent was pumped into the reactor by an HPLC pump. Under the same reaction conditions, the catalysts studied presented the following order of activity: Amberlyst Wet ≈ Zeolite ≈ Amberlyst Dry > sulfated zirconia > montmorillonite > Polymax. This behavior was mainly attributed to the higher number of acid sites possessed by the more active catalysts. The authors obtained the highest yield at solketal (88%) by carrying out the experiments using Amberlyst Wet as catalyst and the following reaction conditions: 40 °C, 4.1 MPa, WHSV = 4 h^{-1} and a molar ratio of A/G = 6 [207].

Olivera et al. studied the solketal synthesis reaction in a continuous reactor at atmospheric pressure. The experimental setup consisted of three packed columns with different volumes, which allowed the researchers to study the effect of catalyst mass. The operating variables studied were the flow rate (0.1–1 mL min^{-1}), temperature (30–50 °C), type of catalyst (Amberlyst 15 or montmorillonite K10), amount of catalyst (1–7 g), A/G molar ratio (2–20) and solvent used to homogenize the reactive mixture (dimethyl sulfoxide or dimethylformamide). The results showed that, in order to obtain the maximum glycerol conversion, the reaction should be carried out at 50 °C, A/G = 20, with a flow rate of 1 mL min^{-1}, an Amberlyst-15 catalyst mass of 7 g and dimethylformamide as solvent. Under these conditions, the glycerol conversion was 92%, with a selectivity towards solketal of 96% [218].

Konwar et al. carried out the ketalization reaction of glycerol with acetone in a Pyrex continuous reactor with a 0.5 g catalyst bed that was supported on both sides by a 1 mm glass bed column. The reagent mixture with ethanol as solvent was pumped with different flow rates by means of an HPLC pump, at different temperatures (30–50 °C) and different A/G molar ratios (6 and 8). The experiments were carried out at atmospheric pressure. As a catalyst, the authors synthesized sulfonated carbons from sodium lignosulfonate, which was subjected to pyrolysis at low temperature and acid exchange with H_2SO_4. The results showed that, so as to achieve the highest yield at solketal, one should operate at 30 °C, with A/G = 8 and a flow rate of 0.1 mL min^{-1}. Under these conditions, it is possible to achieve a glycerol conversion of 92%, with a selectivity towards solketal of 99.5% [133].

Aghbashlo et al. employed theoretical methods to optimize the operating variables of a continuous solketal synthesis reactor, with the objective of maximizing the exergy efficiency and minimizing the exergy destroyed. For this purpose, they also used experimental data, using a continuous reactor. The reactor consisted of a 316 stainless steel tube with a certain amount of catalyst (PD206 resin) inside that was mixed with Pyrex glass. The reagent mixture with ethanol as solvent was pumped by an HPLC pump. Different experiments were carried out by varying the temperature, pressure, A/G molar ratio, flow rate and amount of catalyst. The results showed that the flow rate had the greatest effect on the exergy efficiency, while the pressure had the least effect. The optimum conditions were as follows: 40.66 °C, 4.2 MPa, flow rate of 0.49 mL min^{-1}, A/G molar ratio of 4.97 and 0.5 g of catalyst. Under these conditions, the exergy efficiency was 90.36% [219].

Domínguez-Barroso et al. synthesized sulfonated carbons as catalysts by pyrolysis of cellulose with subsequent oxidation with HNO_3 and treatment with methanesulfonic acid. These solids were initially evaluated in a batch reactor in order to optimize the temperature, reaction time and A/G molar ratio. Subsequently, the reaction was carried out in a continuous downflow reactor, connected to distillation equipment. In this system, the effect of space velocity (WHSV = 2.9–8.9 h^{-1}) for a molar ratio A/G = 8 and a temperature of 57 °C was evaluated. The results showed that, for a WHSV = 2.9 h^{-1}, the complete conversion of glycerol with 99% selectivity towards solketal was achieved. An increase in the WHSV value led to a decrease in conversion because the residence time decreased [220].

Kowalska-Kuś et al. carried out the solketal synthesis reaction in a continuous downflow tubular reactor at atmospheric pressure, using H-ZSM5, Hβ and H-Mordenite zeolites as catalysts, which were mixed with SiO_2 to form the bed. In turn, the catalysts were subjected to treatment with NaOH to partially remove silicon and with citric acid to remove residual aluminum. The unmodified zeolites were named H-ZSM5 (P), Hβ (P) and H-Mordenite (P) and the modified zeolites were named H-ZSM5 (H), Hβ (H) and H-Mordenite (H). All catalysts were evaluated at 50 °C, 1 atm, a molar ratio A/G = 3 and a WHSV = 3.4 h^{-1}. As for the unmodified zeolites, it was observed that the Hβ (P) and H-Mordenite (P) solids exhibited high reaction activity, while the H-ZSM5 (P) solid led to low glycerol conversions. This was attributed to the small pore size of the ZSM5 zeolite, leading to diffusional problems. However, after being treated, the solid H-ZSM5 (H) presented a 90% conversion due to the generation of mesoporosity by the leaching of silicon and aluminum from the structure, while the solids Hβ (H) and H-Mordenite (H) did not significantly modify their activity. Subsequently, the effect of the increasing WHSV on productivity (kg solketal/kg catalyst h) was evaluated. The results showed that an increase in WHSV led to an increase in productivity [75].

Few authors have reported the study of the esterification reaction of glycerol with acetic acid in continuous processes. Most studies have focused on the reactive distillation process; they are referred to in the following sections. Rastegari et al. are the only ones who studied the esterification reaction of glycerol with acetic acid in a continuous process. These authors employed a Pyrex glass reactor, showing that the main operating variables were the AA/G molar ratio, temperature and feed flow rate. In addition, they used an HB zeolite as the catalyst, achieving a glycerol conversion of 26%, with a selectivity towards MAG of 91% [221].

6.2. Immiscibility of the Reagent Mixture

As previously explained, the glycerol ketalization reaction with acetone presents an operational complexity: glycerol is not fully soluble in acetone, so the reaction mixture turns out to be biphasic at the beginning. Rahamn et al. demonstrated that the low miscibility of acetone in glycerol causes a slow supply of acetone for solketal formation and that, when the glycerol conversion is above 30%, solketal acts as a solubilizer and the reaction mixture becomes homogeneous, followed by a rapid product formation. For this reason, it is advisable to carry out the reaction in the presence of excess acetone [83].

Figure 11 shows the glycerol–acetone–solketal phase equilibrium diagram that was obtained experimentally by Esteban et al. [222]. As can be observed, for the initial glycerol–acetone mixture to be totally soluble, the mole fraction of acetone should be approximately 0.9375, which is equivalent to a molar ratio A/G = 15. The authors also demonstrated that solubility is not significantly affected by temperature in the 30–50 °C range studied; therefore, the equilibrium diagram obtained at 40 °C is presented.

A molar ratio of A/G = 15 represents a significant excess of acetone with respect to glycerol, so it is important to study what effect the excess of acetone in the initial reaction mixture has on the achieved glycerol conversion in order to optimize the A/G molar ratio. In order to overcome these disadvantages, some authors have used different solvents.

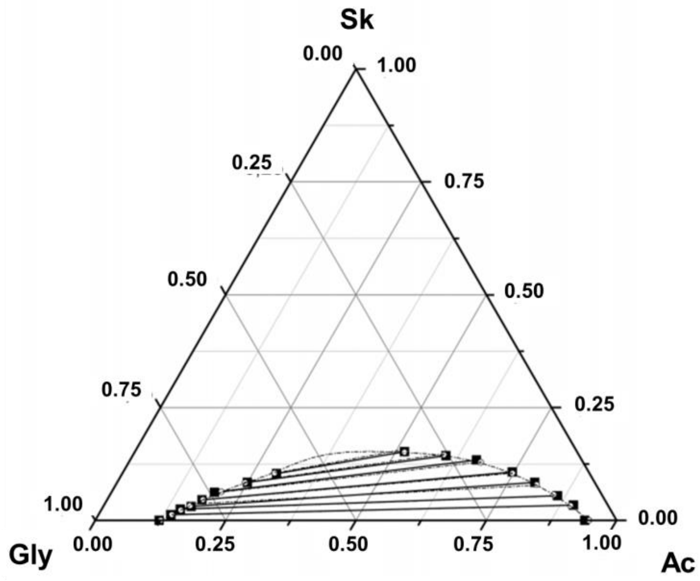

Figure 11. Solubility of the glycerol–acetone–solketal system at 40 °C, in mole fractions, reported by Esteban et al. [222]. Reprinted (adapted) with permission from J. Chem. Eng. Data 2014, 59, 9, 2850–2855. Copyright 2023 American Chemical Society.

In general, two types of polar solvents have been studied: protic and aprotic solvents. As protic solvents, the use of tert-butanol, methanol and ethanol was evaluated. Pescarmona et al. carried out the solketal synthesis reaction using tert-butanol as the solvent [44]. As catalysts, they used mesoporous silicates TUD-1 and MCM-41 substituted with different metals, such as Zr, Hf and Sn, conferring Lewis acidity. The synthesized solids were named Zr-TUD-1, Hf-TUD-1 and Sn-MCM-41, respectively. Under the same reaction conditions, the order of activity was as follows: Hf-TUD-1 > Zr-TUD-1 > Sn-MCM-41. This behavior was attributed to the high specific surface area, the relative hydrophobicity of the surface and the larger number of accessible sites in the more active solids. Under optimal reaction conditions, the Hf-TUD-1 catalyst achieved 52% glycerol conversion with 100% selectivity towards solketal.

Subsequently, the same authors synthesized Ga-MCM-41 in the form of nanoparticles (<150 nm) with different Ga content [167]. The solids with a higher content of the metal were named XS-Ga-MCM-41-H, and those with a lower content were subjected to ion exchange with NH_4OH and calcined to transform them into their protonated form (XS-Ga-MCM-41-L). It has been shown that other similar materials improved their catalytic properties due to the decrease in size at the nanoscale, which increased the specific surface area and decreased the pore length. The synthesized catalysts were evaluated in solketal synthesis by using tert-butanol as solvent. The results showed that, under the same reaction conditions, both catalysts showed the same conversion. However, the solid XS-Ga-MCM-41-L presented a higher TON value, which was due mostly to the presence of Brønsted sites.

Regarding the use of ethanol as a solvent, Dmitriev et al. [40] carried out the solketal synthesis reaction by screening different catalysts, such as beta zeolite, H_2SO_4 as a homogeneous catalyst and KU-2-8 and Amberlyst 35 dry-exchange resins, adjusting the mass of each so as to maintain the same number of acid sites in the reaction. Under the same conditions, the best results were obtained for H_2SO_4 and beta zeolite, which reached equilibrium after 50 min of reaction [40].

On the other hand, Moreira et al. studied the thermodynamics of the solketal synthesis reaction by using ethanol as solvent, after experimentally evaluating methanol and ethanol as protic solvents and dimethyl sulfoxide as aprotic solvent. In their study, they also evaluated the performance of different catalysts, such as Amberlyst 35, Amberlyst 15 and beta zeolite in its protonated form [39]. The combination of Amberlyst 35 resin with ethanol as a solvent led to higher glycerol conversions and selectivity towards solketal, so this combination was selected for the thermodynamic study. With respect to dimethyl sulfoxide, it led to lower conversions, which was attributed to its strong adsorption on the solid or possible limitation to matter transport.

Recently, Mahreni et al. synthesized solids based on a polymer called alginate, a polysaccharide that is present in the cell wall of brown seaweeds, precipitated by $FeCl_3$. The solid was named Fe-Alg and was used as a catalyst in the synthesis of solketal, using ethanol as solvent. As a result, a selectivity towards solketal of 56% was obtained, with no report of the glycerol conversion achieved [223].

With respect to the use of aprotic polar solvents, only a few articles have been published on the topic. In addition to the work of Moreira et al. described in the previous paragraph, the only reports so far correspond to Timofeeva et al., who used acetonitrile as solvent in two studies.

In their first work, they synthesized MIL-type MOFs (100, 53 and 47) to which a metal, M, was incorporated, where M = V^{+3}, Al^{+3}, Fe^{+3}, Cr^{+3} and V/Al, which were evaluated in solketal synthesis by using acetonitrile as a solvent [198]. According to the results obtained, it was concluded that the nature of the metal ion affects the catalytic activity of the catalyst. In general, glycerol conversion decreases according to the following order: $V^{+3} > Al^{+3} > Fe^{+3} > Cr^{+3}$. This behavior was attributed to the difference in surface acidity conferred by each metal and the difference in terms of the interaction of the ions with the water molecules formed as a reaction product. In addition, they studied the simultaneous incorporation of Al and V to the solid in different proportions, verifying that the addition of V in excess leads to better activity, and the activity is maximal when only V is added. Under optimal reaction conditions, the MIL-100-(V) solid led to 85.4% glycerol conversion with 97.7% selectivity.

Subsequently, the same authors acidified bentonites with HNO_3 for subsequent use as catalysts in solketal synthesis, using acetonitrile as solvent [185]. In their study, they evaluated the effect of HNO_3 concentration (0.125–3 M) on the activity of the catalysts. Under the same reaction conditions, catalysts treated with HNO_3 from 0.125 to 0.5 M led to an increase in glycerol conversion from 62% to 94%, respectively, which was attributed to the higher number of Brønsted sites generated by the acid treatment. Higher concentrations of HNO_3 failed to increase catalyst activity, and this result was attributed to aluminum leaching from the clay structure and the lack of new site generation. In all cases, the selectivity towards solketal was higher than 96%. In this work, the activity of the catalysts was compared in the absence of solvent and using acetonitrile. The results showed that the use of a solvent improves the activity of the catalysts, allowing higher conversions to be achieved. However, the reaction variables were modified between one experience and the other, making it difficult to compare the activity under these conditions.

According to previous work, the use of solvents improves the solubility of the reagents in the initial reaction mixture. However, the catalytic results are not significantly favored. Moreover, the introduction of a third component to the system complicates the technological scheme due to the need to separate the solvent from the rest of the components, coupled with the fact that, as the initial concentration of the reactants decreases, the reaction rate also decreases [40]. The combination of these negative aspects makes it more convenient to work with excess acetone, which can subsequently be distilled and recirculated to the process.

As for the esterification reaction of glycerol with acetic acid, the reagents are completely miscible, so the use of solvents in the reaction has not been reported.

6.3. Extraction of the Water Generated as a Reaction Product

As previously explained, one of the main disadvantages of ketalization and esterification reactions is the formation of water as a reaction product. Since the first published reports [57–59,224,225], strategies have been implemented for the elimination of water and the shift of equilibrium towards higher conversions.

Deutsch et al. carried out the solketal synthesis reaction by using a Dean–Stark trap to collect the water formed, using Amberlyst 36 resin as catalyst and dichloromethane as solvent. After 8 h of reaction at 40 °C, with a molar ratio A/G = 1.5 and a catalyst percentage of 5.4% by weight with respect to glycerol, a solketal yield of 88% was achieved [226].

Roldán et al. studied the synthesis of solketal by using a NaA zeolite membrane reactor, using K10 montmorillonite as catalyst. The experimental device consists of a three-hole balloon that is equipped with a condenser in one of its holes, and, in the central hole, it contains the NaA zeolite membrane. Water removal was carried out via the vapor permeation method, since this avoids contact of the membrane with the liquid, which is unstable in acidic media. After 50 h of reaction, for an A/G molar ratio of 2 and a catalyst percentage of 1 wt.% with respect to glycerol, a solketal yield of 90% was obtained [227].

Vicente et al. carried out the solketal synthesis reaction in a two-stage batch process. In the first stage, the reactants, together with the catalyst, were introduced into a balloon equipped with a condenser, and the reaction was carried out at 70 °C. In the second stage, the reaction water and excess acetone were extracted under vacuum. As catalysts, mesoporous silicas functionalized with sulfonic groups were synthesized, which were evaluated in solketal synthesis and compared with commercial solids. From all of them, the Ar-SBA-15 catalyst was selected and functionalized with arenesulfonic acid, which presented a similar activity to the commercial resin Amberlyst 15. Subsequently, the number of batch stages required to significantly shift the equilibrium was studied. The results showed that, after three stages, 89.5% glycerol conversion was achieved, while in a simple batch process, 80% conversion was obtained [171].

On the other hand, Esposito et al. synthesized different Fe(III) complexes, which were evaluated as homogeneous catalysts with Lewis acids in the synthesis of solketal. In this case, the authors carried out the reactions by using a balloon as a reactor, equipped with a condenser containing a small 3 Å molecular sieve column at the top in order to retain the water formed during the reaction. Of all the catalysts, the solid $FeCl_3(1\text{-}NO_2)$ presented higher activity, solubility in the reactive mixture and stability. Under optimal reaction conditions, 99% glycerol conversion was achieved with 98% selectivity towards solketal [228].

Recently, Li et al. carried out the reaction of glycerol ketalization with acetone in a pilot-scale reactive distillation process, employing an NKC-9 resin as the catalyst. The authors reported optimum results for five theoretical plates in the rectification zone and six theoretical plates in the depletion zone, at a pressure of 101.325 kPa, A/G molar ratio of 2–3 and reflux ratio of 2.4, indicating that substantial improvement in glycerol conversion was achieved by this type of process [229].

All of these previously described experiences demonstrate that it is possible to shift the reaction equilibrium towards values close to 100% glycerol conversion if a correct combination between an active catalyst and an adequate water removal method is used.

Regarding the esterification reaction of glycerol with acetic acid, Liu et al. carried out the reaction by using a three-necked balloon coupled to a distillation column, which allowed the water product of the reaction to be constantly removed. In this way, it was possible to achieve a TAG selectivity of more than 90%, with complete conversion of glycerol [230]. Li et al. simulated a reactive distillation process for TAG production. The results showed that it is possible to achieve complete conversion of glycerol with high selectivity towards TAG, using an AA/G molar ratio of 4, 50 theoretical plates for the reactive section, a reflux ratio between 4 and 6 and a top pressure of 35 kPa [231].

Recently, Bhaduri et al. carried out the esterification reaction of glycerol with acetic acid by employing a catalyst based on a silica–carbon nanocomposite prepared by the modified evaporation-induced self-assembly (EISA) method, subsequently pyrolyzed at 400 and 550 °C and finally functionalized with phosphoric acid. To displace the water product of the reaction, the tests were carried out using a Dean-Stark trap, achieving a TAG selectivity of 36% after 3 h of reaction at 110 °C [232].

6.4. Use of Crude Glycerol

The economics of solketal and acetylglycerols synthesis are directly related to the price of the raw material (glycerol). Therefore, the excessive purification of glycerol could compromise the profitability of the process. For this reason, it is necessary to evaluate the catalytic activity of the synthesized solids in a more realistic context, which includes the use of crude glycerol as feedstock.

Crude glycerol contains a large number of impurities, including inorganic sodium or potassium bases; traces of methanol (MeOH); and non-glycerol organic matter (MONG) such as free fatty acids, traces of oils and non-transesterified fats [233]. The nature of these impurities and their concentration can have, to a greater or lesser extent, a different impact on glycerol esterification and ketalization reactions, mainly linked to the effect they have on the catalysts used.

Da Silva et al. were among the first researchers to study the effect of impurities in crude glycerol on the activity of beta zeolites and an Amberlyst 15 resin in the reaction of glycerol ketalization with acetone. As a result, they concluded that the presence of water and NaCl in the reaction medium drastically reduces the activity of both catalysts, attributing this result to the mobility of Na^+ ions into the pores of the solids, which would facilitate the diffusion of water and thus the neutralization of the acid sites. In their study, the authors concluded that beta zeolite is more resistant to the presence of water than Amberlyst 15 resin [234].

Vicente et al. evaluated the activity of an SBA-15 functionalized with arenesulfonic groups by using crude glycerol as a reagent and compared these results with those obtained using analytical- and pharmaceutical-grade glycerol. As a result, they concluded that the activity of the solids is similar in all cases, emphasizing that, if crude glycerol is used as reagent, the solid must be regenerated to be reused. The authors attributed this deactivation to the cation exchange that occurs between the Na^+ and H^+ ions of the active sites of the catalyst [171].

Talebian-Kiakalaieh et al. evaluated the effect of crude glycerol impurities on the activity of a NaY zeolite modified with citric acid to impart mesoporosity. In conclusion, they reported that the presence of methanol and NaCl led to a decrease in selectivity towards solketal from 97.75% to 88.21%, although the glycerol conversion remained relatively constant. The authors did not justify this decrease [147].

Kowalska-Kus et al. evaluated the activity of different zeolites (BEA, MFI and FAU) in the presence of crude glycerol, using a continuous reactor. The authors reported that the presence of salts and MONG negatively affects the glycerol conversion and the selectivity towards solketal, due to their adsorption on the surface of the catalysts. In this sense, since the process is continuous, as time progresses, the number of adsorbed impurities increases, evidencing a decrease in glycerol conversion and selectivity towards solketal. In turn, the authors concluded that the presence of water or only inorganic salts does not significantly modify the activity of the catalysts [235].

Recently, Saini et al. employed a NaOH-modified H-MOR-type zeolite to partially remove silicon from the structure. This catalyst proved to be tolerant to water and other impurities present in crude glycerol, as well as stable after three uses. The good results were attributed to the high strength of the acid sites in combination with a high specific surface area [79].

With respect to the esterification reaction of glycerol with acetic acid, very few articles have been reported where glycerol is used as a raw material.

Zhu et al. evaluated the activity of a HSiW-supported zirconia in the esterification reaction of glycerol with acetic acid, using crude glycerol. The authors reported that the presence of NaCl and methanol did not affect glycerol conversion and product distribution. On the other hand, the presence of water slightly decreased the glycerol conversion and selectivity towards TAG, confirming the good tolerance of the catalyst to water, which was attributed to the strong interaction between the highly dispersed HSiW compounds and the $\equiv$Zr- OH groups on the surface of the solid [55].

Popova et al. synthesized KIL-2-type silica-impregnated zirconia nanomaterials, which were evaluated using crude glycerol. The results showed that the presence of impurities in the crude decreased the conversion of glycerol and led to a higher selectivity towards MAGs. The authors did not study the effect of each impurity [236].

Finally, Oh et al. employed Novozym 435 enzymes for the esterification of glycerol with acetic acid, obtaining a decrease in glycerol conversion when compared to the use of analytical glycerol. However, the authors did not discuss these results [237].

6.5. Latest Technological Advances

Within the latest advances related to the reaction of glycerol ketalization with acetone, photocatalysis and the simulation of the large-scale production process have played a leading role in this research field.

On the one hand, heterogeneous photocatalysis has been studied in recent years as an alternative for the conversion of glycerol into different compounds, such as solketal, because the reactions are carried out under moderate conditions and a relatively low energy consumption is required [238]. In this context, Hidalgo-Carillo et al. recently carried out, for the first time, the photocatalytic reaction of glycerol ketalization with acetone, calling it the fourth-generation solketal synthesis, after the synthesis using homogeneous, heterogeneous and solvent-free catalysts. The authors used the commercial TiO_2 Aeroxide® Evonik P25 TiO_2 catalyst, carrying out the reaction under simulated solar irradiation, using an Xe lamp. The results showed that a solketal yield of 87% at 30 °C can be achieved, although with high reaction times (24 h), due to the low energy utilization by the catalyst (about 5%). These results open the possibility of studying new sources of active radiation in photocatalysis, as well as of studying continuous processes and reaction mechanisms [239].

Following this line, Gomes et al. carried out the reaction by photochemically exciting an Nb_2O_5 catalyst with UV-C radiation. In this paper, the authors developed a dual process in which the catalyst first converts isopropyl alcohol to acetone, generating H^+ as a by-product, which then catalyzes the synthesis of solketal. The results showed glycerol conversions of 47.8%, with a selectivity towards solketal of 69.8% [240].

In addition to the catalytic studies, it is important to analyze the technical and economic feasibility of the production process, in order to think of a large-scale process. In this sense, Vannucci et al. carried out a feasibility study of a small–medium plant capable of processing between 4000 and 20,000 tons of glycerol per year. The authors demonstrated that, if the price of solketal remains above 2400 USD/Tn, even plants processing 4000 Tn/year of glycerol are economically viable. Furthermore, they noted that the reduction in the cost of cooling water required to condense the excess acetone used in the process is more critical than the lifetime of the catalyst [241].

In addition to technoeconomic studies, it is important to consider aspects related to process intensification, an area of chemical engineering that has grown exponentially in recent years, whose objective is to improve existing technologies to allow greater efficiency, reducing energy consumption, costs and environmental impact, involving downsizing and efficient integration with other equipment [242]. In this regard, Li et al. proposed a reactive partition wall distillation (RDWC) process for solketal synthesis, whose scheme is shown in Figure 12. The authors divided the column into four zones: zone I is reaction, zone II is product purification, zone III is distillation and zone IV is rectification. By optimizing the total annual cost (TAC) and energy consumed, the authors concluded that the RDWC process achieves a 13.9% reduction in energy consumption, an 18.2% reduction in TAC and a 16.4% reduction in CO_2 emissions compared to conventional reactive distillation [229].

Recently, Corrêa et al. proposed a continuous process of the Simulated Moving Bed Reactor (SMBR) type. This type of technology is recommended when the reaction is limited by the thermodynamic equilibrium, as in the case of glycerol ketalization with acetone, since the SMBR combines the chemical reaction with the separation by adsorption of some compound involved in it. In the case of solketal synthesis, the equilibrium is shifted by the adsorption of the water product of the reaction. In their work, the authors proposed the scheme shown in Figure 13, where a process with several feeds is used, in which the eluent is ethanol, obtaining two output streams: a binary mixture of solketal–ethanol and another of acetone–ethanol. The inputs are the reactive mixture (glycerol + acetone) and the eluent (ethanol). The authors studied the effect of temperature on the efficiency of the process, using an Amberlyst 35 as catalyst and adsorbent, concluding that 30 °C turns out to be the optimum temperature. Previous studies have shown that, if an efficient process integration strategy is achieved and the eluent is recirculated to the process, production costs could be decreased by 44% compared to conventional processes [243]. Subsequently, the same authors carried out a process improvement, finding that, under optimum conditions, the maximum productivity is 10 kg of solketal per liter of adsorbent per day, with the desorbent (ethanol) consumption being below 6 L per kg of solketal produced [244].

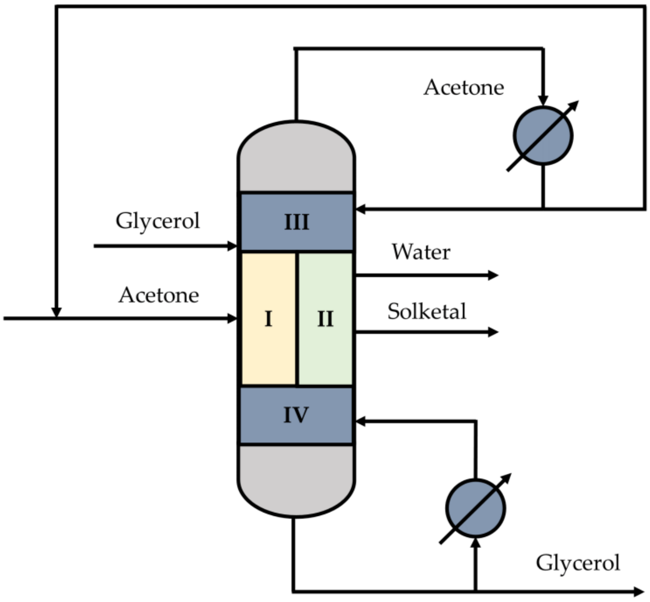

Figure 12. Reactive split-wall distillation (RDWC) process for solketal synthesis proposed by Li et al. [225]. Zone I is reaction, zone II is product purification, zone III is distillation and zone IV is rectification.

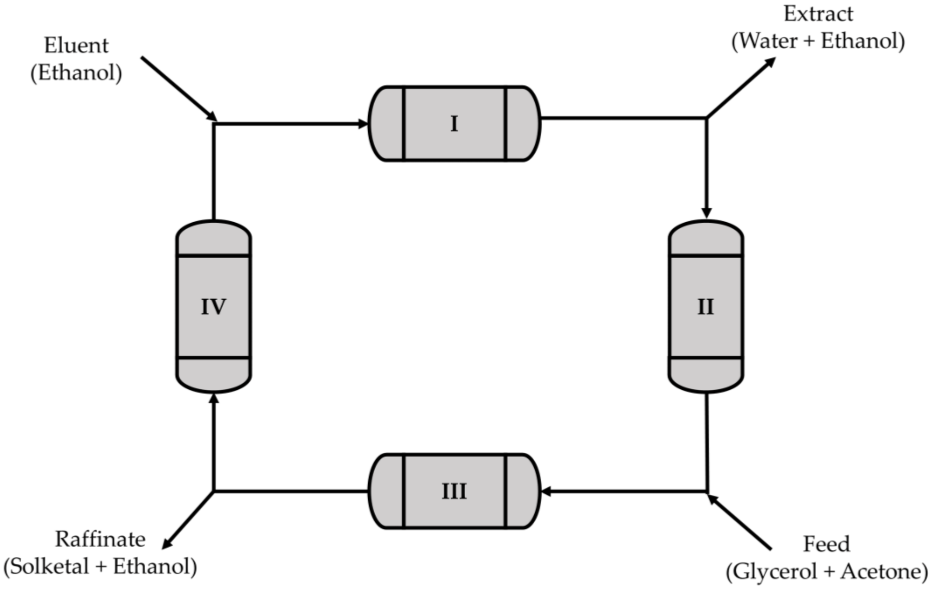

Figure 13. Continuous Simulated Moving Bed Reactor (SMBR)-type process proposed by Corrêa et al. [244].

7. Conclusions, Perspectives and Future Work

Glycerol obtained as a by-product in biodiesel synthesis is configured as a platform molecule for the production of a wide variety of industrial chemical compounds through energetically integrated processes in the biorefinery environment. In particular, the reactions of ketalization and esterification of glycerol have gained increasing interest in recent years because the compounds that are obtained can be used in several industrial applications. In this work, a literature review of more than 200 publications on the reactions of glycerol ketalization with acetone and esterification with acetic acid was carried out, covering mechanistic, thermodynamic, catalytic and kinetic aspects.

With respect to the products obtained, the reaction of glycerol ketalization with acetone leads to the generation of solketal with a selectivity higher than 90% in most of the articles. On the other hand, in the esterification reaction of glycerol with acetic acid, a mixture of mono- (MAG), di- (DAG) and tri-substituted (TAG) acetylglycerols is obtained, with selectivity values that vary according to the catalyst and reaction conditions. Most articles report selectivity values for TAG of 35%, which is the most commercially valuable compound, with only a few reporting selectivity values close to 90%.

Both reactions have been studied in liquid phase, using batch and continuous flow reactors. The ketalization reaction has been studied between room temperature and 90 °C, while the esterification reaction was studied between 80 °C and 170 °C, which implies that higher operating pressures are required in this case to maintain the liquid phase condition.

Both the ketalization reaction with acetone and esterification with acetic acid are globally exothermic. For ketalization, reaction enthalpies in the range of $-6.43/-30.0$ kJ mol^{-1} have been reported, while for esterification, no thermodynamic properties have been reported for the individual reactions in liquid phase.

From the mechanistic point of view, both reactions are catalyzed by acid sites, both Brønsted and Lewis. In this regard, both reactions have been catalyzed by acidic solids of the same nature, including ionic liquids, zeolites, exchange resins, carbonaceous materials, sulfated zirconia, heteropolyacids, silica-based catalysts and clays. Regardless of their nature and the strength of the acid sites, their density and pore size have been found to be determining factors in catalytic activity. It turns out that the higher the density and acidic strength of the sites, the higher the activity of the catalyst. In addition, more porous solids allow for the diffusion of reactants and products, facilitating the transport processes and improving their performance.

In particular, for the reaction of glycerol ketalization with acetone, the most active solids are exchange resins, functionalized carbons and heteropolyacids, reaching glycerol conversions and selectivity values to solketal higher than 95%. For the esterification reaction with acetic acid, most solids lead to complete glycerol conversion, but functionalized carbons, ionic liquids and clays allow higher selectivity values to TAG.

It has been reported that the main causes of the deactivation of solids used as catalysts have been attributed to the adsorption of reagents and/or products on the surface of the catalysts, water generated during the reaction, modifications of the specific surface area and pore size of the solids and leaching of active sites and attrition due to mechanical wear from agitation during the reaction.

With respect to kinetic expressions, for the reaction of glycerol ketalization with acetone, the power law, the pseudo-homogeneous model, Eley–Rideal and Langmuir–Hinshelwood–Hougen–Watson have been proposed as models. These expressions have allowed the determination of activation energies, depending on the solid used.

In order to scale up the reactions for industrial application, it is necessary to take several aspects into account, such as the immiscibility of the glycerol–acetone mixture in the case of ketalization, and the formation of water as a product of both reactions. In the first case, the use of solvents to improve miscibility has been evaluated, determining that the activity does not improve significantly. This fact, added to the need for separating the solvent after the reaction, makes it preferable to work with excess acetone, which shifts the thermodynamic equilibrium towards the products and, after being separated, can be recirculated to be used again as a reagent.

With respect to the formation of water as a product, several strategies have been reported to remove it from the reaction medium and shift the thermodynamic equilibrium to the products, such as reactive distillation, the use of membrane reactors, Dean-Stark traps and molecular sieves. Other authors have carried out the reactions in several stages until equilibrium is reached, with water extraction between stages. All of these experiences have shown that it is possible to obtain values close to 100% conversion of glycerol for the ketalization reaction and more than 90% selectivity towards TAG for the esterification reaction if a correct combination of an active catalyst and an adequate water removal method is used.

Another aspect studied and of great importance for process scale-up is the use of crude glycerol as a reagent. It has been determined for both reactions that, depending on the solid used, the presence of water, salts, methanol and non-glycerol organic matter (MONG) can affect the activity and stability of the catalysts, so that it is of great importance to study the effect of impurities when synthesizing new materials as catalysts.

Among the latest advances related to the reaction of glycerol ketalization with acetone, the research has focused on photocatalysis and the simulation of production processes.

The need to develop industrially applicable technologies leads to several challenges in relation to both glycerol conversion reactions. Firstly, simulation studies need to be carried out to determine whether these processes are economically viable and what yields they will produce at market levels. Secondly, experimental tests should be carried out in the presence of catalyst pellets to assess the loss of activity due to the effect of internal and external resistances on mass transport and energy transfer. The possibility of carrying out the reactions in the presence of crude glycerol and its impurities should then be evaluated, since these impurities affect the catalytic activity. Then, when thinking about process scale-up, a technology should be considered that allows for the easy and efficient removal of water from the reaction medium to increase the achievable conversions. Finally, as these processes are limited to glycerol biorefineries, the intensification of energy-saving processes with other catalytic biorefinery processes could be considered.

It is hoped that this work will be the starting point for the search for new technologies that will allow for the efficient integration of glycerol conversion processes in the environment of new biorefineries, reducing the investment and equipment maintenance costs, as well as the energy consumption and environmental impact.

Author Contributions: Conceptualization, F.M.P. and M.N.G.; methodology, F.M.P.; validation, M.N.G., G.F.S. and F.P.; formal analysis, F.M.P. and M.N.G.; investigation, F.M.P.; resources, G.F.S. and F.P.; data curation, M.N.G., G.F.S. and F.P.; writing—original draft preparation, F.M.P.; writing—review and editing, M.N.G., G.F.S. and F.P.; visualization, F.M.P. and M.N.G.; supervision, G.F.S. and F.P.; project administration, G.F.S. and F.P.; funding acquisition, G.F.S. and F.P. All authors have read and agreed to the published version of the manuscript.

Funding: This research was funded by the Consejo Nacional de Investigaciones Científicas y Técnicas (CONICET), grant number PIP 0386; and the University of La Plata (UNLP), grant number I-248.

Data Availability Statement: The data reported were taken from papers included in the references.

Acknowledgments: F.M.P. and M.N.G. thank the University of La Plata (UNLP) for awarding them the Young Research Grant in 2022 and 2023, respectively.

Conflicts of Interest: The authors declare no conflict of interest.

References

1. Fundación Leia—Centro de Desarrollo Tecnológico Industria Química Basada En Biomasa: Implicaciones Tecnológicas. 2007. Available online: https://www.leia.es (accessed on 15 July 2023).
2. Romanelli, G.P.; Ruiz, D.M.; Pasquale, G.A. *Química de La Biomasa y Los Biocombustibles*; Universidad Nacional de La Plata: La Plata, Argentina, 2017; ISBN 978-950-34-1425-5.

3. Ning, P.; Yang, G.; Hu, L.; Sun, J.; Shi, L.; Zhou, Y.; Wang, Z.; Yang, J. Recent Advances in the Valorization of Plant Biomass. *Biotechnol. Biofuels* **2021**, *14*, 102. [CrossRef]
4. Mota, C.J.A.; Pinto, B.P.; de Lima, A.L. *Glycerol: A Versatile Renewable Feedstock for the Chemical Industry*; Springer: Cham, Switzerland, 2017; ISBN 9783319593753.
5. Ma, F.; Hanna, M.A. Biodiesel Production: A Review. *Bioresour. Technol.* **1999**, *70*, 1–15. [CrossRef]
6. Torroba, A.; Carvalho, A. *Atlas de Los Biocombustibles Líquidos 2020–2021*; Interamerican Institute for Agriculture Cooperation: San Jose, CA, USA, 2022; ISBN 9789292489199.
7. Torroba, A. *Atlas de Los Biocombustibles Líquidos 2019–2020*; Interamerican Institute for Agriculture Cooperation: San Jose, CA, USA, 2020.
8. Anitha, M.; Kamarudin, S.K.; Kofli, N.T. The Potential of Glycerol as a Value-Added Commodity. *Chem. Eng. J.* **2016**, *295*, 119–130. [CrossRef]
9. Bianchi, C.L.; Canton, P.; Dimitratos, N.; Porta, F.; Prati, L. Selective Oxidation of Glycerol with Oxygen Using Mono and Bimetallic Catalysts Based on Au, Pd and Pt Metals. *Catal. Today* **2005**, *102–103*, 203–212. [CrossRef]
10. Pagliaro, M.; Rossi, M. *The Future of Glycerol New Uses of a Versatile Raw Material*; RSC Publishing: Cambridge, UK, 2008; ISBN 9780854041244.
11. Perez, F.M.; Gatti, M.N.; Nichio, N.N.; Pompeo, F. Bio-Additives from Glycerol Acetylation with Acetic Acid: Chemical Equilibrium Model. *Results Eng.* **2022**, *15*, 100502. [CrossRef]
12. Aloui, M.; Cecilia, J.A.; Moreno-Tost, R.; Ghorbel, S.B.; Saïd Zina, M.; Rodríguez-Castellón, E. Glycerol Etherification towards Selective Diglycerol over Mixed Oxides Derived from Hydrotalcites: Effect of Ni Loading. *J. Sol-Gel Sci. Technol.* **2021**, *97*, 351–364. [CrossRef]
13. Buffoni, I.N.; Gatti, M.N.; Santori, G.F.; Pompeo, F.; Nichio, N.N. Hydrogen from Glycerol Steam Reforming with a Platinum Catalyst Supported on a SiO_2-C Composite. *Int. J. Hydrogen Energy* **2017**, *42*, 12967–12977. [CrossRef]
14. Almena, A.; Martín, M. Technoeconomic Analysis of the Production of Epichlorohydrin from Glycerol. *Ind. Eng. Chem. Res.* **2016**, *55*, 3226–3238. [CrossRef]
15. Rittiron, P.; Niamnuy, C.; Donphai, W.; Chareonpanich, M.; Seubsai, A. Production of Glycerol Carbonate from Glycerol over Templated-Sodium-Aluminate Catalysts Prepared Using a Spray-Drying Method. *ACS Omega* **2019**, *4*, 9001–9009. [CrossRef]
16. Liu, S.; Yu, Z.; Wang, Y.; Sun, Z.; Liu, Y.; Shi, C.; Wang, A. Catalytic Dehydration of Glycerol to Acrolein over Unsupported MoP. *Catal. Today* **2021**, *379*, 132–140. [CrossRef]
17. Gatti, M.N.; Pompeo, F.; Santori, G.F.; Nichio, N.N. Bio-Propylene Glycol by Liquid Phase Hydrogenolysis of Glycerol with Ni/SiO_2-C Catalysts. *Catal. Today* **2017**, *296*, 26–34. [CrossRef]
18. Perez, F.M.; Legarto, C.; Lombardi, M.B.; Santori, G.F.; Pompeo, F.; Nichio, N.N. Activated Bentonite Nanocomposite for the Synthesis of Solketal from Glycerol in the Liquid Phase. *Catalysts* **2022**, *12*, 673. [CrossRef]
19. Pirzadi, Z.; Meshkani, F. From Glycerol Production to Its Value-Added Uses: A Critical Review. *Fuel* **2022**, *329*, 125044. [CrossRef]
20. Kaur, J.; Sarma, A.K.; Jha, M.K.; Gera, P. Valorisation of Crude Glycerol to Value-Added Products: Perspectives of Process Technology, Economics and Environmental Issues. *Biotechnol. Rep.* **2020**, *27*, e00487. [CrossRef]
21. National Institute of Standards and Technology (NIST). Available online: https://webbook.nist.gov/chemistry/name-ser/ (accessed on 10 June 2023).
22. Seyferth, D. The Rise and Fall of Tetraethyllead. 2. *Organometallics* **2003**, *22*, 5154–5178. [CrossRef]
23. Mota, C.J.A.; Da Silva, C.X.A.; Rosenbach, N.; Costa, J.; Da Silva, F. Glycerin Derivatives as Fuel Additives: The Addition of Glycerol/Acetone Ketal (Solketal) in Gasolines. *Energy Fuels* **2010**, *24*, 2733–2736. [CrossRef]
24. García, H.; García, J.I.; Fraile, J.M.; Mayoral, J.A. Solketal: Green and Catalytic Synthesis and Its Classification as a Solvent—2,2-Dimethyl-4-hidroxymethyl-1,3-dioxolane, an Interesting Green Solvent Produced through Heterogeneous Catalysis. *Chim. Oggi/Chem. Today* **2008**, *26*, 10–12.
25. Liao, X.; Zhu, Y.; Wang, S.G.; Chen, H.; Li, Y. Theoretical Elucidation of Acetylating Glycerol with Acetic Acid and Acetic Anhydride. *Appl. Catal. B Environ.* **2010**, *94*, 64–70. [CrossRef]
26. Fiume, M.Z. Final Report on the Safety Assessment of Triacetin. *Int. J. Toxicol.* **2003**, *22*, 1–10.
27. Scopus. Available online: https://www.scopus.com/home.uri (accessed on 9 July 2023).
28. Nanda, M.R.; Zhang, Y.; Yuan, Z.; Qin, W.; Ghaziaskar, H.S.; Xu, C. Catalytic Conversion of Glycerol for Sustainable Production of Solketal as a Fuel Additive: A Review. *Renew. Sustain. Energy Rev.* **2016**, *56*, 1022–1031. [CrossRef]
29. Zahid, I.; Ayoub, M.; Abdullah, B.B.; Mukhtar, A.; Saqib, S.; Rafiq, S.; Ullah, S.; Al-Sehemi, A.G.; Farrukh, S.; Danish, M. Glycerol Conversion to Solketal: Catalyst and Reactor Design, and Factors Affecting the Yield. *ChemBioEng Rev.* **2021**, *8*, 227–238. [CrossRef]
30. Talebian-Kiakalaieh, A.; Amin, N.A.S.; Najaafi, N.; Tarighi, S. A Review on the Catalytic Acetalization of Bio-Renewable Glycerol to Fuel Additives. *Front. Chem.* **2018**, *6*, 573. [CrossRef]
31. Khodadadi, M.R.; Thiel, J.; Varma, R.S.; Len, C. Innovative Continuous Synthesis of Solketal. *J. Flow Chem.* **2021**, *11*, 725–735. [CrossRef]
32. Ao, S.; Rokhum, S.L. Recent Advances in the Valorization of Biodiesel By-Product Glycerol to Solketal. *J. Chem.* **2022**, *2022*, 4938672. [CrossRef]

33. Len, C.; Delbecq, F.; Cara Corpas, C.; Ruiz Ramos, E. Continuous Flow Conversion of Glycerol into Chemicals: An Overview. *Synthesis* **2018**, *50*, 723–741. [CrossRef]
34. Da Silva, M.J.; Lopes, N.P.G.; Rodrigues, A.A. Biodiesel Additives Synthesis Using Solid Heteropolyacid Catalysts. *Energies* **2023**, *16*, 1332. [CrossRef]
35. Nda-Umar, U.I.; Ramli, I.; Taufiq-Yap, Y.H.; Muhamad, E.N. An Overview of Recent Research in the Conversion of Glycerol into Biofuels, Fuel Additives and Other Bio-Based Chemicals. *Catalysts* **2019**, *9*, 15. [CrossRef]
36. Nda-Umar, U.I.; Ramli, I.B.; Muhamad, E.N.; Azri, N.; Amadi, U.F.; Taufiq-Yap, Y.H. Influence of Heterogeneous Catalysts and Reaction Parameters on the Acetylation of Glycerol to Acetin: A Review. *Appl. Sci.* **2020**, *10*, 7155. [CrossRef]
37. Ozorio, L.P.; Pianzolli, R.; Mota, M.B.S.; Mota, C.J.A. Reactivity of Glycerol/Acetone Ketal (Solketal) and Glycerol/Formaldehyde Acetals toward Acid-Catalyzed Hydrolysis. *J. Braz. Chem. Soc.* **2012**, *23*, 931–937. [CrossRef]
38. Nanda, M.R.; Yuan, Z.; Qin, W.; Ghaziaskar, H.S.; Poirier, M.A.; Xu, C.C. Thermodynamic and Kinetic Studies of a Catalytic Process to Convert Glycerol into Solketal as an Oxygenated Fuel Additive. *Fuel* **2014**, *117*, 470–477. [CrossRef]
39. Moreira, M.N.; Faria, R.P.V.; Ribeiro, A.M.; Rodrigues, A.E. Solketal Production from Glycerol Ketalization with Acetone: Catalyst Selection and Thermodynamic and Kinetic Reaction Study. *Ind. Eng. Chem. Res.* **2019**, *58*, 17746–17759. [CrossRef]
40. Dmitriev, G.S.; Terekhov, A.V.; Zanaveskin, L.N.; Khadzhiev, S.N.; Zanaveskin, K.L.; Maksimov, A.L. Choice of a Catalyst and Technological Scheme for Synthesis of Solketal. *Russ. J. Appl. Chem.* **2016**, *89*, 1619–1624. [CrossRef]
41. Cornejo, A.; Campoy, M.; Barrio, I.; Navarrete, B.; Lázaro, J. Solketal Production in a Solvent-Free Continuous Flow Process: Scaling from Laboratory to Bench Size. *React. Chem. Eng.* **2019**, *4*, 1803–1813. [CrossRef]
42. Vannucci, J.A.; Nichio, N.N.; Pompeo, F. Solketal Synthesis from Ketalization of Glycerol with Acetone: A Kinetic Study over a Sulfated Zirconia Catalyst. *Catal. Today* **2021**, *372*, 238–245. [CrossRef]
43. Perez, F.M.; Nichio, N.; Pompeo, F. Thermodynamic Assessment of Chemical Equilibrium for the Synthesis of Solketal in the Liquid Phase. *Chem. Eng. Technol.* **2021**, *44*, 1356–1363. [CrossRef]
44. Li, L.; Korányi, T.I.; Sels, B.F.; Pescarmona, P.P. Highly-Efficient Conversion of Glycerol to Solketal over Heterogeneous Lewis Acid Catalysts. *Green Chem.* **2012**, *14*, 1611–1619. [CrossRef]
45. da Silva, M.J.; de Ávila Rodrigues, F.; Júlio, A.A. SnF_2-Catalyzed Glycerol Ketalization: A Friendly Environmentally Process to Synthesize Solketal at Room Temperature over on Solid and Reusable Lewis Acid. *Chem. Eng. J.* **2017**, *307*, 828–835. [CrossRef]
46. Priya, S.S.; Selvakannan, P.R.; Chary, K.V.R.; Kantam, M.L.; Bhargava, S.K. Solvent-Free Microwave-Assisted Synthesis of Solketal from Glycerol Using Transition Metal Ions Promoted Mordenite Solid Acid Catalysts. *Mol. Catal.* **2017**, *434*, 184–193. [CrossRef]
47. Janiszewska, E.; Kowalska-Kuś, J.; Góra-Marek, K.; Szymocha, A.; Nowińska, K.; Kowalak, S. Modification of Silicalite-1 with Ammonium Compounds Aimed at Preparation of Acidic Catalyst for Acetalization of Glycerol with Acetone. *Appl. Catal. A Gen.* **2019**, *581*, 1–10. [CrossRef]
48. Troncea, S.B.; Wuttke, S.; Kemnitz, E.; Coman, S.M.; Parvulescu, V.I. Hydroxylated Magnesium Fluorides as Environmentally Friendly Catalysts for Glycerol Acetylation. *Appl. Catal. B Environ.* **2011**, *107*, 260–267. [CrossRef]
49. Kale, S.; Umbarkar, S.B.; Dongare, M.K.; Eckelt, R.; Armbruster, U.; Martin, A. Selective Formation of Triacetin by Glycerol Acetylation Using Acidic Ion-Exchange Resins as Catalyst and Toluene as an Entrainer. *Appl. Catal. A Gen.* **2015**, *490*, 10–16. [CrossRef]
50. Zhou, L.; Nguyen, T.H.; Adesina, A.A. The Acetylation of Glycerol over Amberlyst-15: Kinetic and Product Distribution. *Fuel Process. Technol.* **2012**, *104*, 310–318. [CrossRef]
51. Swati, L.; Pandhare, T.V.K.; Dongare, M.K.; Umbarkar, S.B. In Situ Formed Supported Silicomolybdic Heteropolyanions: Efficient Solid Catalyst for Acetylation of Glycerol. *J. Environ. Anal. Chem.* **2015**, *2*, 2380–2391. [CrossRef]
52. Venkatesha, N.J.; Bhat, Y.S.; Prakash, B.S.J. Volume Accessibility of Acid Sites in Modified Montmorillonite and Triacetin Selectivity in Acetylation of Glycerol. *RSC Adv.* **2016**, *6*, 45819–45828. [CrossRef]
53. Kong, P.S.; Aroua, M.K.; Daud, W.M.A.W.; Lee, H.V.; Cognet, P.; Pérès, Y. Catalytic Role of Solid Acid Catalysts in Glycerol Acetylation for the Production of Bio-Additives: A Review. *RSC Adv.* **2016**, *6*, 68885–68905. [CrossRef]
54. Sandesh, S.; Manjunathan, P.; Halgeri, A.B.; Shanbhag, G.V. Glycerol Acetins: Fuel Additive Synthesis by Acetylation and Esterification of Glycerol Using Cesium Phosphotungstate Catalyst. *RSC Adv.* **2015**, *5*, 104354–104362. [CrossRef]
55. Zhu, S.; Zhu, Y.; Gao, X.; Mo, T.; Zhu, Y.; Li, Y. Bioresource Technology Production of Bioadditives from Glycerol Esterification over Zirconia Supported Heteropolyacids. *Bioresour. Technol.* **2013**, *130*, 45–51. [CrossRef] [PubMed]
56. Alves, N.F.; Santiago Neto, A.D.B.; Bessa, B.D.S.; Oliveira, A.C.; Mendes Filho, J.; Campos, A.F.; Oliveira, A.C. Binary Oxides with Defined Hierarchy of Pores in the Esterification of Glycerol. *Catalysts* **2016**, *6*, 151. [CrossRef]
57. Mushrush, G.W.; Stalick, W.M.; Beal, E.J.; Basu, S.C.; Eric Slone, J.; Cummings, J. The Synthesis of Acetals and Ketals of the Reduced Sugar Mannose as Fuel System Icing Inhibitors. *Pet. Sci. Technol.* **1997**, *15*, 237–244. [CrossRef]
58. Bruchmann, B.; Haberle, K.; Gruner, H.; Hirn, M. Preparation of Cyclic Acetals or Ketals. U.S. Patent No. 5,917,059, 29 June 1999.
59. García, E.; Laca, M.; Pérez, E.; Garrido, A.; Peinado, J. New Class of Acetal Derived from Glycerin as a Biodiesel Fuel Component. *Energy Fuels* **2008**, *22*, 4274–4280. [CrossRef]
60. Suriyaprapadilok, N.; Kitiyanan, B. Synthesis of Solketal from Glycerol and Its Reaction with Benzyl Alcohol. *Energy Procedia* **2011**, *9*, 63–69. [CrossRef]
61. Menezes, F.D.L.; Guimaraes, M.D.O.; Da Silva, M.J. Highly Selective $SnCl_2$-Catalyzed Solketal Synthesis at Room Temperature. *Ind. Eng. Chem. Res.* **2013**, *52*, 16709–16713. [CrossRef]

62. Zaher, S.; Christ, L.; Abd El Rahim, M.; Kanj, A.; Karamé, I. Green Acetalization of Glycerol and Carbonyl Catalyzed by $FeCl_3 \cdot 6H_2O$. *Mol. Catal.* **2017**, *438*, 204–213. [CrossRef]
63. Nascimento, J.A.C.; Pinto, B.P.; Calado, V.M.A.; Mota, C.J.A. Synthesis of Solketal Fuel Additive from Acetone and Glycerol Using CO_2 as Switchable Catalyst. *Front. Energy Res.* **2019**, *7*, 58. [CrossRef]
64. Jayakumar, M.; Karmegam, N.; Gundupalli, M.P.; Bizuneh Gebeyehu, K.; Tessema Asfaw, B.; Chang, S.W.; Ravindran, B.; Kumar Awasthi, M. Heterogeneous Base Catalysts: Synthesis and Application for Biodiesel Production—A Review. *Bioresour. Technol.* **2021**, *331*, 125054. [CrossRef]
65. Vekariya, R.L. A Review of Ionic Liquids: Applications towards Catalytic Organic Transformations. *J. Mol. Liq.* **2017**, *227*, 44. [CrossRef]
66. Ji, Y.; Zhang, T.; Gui, X.; Shi, H.J.; Yun, Z. Solventless Ketalization of Glycerol to Solketal with Acetone over the Ionic Liquid $[P(C_4H_9)3C_{14}H_{29}][TsO]$. *Chinese J. Chem. Eng.* **2020**, *28*, 158–164. [CrossRef]
67. Gui, Z.; Zahrtmann, N.; Saravanamurugan, S.; Reyero, I.; Qi, Z.; Bañares, M.A.; Riisager, A.; Garcia-Suarez, E.J. Brønsted Acid Ionic Liquids (BAILs) as Efficient and Recyclable Catalysts in the Conversion of Glycerol to Solketal at Room Temperature. *ChemistrySelect* **2016**, *1*, 5869–5873. [CrossRef]
68. Li, L.; Yu, S.T.; Xie, C.X.; Liu, F.S.; Li, H.J. Synthesis of Glycerol Triacetate Using Functionalized Ionic Liquid as Catalyst. *J. Chem. Technol. Biotechnol.* **2009**, *84*, 1649–1652. [CrossRef]
69. Liu, X.; Ma, H.; Wu, Y.; Wang, C.; Yang, M.; Yan, P.; Welz-Biermann, U. Esterification of Glycerol with Acetic Acid Using Double SO_3H-Functionalized Ionic Liquids as Recoverable Catalysts. *Green Chem.* **2011**, *13*, 697–701. [CrossRef]
70. Keogh, J.; Tiwari, M.S.; Manyar, H. Esterification of Glycerol with Acetic Acid Using Nitrogen-Based Brønsted-Acidic Ionic Liquids. *Ind. Eng. Chem. Res.* **2019**, *58*, 17235–17243. [CrossRef]
71. Guang, B.; Zhang, W.; Wu, Y.; Xiao, Y.; Su, M.; Liu, Y. Dual Sulfonic Acid Functionalized Heteropolyacid-Based Ionic Liquids for Esterification of Glycerol Toward Triacetylglycerol. *Catal. Lett.* **2023**, *153*, 1625–1634. [CrossRef]
72. International Zeolite Association Database of Zeolite Structures. Available online: http://www.iza-structure.org/databases/ (accessed on 15 July 2023).
73. Manjunathan, P.; Maradur, S.P.; Halgeri, A.B.; Shanbhag, G.V. Room Temperature Synthesis of Solketal from Acetalization of Glycerol with Acetone: Effect of Crystallite Size and the Role of Acidity of Beta Zeolite. *J. Mol. Catal. A Chem.* **2015**, *396*, 47–54. [CrossRef]
74. Sandesh, S.; Halgeri, A.B.; Shanbhag, G.V. Utilization of Renewable Resources: Condensation of Glycerol with Acetone at Room Temperature Catalyzed by Organic-Inorganic Hybrid Catalyst. *J. Mol. Catal. A Chem.* **2015**, *401*, 73–80. [CrossRef]
75. Kowalska-Kus, J.; Held, A.; Frankowski, M.; Nowinska, K. Solketal Formation from Glycerol and Acetone over Hierarchical Zeolites of Different Structure as Catalysts. *J. Mol. Catal. A Chem.* **2017**, *426*, 205–212. [CrossRef]
76. Rossa, V.; Pessanha, Y.D.S.P.; Díaz, G.C.; Câmara, L.D.T.; Pergher, S.B.C.; Aranda, D.A.G. Reaction Kinetic Study of Solketal Production from Glycerol Ketalization with Acetone. *Ind. Eng. Chem. Res.* **2017**, *56*, 479–488. [CrossRef]
77. Rossa, V.; Treichel, H.; Alexandre, D.; Aranda, G. Transformation of Glycerol Into Solketal By Beta and Ferrierite Acid. *Perspectiva* **2017**, *41*, 101–112.
78. Silva, L.S.D.; Araki, C.A.; Marcucci, S.M.P.; Silva, V.L.D.S.T.D.; Arroyo, P.A. Desilication of ZSM-5 and ZSM-12 Zeolites with Different Crystal Sizes: Effect on Acidity and Mesoporous Initiation. *Mater. Res.* **2019**, *22*, e20180872. [CrossRef]
79. Saini, B.; Tathod, A.P.; Saxena, S.K.; Arumugam, S.; Viswanadham, N. Sustainable Upgrade of Bioderived Glycerol to Solketal through Acetalization over Metal-Free Mordenite Catalysts. *ACS Sustain. Chem. Eng.* **2022**, *10*, 1172–1181. [CrossRef]
80. da Silva, C.X.A.; Gonçalves, V.L.C.; Mota, C.J.A. Water-Tolerant Zeolite Catalyst for the Acetalisation of Glycerol. *Green Chem.* **2009**, *11*, 38–41. [CrossRef]
81. Venkatesha, N.J.; Bhat, Y.S.; Jai Prakash, B.S. Dealuminated BEA Zeolite for Selective Synthesis of Five-Membered Cyclic Acetal from Glycerol under Ambient Conditions. *RSC Adv.* **2016**, *6*, 18824–18833. [CrossRef]
82. Ferreira, C.; Araujo, A.; Calvino-Casilda, V.; Cutrufello, M.G.; Rombi, E.; Fonseca, A.M.; Bañares, M.A.; Neves, I.C. Y Zeolite-Supported Niobium Pentoxide Catalysts for the Glycerol Acetalization Reaction. *Microporous Mesoporous Mater.* **2018**, *271*, 243–251. [CrossRef]
83. Rahaman, M.S.; Phung, T.K.; Hossain, M.A.; Chowdhury, E.; Tulaphol, S.; Lalvani, S.B.; O'Toole, M.; Willing, G.A.; Jasinski, J.B.; Crocker, M.; et al. Hydrophobic Functionalization of HY Zeolites for Efficient Conversion of Glycerol to Solketal. *Appl. Catal. A Gen.* **2020**, *592*, 117369. [CrossRef]
84. Li, Y.; Xie, Q.; Wang, M.; Wang, Z.; Liu, J.; Du, Y.; Zhang, D.; Liu, M.; Zhang, G.; Jin, X.; et al. Fe^{3+} and Chlorotrimethylsilane Modified NaY Catalysts Display Enhanced Activity and Durability for Acetalization of Glycerol to Solketal. *Chem. Eng. J.* **2023**, *452*, 139303. [CrossRef]
85. Gonçalves, V.L.C.; Pinto, B.P.; Silva, J.C.; Mota, C.J.A. Acetylation of Glycerol Catalyzed by Different Solid Acids. *Catal. Today* **2008**, *133*, 673–677. [CrossRef]
86. Dalla Costa, B.O.; Decolatti, H.P.; Legnoverde, M.S.; Querini, C.A. Influence of Acidic Properties of Different Solid Acid Catalysts for Glycerol Acetylation. *Catal. Today* **2017**, *289*, 222–230. [CrossRef]
87. Popova, M.; Lazarova, H.; Kalvachev, Y.; Todorova, T.; Szegedi, Á.; Shestakova, P.; Mali, G.; Dasireddy, V.D.B.C.; Likozar, B. Zr-Modified Hierarchical Mordenite as Heterogeneous Catalyst for Glycerol Esterification. *Catal. Commun.* **2017**, *100*, 10–14. [CrossRef]

88. Chakrabarti, A.; Sharma, M.M. Cationic Ion Exchange Resins as Catalyst. *React. Polym.* **1993**, *20*, 1–45. [CrossRef]
89. Harmer, M.A.; Sun, Q. Solid Acid Catalysis Using Ion-Exchange Resins. *Appl. Catal. A Gen.* **2001**, *221*, 45–62. [CrossRef]
90. Nandan, D.; Sreenivasulu, P.; Sivakumar Konathala, L.N.; Kumar, M.; Viswanadham, N. Acid Functionalized Carbon-Silica Composite and Its Application for Solketal Production. *Microporous Mesoporous Mater.* **2013**, *179*, 182–190. [CrossRef]
91. Esteban, J.; Ladero, M.; García-Ochoa, F. Kinetic Modelling of the Solventless Synthesis of Solketal with a Sulphonic Ion Exchange Resin. *Chem. Eng. J.* **2015**, *269*, 194–202. [CrossRef]
92. Sulistyo, H.; Hapsari, I.; Budhijanto; Sediawan, W.B.; Rahayu, S.S.; Azis, M.M. Heterogeneous Catalytic Reaction of Glycerol with Acetone for Solketal Production. *MATEC Web Conf.* **2019**, *268*, 07004. [CrossRef]
93. Ilgen, O.; Yerlikaya, S.; Akyurek, F.O. Synthesis of Solketal from Glycerol and Acetone over Amberlyst-46 to Produce an Oxygenated Fuel Additive. *Period. Polytech. Chem. Eng.* **2017**, *61*, 144–148. [CrossRef]
94. Santos-Vieira, I.C.M.S.; Mendes, R.F.; Paz, F.A.A.; Rocha, J.; Simões, M.M.Q. Solketal Production via Solvent-Free Acetalization of Glycerol over Triphosphonic-Lanthanide Coordination Polymers. *Catalysts* **2021**, *11*, 598. [CrossRef]
95. Lopes, N.F.; Caiado, M.; Canhao, P.; Castanheiro, J.E. Synthesis of Bio-Fuel Additives from Glycerol over Poly(Vinyl Alcohol) with Sulfonic Acid Groups. *Energy Sources Part A Recover. Util. Environ. Eff.* **2015**, *37*, 1928–1936. [CrossRef]
96. Churipard, S.R.; Manjunathan, P.; Chandra, P.; Shanbhag, G.V.; Ravishankar, R.; Rao, P.V.C.; Sri Ganesh, G.; Halgeri, A.B.; Maradur, S.P. Remarkable Catalytic Activity of a Sulfonated Mesoporous Polymer (MP-SO_3H) for the Synthesis of Solketal at Room Temperature. *New J. Chem.* **2017**, *41*, 5745–5751. [CrossRef]
97. Tokuyama, H.; Ohno, H.; Fujita, T. Effect of Polymer Matrices of Gels Bearing a Sulfo Group on Their Catalytic Properties for Acetalization of Glycerol to Solketal and Esterification of Oleic Acid to Ethyl Oleate. *React. Funct. Polym.* **2021**, *165*, 104943. [CrossRef]
98. Laskar, I.B.; Rajkumari, K.; Gupta, R.; Rokhum, L. Acid-Functionalized Mesoporous Polymer-Catalyzed Acetalization of Glycerol to Solketal, a Potential Fuel Additive under Solvent-Free Conditions. *Energy Fuels* **2018**, *32*, 12567–12576. [CrossRef]
99. Yang, J.; Li, N.; Ma, W.J.; Zhou, J.H.; Sun, H.Z. Synthesis of Solketal with Catalyst Sulfonic Acid Resin. *Adv. Mater. Res.* **2014**, *830*, 176–179. [CrossRef]
100. Dosuna-Rodríguez, I.; Gaigneaux, E.M. Glycerol Acetylation Catalysed by Ion Exchange Resins. *Catal. Today* **2012**, *195*, 14–21. [CrossRef]
101. Zhou, L.; Al-Zaini, E.; Adesina, A.A. Catalytic Characteristics and Parameters Optimization of the Glycerol Acetylation over Solid Acid Catalysts. *Fuel* **2013**, *103*, 617–625. [CrossRef]
102. Banu, I.; Bozga, G.; Bumbac, G.; Vintila, A.; Velea, S.; Galan, A.M.; Bombos, M.; Blajan, O.; Crucean, A.C. A Kinetic Study of Glycerol Esterification with Acetic Acid over a Commercial Amberlyst-35 Ion Exchange Resin. *Rev. Chim.* **2019**, *70*, 2325–2329. [CrossRef]
103. Caballero, K.V.; Guerrero-Amaya, H.; Baldovino-Medrano, V.G. Revisiting Glycerol Esterification with Acetic Acid over Amberlyst-35 via Statistically Designed Experiments: Overcoming Transport Limitations. *Chem. Eng. Sci.* **2019**, *207*, 91–104. [CrossRef]
104. Liao, X.; Zhu, Y.; Wang, S.G.; Li, Y. Producing Triacetylglycerol with Glycerol by Two Steps: Esterification and Acetylation. *Fuel Process. Technol.* **2009**, *90*, 988–993. [CrossRef]
105. Bedogni, G.A.; Padró, C.L.; Okulik, N.B. A Combined Experimental and Computational Study of the Esterification Reaction of Glycerol with Acetic Acid. *J. Mol. Model.* **2014**, *20*, 2167. [CrossRef]
106. Reinoso, D.M.; Tonetto, G.M. Bioadditives Synthesis from Selective Glycerol Esterification over Acidic Ion Exchange Resin as Catalyst. *J. Environ. Chem. Eng.* **2018**, *6*, 3399–3407. [CrossRef]
107. Setyaningsih, L.; Siddiq, F.; Pramezy, A. Esterification of Glycerol with Acetic Acid over Lewatit Catalyst. *MATEC Web Conf.* **2018**, *154*, 2–5. [CrossRef]
108. Setyaningsih, L.; Mutiara, T.; Chafidz, A.; Zulkania, A.; Andrianto, M.A.; Farikha, N.L. Kinetic Modelling of Esterification of Glycerol with Acetic Acid Catalyzed by Lewatite. *IOP Conf. Ser. Mater. Sci. Eng.* **2019**, *543*, 012008. [CrossRef]
109. Jiang, Y.; Li, X.; Zhao, H.; Hou, Z. Esterification of Glycerol with Acetic Acid over SO_3H-Functionalized Phenolic Resin. *Fuel* **2019**, *255*, 115842. [CrossRef]
110. Mou, R.; Wang, X.; Wang, Z.; Zhang, D.; Yin, Z.; Lv, Y.; Wei, Z. Synthesis of Fuel Bioadditive by Esterification of Glycerol with Acetic Acid over Hydrophobic Polymer-Based Solid Acid. *Fuel* **2021**, *302*, 121175. [CrossRef]
111. Besson, M.; Gallezot, P.; Perrard, A.; Pinel, C. Active Carbons as Catalysts for Liquid Phase Reactions. *Catal. Today* **2005**, *102*, 160–165. [CrossRef]
112. Boehm, H.-P. Functional Groups on the Surfaces of Solids. *Angew. Chemie Int. Ed. Engl.* **1966**, *5*, 533–544. [CrossRef]
113. Konwar, L.J.; Mäki-Arvela, P.; Mikkola, J.P. SO3H-Containing Functional Carbon Materials: Synthesis, Structure, and Acid Catalysis. *Chem. Rev.* **2019**, *119*, 11576–11630. [CrossRef]
114. Schröder, E.; Thomauske, K.; Weber, C.; Hornung, A.; Tumiatti, V. Experiments on the Generation of Activated Carbon from Biomass. *J. Anal. Appl. Pyrolysis* **2007**, *79*, 106–111. [CrossRef]
115. Duan, D.; Chen, D.; Huang, L.; Zhang, Y.; Zhang, Y.; Wang, Q.; Xiao, G.; Zhang, W.; Lei, H.; Ruan, R. Activated Carbon from Lignocellulosic Biomass as Catalyst: A Review of the Applications in Fast Pyrolysis Process. *J. Anal. Appl. Pyrolysis* **2021**, *158*, 105246. [CrossRef]

116. Sánchez, J.A.; Hernández, D.L.; Moreno, J.A.; Mondragón, F.; Fernández, J.J. Alternative Carbon Based Acid Catalyst for Selective Esterification of Glycerol to Acetylglycerols. *Appl. Catal. A Gen.* **2011**, *405*, 55–60. [CrossRef]
117. Goscianska, J.; Malaika, A. A Facile Post-Synthetic Modification of Ordered Mesoporous Carbon to Get Efficient Catalysts for the Formation of Acetins. *Catal. Today* **2020**, *357*, 84–93. [CrossRef]
118. Galhardo, T.S.; Simone, N.; Gonçalves, M.; Figueiredo, F.C.A.; Mandelli, D.; Carvalho, W.A. Preparation of Sulfonated Carbons from Rice Husk and Their Application in Catalytic Conversion of Glycerol. *ACS Sustain. Chem. Eng.* **2013**, *1*, 1381–1389. [CrossRef]
119. Chandrakala, U.; Prasad, R.B.N.; Prabhavathi Devi, B.L.A. Glycerol Valorization as Biofuel Additives by Employing a Carbon-Based Solid Acid Catalyst Derived from Glycerol. *Ind. Eng. Chem. Res.* **2014**, *53*, 16164–16169. [CrossRef]
120. Rodrigues, R.; Gonçalves, M.; Mandelli, D.; Pescarmona, P.P.; Carvalho, W.A. Solvent-Free Conversion of Glycerol to Solketal Catalysed by Activated Carbons Functionalised with Acid Groups. *Catal. Sci. Technol.* **2014**, *4*, 2293–2301. [CrossRef]
121. Fernández, P.; Fraile, J.M.; García-Bordejé, E.; Pires, E. Sulfonated Hydrothermal Carbons from Cellulose and Glucose as Catalysts for Glycerol Ketalization. *Catalysts* **2019**, *9*, 804. [CrossRef]
122. Ao, S.; Alghamdi, L.A.; Kress, T.; Selvaraj, M.; Halder, G.; Wheatley, A.E.H.; Lalthazuala Rokhum, S. Microwave-Assisted Valorization of Glycerol to Solketal Using Biomass-Derived Heterogeneous Catalyst. *Fuel* **2023**, *345*, 128190. [CrossRef]
123. Konwar, L.J.; Mäki-Arvela, P.; Begum, P.; Kumar, N.; Thakur, A.J.; Mikkola, J.P.; Deka, R.C.; Deka, D. Shape Selectivity and Acidity Effects in Glycerol Acetylation with Acetic Anhydride: Selective Synthesis of Triacetin over Y-Zeolite and Sulfonated Mesoporous Carbons. *J. Catal.* **2015**, *329*, 237–247. [CrossRef]
124. Carvalho Ballotin, F.; da Silva, M.J.; Paula de Carvalho Teixeira, A.; Montero Lago, R. Amphiphilic Acid Carbon Catalysts Produced by Bio-Oil Sulfonation for Solvent-Free Glycerol Ketalization. *Fuel* **2020**, *274*, 117799. [CrossRef]
125. Balotin, G.; De Almeida, J.; Silva, R.S.; Carvalho, W.A.; Carvalho, C.T.; Rodrigues, R. Upgrading Catalytic Efficiency of Activated Carbons by Tailoring Lignocellulosic Biomass Waste for Sustainable Conversion of Glycerol to Solketal. *Mol. Catal.* **2023**, *538*, 112976. [CrossRef]
126. Mahammad Rafi, J.; Rajashekar, A.; Srinivas, M.; Rao, B.V.S.K.; Prasad, R.B.N.; Lingaiah, N. Esterification of Glycerol over a Solid Acid Biochar Catalyst Derived from Waste Biomass. *RSC Adv.* **2015**, *5*, 44550–44556. [CrossRef]
127. Tao, M.L.; Guan, H.Y.; Wang, X.H.; Liu, Y.C.; Louh, R.F. Fabrication of Sulfonated Carbon Catalyst from Biomass Waste and Its Use for Glycerol Esterification. *Fuel Process. Technol.* **2015**, *138*, 355–360. [CrossRef]
128. Bartoli, M.; Zhu, C.; Chae, M.; Bressler, D.C. Glycerol Acetylation Mediated by Thermally Hydrolysed Biosolids-Based Material. *Catalysts* **2020**, *10*, 5. [CrossRef]
129. Nda-Umar, U.I.; Ramli, I.; Muhamad, E.N.; Taufiq-Yap, Y.H.; Azri, N. Synthesis and Characterization of Sulfonated Carbon Catalysts Derived from Biomass Waste and Its Evaluation in Glycerol Acetylation. *Biomass Convers. Biorefinery* **2022**, *12*, 2045–2060. [CrossRef]
130. Malaika, A.; Ptaszyńska, K.; Kozłowski, M. Conversion of Renewable Feedstock to Bio-Carbons Dedicated for the Production of Green Fuel Additives from Glycerol. *Fuel* **2021**, *288*, 119609. [CrossRef]
131. Khayoon, M.S.; Abbas, A.; Hameed, B.H.; Triwahyono, S.; Jalil, A.A.; Harris, A.T.; Minett, A.I. Selective Acetalization of Glycerol with Acetone over Nickel Nanoparticles Supported on Multi-Walled Carbon Nanotubes. *Catal. Lett.* **2014**, *144*, 1009–1015. [CrossRef]
132. Gonçalves, M.; Rodrigues, R.; Galhardo, T.S.; Carvalho, W.A. Highly Selective Acetalization of Glycerol with Acetone to Solketal over Acidic Carbon-Based Catalysts from Biodiesel Waste. *Fuel* **2016**, *181*, 46–54. [CrossRef]
133. Konwar, L.J.; Samikannu, A.; Mäki-Arvela, P.; Boström, D.; Mikkola, J.P. Lignosulfonate-Based Macro/Mesoporous Solid Protonic Acids for Acetalization of Glycerol to Bio-Additives. *Appl. Catal. B Environ.* **2018**, *220*, 314–323. [CrossRef]
134. Saikia, K.; Rajkumari, K.; Moyon, N.S.; Basumatary, S.; Halder, G.; Rashid, U.; Rokhum, S.L. Sulphonated Biomass-Based Catalyst for Solketal Synthesis by Acetalization of Glycerol—A Byproduct of Biodiesel Production. *Fuel Process. Technol.* **2022**, *238*, 107482. [CrossRef]
135. Khayoon, M.S.; Hameed, B.H. Solventless Acetalization of Glycerol with Acetone to Fuel Oxygenates over Ni-Zr Supported on Mesoporous Activated Carbon Catalyst. *Appl. Catal. A Gen.* **2013**, *464–465*, 191–199. [CrossRef]
136. Cheruvathoor Poulose, A.; Medved', M.; Bakuru, V.R.; Sharma, A.; Singh, D.; Kalidindi, S.B.; Bares, H.; Otyepka, M.; Jayaramulu, K.; Bakandritsos, A.; et al. Acidic Graphene Organocatalyst for the Superior Transformation of Wastes into High-Added-Value Chemicals. *Nat. Commun.* **2023**, *14*, 1373. [CrossRef]
137. Kumar, S.; Viswanadham, N.; Saxena, S.K.; Selvamani, A.; Diwakar, J.; Al-Muhtaseb, A.H. Single-Pot Template-Free Synthesis of a Glycerol-Derived C-Si-Zr Mesoporous Composite Catalyst for Fuel Additive Production. *New J. Chem.* **2020**, *44*, 8254–8263. [CrossRef]
138. Reddy, P.S.; Sudarsanam, P.; Mallesham, B.; Raju, G.; Reddy, B.M. Acetalisation of Glycerol with Acetone over Zirconia and Promoted Zirconia Catalysts under Mild Reaction Conditions. *J. Ind. Eng. Chem.* **2011**, *17*, 377–381. [CrossRef]
139. Reena, S.; Shamshuddin, S.; Vasantha, V.; D'Souza, J. Synthesis of Solketal over Zirconia Based Acid Catalysts. *Bangladesh J. Sci. Ind. Res.* **2019**, *54*, 31–38. [CrossRef]
140. Vasantha, V.T.; Venkatesha, N.J.; Shamshuddin, S.Z.M.; Reddy, B.G.V. Sulphated Zirconia Supported on Cordierite Honeycomb Monolith for Effective Synthesis of Solketal from Acetalisation of Glycerol with Acetone. *ChemistrySelect* **2018**, *3*, 4–6. [CrossRef]
141. Lei, Q.; Li, D.; Li, J.; Liu, C.; Xu, C.; Dong, W. Glycerol Esterification to Glyceryl Diacetate over SO 42 À / W-Zr Complex Solid Super Acid Catalysts. *ChemistrySelect* **2019**, *4*, 2780–2786. [CrossRef]

142. Abida, K.; Ali, A. Sulphuric Acid—Functionalized Siliceous Zirconia as an Efficient and Reusable Catalyst for the Synthesis of Glycerol Triacetate. *Chem. Pap.* **2020**, *74*, 3627–3639. [CrossRef]
143. Mizuno, N.; Misono, M. Heteropolyacid Catalysts. *Curr. Opin. Solid State Mater. Sci.* **1997**, *2*, 84–89. [CrossRef]
144. Ren, Y.; Yue, B.; Gu, M.; He, H. Progress of the Application of Mesoporous Silica-Supported Heteropolyacids in Heterogeneous Catalysis and Preparation of Nanostructured Metal Oxides. *Materials* **2010**, *3*, 764–785. [CrossRef]
145. Ferreira, P.; Fonseca, I.M.; Ramos, A.M.; Vital, J.; Castanheiro, J.E. Valorisation of Glycerol by Condensation with Acetone over Silica-Included Heteropolyacids. *Appl. Catal. B Environ.* **2010**, *98*, 94–99. [CrossRef]
146. Chen, L.; Nohair, B.; Zhao, D.; Kaliaguine, S. Highly Efficient Glycerol Acetalization over Supported Heteropoly Acid Catalysts. *ChemCatChem* **2018**, *10*, 1918–1925. [CrossRef]
147. Talebian-Kiakalaieh, A.; Tarighi, S. Hierarchical Faujasite Zeolite-Supported Heteropoly Acid Catalyst for Acetalization of Crude-Glycerol to Fuel Additives. *J. Ind. Eng. Chem.* **2019**, *79*, 452–464. [CrossRef]
148. Sadjadi, S.; Tarighi, S.; Moussavi, N.S.; Ahadi, N. Heteropolyacid Supported on the Composite of Bentonite and Ionic Liquid Containing Acidic Polymer: A Highly Selective Catalyst for Glycerol Acetalization to Solketal. *J. Mol. Struct.* **2022**, *1256*, 132556. [CrossRef]
149. Chansorn, N.; Amnuaypanich, S.; Soontaranon, S.; Rugmai, S.; Amnuaypanich, S. Increasing Solketal Production from the Solventless Ketalization of Glycerol Catalyzed by Nanodispersed Phosphotungstic Acid in Poly(N-Methyl-4-Vinylpyridinium) Grafted on Silica Nanoparticles. *J. Ind. Eng. Chem.* **2022**, *112*, 233–243. [CrossRef]
150. da Silva, M.J.; Teixeira, M.G.; Chaves, D.M.; Siqueira, L. An Efficient Process to Synthesize Solketal from Glycerol over Tin (II) Silicotungstate Catalyst. *Fuel* **2020**, *281*, 118724. [CrossRef]
151. Da Silva, M.J.; Rodrigues, A.A.; Teixeira, M.G. Iron (III) Silicotungstate: An Efficient and Recyclable Catalyst for Converting Glycerol to Solketal. *Energy Fuels* **2020**, *34*, 9664–9673. [CrossRef]
152. Gonçalves, C.E.; Laier, L.O.; Cardoso, A.L.; José, M. Bioadditive Synthesis from $H_3PW_{12}O_{40}$-Catalyzed Glycerol Esteri Fi Cation with HOAc under Mild Reaction Conditions. *Fuel Process. Technol.* **2012**, *102*, 46–52. [CrossRef]
153. Ferreira, P.; Fonseca, I.M.; Ramos, A.M.; Vital, J.; Castanheiro, J.E. Glycerol Acetylation over Dodecatungstophosphoric Acid Immobilized into a Silica Matrix as Catalyst. *Appl. Catal. B Environ.* **2009**, *91*, 416–422. [CrossRef]
154. Khayoon, M.S.; Hameed, B.H. Synthesis of Hybrid SBA-15 Functionalized with Molybdophosphoric Acid as Efficient Catalyst for Glycerol Esterification to Fuel Additives. *Appl. Catal. A Gen.* **2012**, *433–434*, 152–161. [CrossRef]
155. Patel, A.; Singh, S. A Green and Sustainable Approach for Esterification of Glycerol Using 12-Tungstophosphoric Acid Anchored to Different Supports: Kinetics and Effect of Support. *Fuel* **2014**, *118*, 358–364. [CrossRef]
156. Balaraju, M.; Nikhitha, P.; Jagadeeswaraiah, K.; Srilatha, K.; Prasad, P.S.S.; Lingaiah, N. Acetylation of Glycerol to Synthesize Bioadditives over Niobic Acid Supported Tungstophosphoric Acid Catalysts. *Fuel Process. Technol.* **2010**, *91*, 249–253. [CrossRef]
157. Ferreira, P.; Fonseca, I.M.; Ramos, A.M.; Vital, J.; Castanheiro, J.E. Esterification of Glycerol with Acetic Acid over Dodecamolybdophosphoric Acid Encaged in USY Zeolite. *Catal. Commun.* **2009**, *10*, 481–484. [CrossRef]
158. Neto, A.B.S.; Oliveira, A.C.; Rodriguez-castellón, E.; Campos, A.F.; Freire, P.T.C.; Sousa, F.F.F.; Filho, J.M.; Araujo, J.C.S.; Lang, R. A Comparative Study on Porous Solid Acid Oxides as Catalysts in the Esteri Fi Cation of Glycerol with Acetic Acid. *Catal. Today* **2020**, *349*, 57–67. [CrossRef]
159. Magar, S.; Mohanraj, G.T.; Jana, S.K.; Rode, C.V. Synthesis and Characterization of Supported Heteropoly Acid: Efficient Solid Acid Catalyst for Glycerol Esterification to Produce Biofuel Additives. *Inorg. Nano-Metal Chem.* **2020**, *50*, 1157–1165. [CrossRef]
160. Kale, S.S.; Armbruster, U.; Eckelt, R.; Bentrup, U.; Umbarkar, S.B.; Dongare, M.K.; Martin, A. Understanding the Role of Keggin Type Heteropolyacid Catalysts for Glycerol Acetylation Using Toluene as an Entrainer. *Appl. Catal. A Gen.* **2016**, *527*, 9–18. [CrossRef]
161. Jagadeeswaraiah, K.; Balaraju, M.; Prasad, P.S.S.; Lingaiah, N. Selective Esterification of Glycerol to Bioadditives over Heteropoly Tungstate Supported on Cs-Containing Zirconia Catalysts. *Appl. Catal. A Gen.* **2010**, *386*, 166–170. [CrossRef]
162. Zhu, S.; Gao, X.; Dong, F.; Zhu, Y.; Zheng, H.; Li, Y. Design of a Highly Active Silver-Exchanged Phosphotungstic Acid Catalyst for Glycerol Esterification with Acetic Acid. *J. Catal.* **2013**, *306*, 155–163. [CrossRef]
163. Da Silva, M.J.; Liberto, N.A.; De Andrade Leles, L.C.; Pereira, U.A. Fe4(SiW12O40)3-Catalyzed Glycerol Acetylation: Synthesis of Bioadditives by Using Highly Active Lewis Acid Catalyst. *J. Mol. Catal. A Chem.* **2016**, *422*, 69–83. [CrossRef]
164. Sun, Z.; Duan, X.; Tao, M.; Wang, X.; Zhou, D. Design of a Highly Efficient Indium-Exchanged Heteropolytungstic Acid for Glycerol Esterification with Acetic Acid. *Catal. Surv. Asia* **2016**, *20*, 82–90. [CrossRef]
165. Kamlesh, N.T.; Manish, M.; Munusamy, K.; Rajesh, S.S. Synthesis of Aluminium Triflate-Grafted MCM-41 as a Water-Tolerant Acid Catalyst for the Ketalization of Glycerol with Acetone. *Catal. Sci. Technol.* **2015**, *5*, 2427–2440.
166. Abreu, T.H.; Meyer, C.I.; Padró, C.; Martins, L. Acidic V-MCM-41 Catalysts for the Liquid-Phase Ketalization of Glycerol with Acetone. *Microporous Mesoporous Mater.* **2019**, *273*, 219–225. [CrossRef]
167. Collard, X.; Li, L.; Lueangchaichaweng, W.; Bertrand, A.; Aprile, C.; Pescarmona, P.P. Ga-MCM-41 Nanoparticles: Synthesis and Application of Versatile Heterogeneous Catalysts. *Catal. Today* **2014**, *235*, 184–192. [CrossRef]
168. Huang, Y.; Zhang, G.; Zhang, Q. Preparation of the WOX/MCM-41 Solid Acid Catalyst and the Catalytic Performance for Solketal Synthesis. *ACS Omega* **2021**, *6*, 3875–3883. [CrossRef]
169. Gadamsetti, S.; Rajan, N.P.; Rao, G.S.; Chary, K.V.R. Acetalization of Glycerol with Acetone to Bio Fuel Additives over Supported Molybdenum Phosphate Catalysts. *J. Mol. Catal. A Chem.* **2015**, *410*, 49–57. [CrossRef]

170. Ammaji, S.; Rao, G.S.; Chary, K.V.R. Acetalization of Glycerol with Acetone over Various Metal—Modified SBA—15 Catalysts. *Appl. Petrochem. Res.* **2018**, *8*, 107–118. [CrossRef]
171. Vicente, G.; Melero, J.A.; Morales, G.; Paniagua, M.; Martín, E. Acetalisation of Bio-Glycerol with Acetone to Produce Solketal over Sulfonic Mesostructured Silicas. *Green Chem.* **2010**, *12*, 899–907. [CrossRef]
172. Li, Z.; Miao, Z.; Wang, X.; Zhao, J.; Zhou, J.; Si, W.; Zhuo, S. One-Pot Synthesis of ZrMo-KIT-6 Solid Acid Catalyst for Solvent-Free Conversion of Glycerol to Solketal. *Fuel* **2018**, *233*, 377–387. [CrossRef]
173. Kao, L.C.; Kan, W.C.; Martin-Aranda, R.M.; Guerrero-Perez, M.O.; Bañares, M.; Liou, S.Y.H. SiO_2 Supported Niobium Oxides with Active Acid Sites for the Catalytic Acetalization of Glycerol. *Catal. Today* **2020**, *356*, 80–87. [CrossRef]
174. Vivian, A.; Soumoy, L.; Fusaro, L.; Louette, P.; Felten, A.; Fiorilli, S.; Debecker, D.P.; Aprile, C. The High Activity of Mesoporous Ga-SiO_2 Catalysts in the Upgrading of Glycerol to Solketal Explained by in-Depth Characterization. *J. Catal.* **2021**, *400*, 83–92. [CrossRef]
175. Hermida, L.; Agustian, J.; Abdullah, A.Z.; Mohamed, A.R. Review of Large-Pore Mesostructured Cellular Foam (MCF) Silica and Its Applications. *Open Chem.* **2019**, *17*, 1000–1016. [CrossRef]
176. Calvino-Casilda, V.; Stawicka, K.; Trejda, M.; Ziolek, M.; Bañares, M.A. Real-Time Raman Monitoring and Control of the Catalytic Acetalization of Glycerol with Acetone over Modified Mesoporous Cellular Foams. *J. Phys. Chem. C* **2014**, *118*, 10780–10791. [CrossRef]
177. Stawicka, K.; Alba, E.D.; Calvino-casilda, V.; Trejda, M.; Ban, M.A.; Ziolek, M. The Role of Brønsted and Lewis Acid Sites in Acetalization of Glycerol over Modi Fi Ed Mesoporous Cellular Foams. *J. Phys. Chem. C* **2016**, *120*, 16699–16711. [CrossRef]
178. Bivona, L.A.; Vivian, A.; Fusaro, L.; Fiorilli, S.; Aprile, C. Design and Catalytic Applications of 1D Tubular Nanostructures: Improving Efficiency in Glycerol Conversion. *Appl. Catal. B Environ.* **2019**, *247*, 182–190. [CrossRef]
179. Melero, J.A.; van Grieken, R.; Morales, G.; Paniagua, M. Acidic Mesoporous Silica for the Acetylation of Glycerol: Synthesis of Bioadditives to Petrol Fuel. *Energy Fuels* **2007**, *21*, 1782–1791. [CrossRef]
180. Popova, M.; Lazarova, H.; Szegedi, A.; Mihályi, M.R.; Rangus, M.; Likozar, B.; Dasireddy, V.D.B.C. Renewable Glycerol Esterification over Sulfonic-Modified Mesoporous Silicas. *J. Serbian Chem. Soc.* **2018**, *83*, 39–50. [CrossRef]
181. Tonutti, L.G.; Dalla Costa, B.O.; Decolatti, H.P.; Mendow, G.; Querini, C.A. Determination of Kinetic Constants for Glycerol Acetylation by Particle Swarm Optimization Algorithm. *Chem. Eng. J.* **2021**, *424*, 130408. [CrossRef]
182. Manurung, R.; Dedi Anggreawan, M.; Gery Siregar, A. Triacetin Production Using SiO_2-H_3PO_4 Catalysts Derived from Bamboo Leaf Biomass Waste for Esterification Reactions of Glycerol and Acetic Acid. *IOP Conf. Ser. Mater. Sci. Eng.* **2020**, *801*, 012052. [CrossRef]
183. Trejda, M.; Stawicka, K.; Dubinska, A.; Ziolek, M. Development of Niobium Containing Acidic Catalysts for Glycerol Esterification. *Catal. Today* **2012**, *187*, 129–134. [CrossRef]
184. Khayoon, M.S.; Triwahyono, S.; Hameed, B.H.; Jalil, A.A. Improved Production of Fuel Oxygenates via Glycerol Acetylation with Acetic Acid. *Chem. Eng. J.* **2014**, *243*, 473–484. [CrossRef]
185. Timofeeva, M.N.; Panchenko, V.N.; Krupskaya, V.V.; Gil, A.; Vicente, M.A. Effect of Nitric Acid Modification of Montmorillonite Clay on Synthesis of Solketal from Glycerol and Acetone. *Catal. Commun.* **2017**, *90*, 65–69. [CrossRef]
186. Alali, K.; Lebsir, F.; Amri, S.; Rahmouni, A.; Srasra, E. Algerian Acid Activated Clays as Efficient Catalysts for a Green Synthesis of Solketal by Chemoselective Acetalization of Glycerol with Acetone. *Bull. Chem. React. Eng. Catal.* **2019**, *14*, 130–141. [CrossRef]
187. Perez, F.M.; Santori, G.F.; Pompeo, F.; Nichio, N.N. Silica-Resin-Bentonite Nanocomposite and Its Application in Catalysis. *Minerals* **2022**, *12*, 1486. [CrossRef]
188. Tangestanifard, M.; Ghaziaskar, H.S. Arenesulfonic Acid-Functionalized Bentonite as Catalyst in Glycerol Esterification with Acetic Acid. *Catalysts* **2017**, *7*, 211. [CrossRef]
189. Fan, C.; Xu, C.; Liu, C.; Huang, Z.; Liu, J.; Ye, Z. Catalytic Acetalization of Biomass Glycerol with Acetone over TiO_2–SiO_2 Mixed Oxides. *React. Kinet. Mech. Catal.* **2012**, *107*, 189–202. [CrossRef]
190. Souza, T.E.; Padula, I.D.; Teodoro, M.M.G.; Chagas, P.; Resende, J.M.; Souza, P.P.; Oliveira, L.C.A. Amphiphilic Property of Niobium Oxyhydroxide for Waste Glycerol Conversion to Produce Solketal. *Catal. Today* **2015**, *254*, 83–89. [CrossRef]
191. Mallesham, B.; Sudarsanam, P.; Reddy, B.M. Production of Biofuel Additives from Esterification and Acetalization of Bioglycerol over SnO_2-Based Solid Acids. *Ind. Eng. Chem. Res.* **2014**, *53*, 18775–18785. [CrossRef]
192. Rodrigues, R.; Mandelli, D.; Gonçalves, N.S.; Pescarmona, P.P.; Carvalho, W.A. Acetalization of Acetone with Glycerol Catalyzed by Niobium-Aluminum Mixed Oxides Synthesized by a Sol–Gel Process. *J. Mol. Catal. A Chem.* **2016**, *422*, 122–130. [CrossRef]
193. Shen, C.; Li, Z.; Park, J.S.; Li, Z.; Li, C.; Hong, G.H.; Lee, J.; Moon, H.; Kim, J.M.; Jin, M. Ordered WOx/Mesoporous SnO_2 Catalysts with Excellent Acetalization Performance for Producing Bio-Additives from Glycerol. *Mol. Catal.* **2022**, *520*, 112179. [CrossRef]
194. Li, X.; Zheng, L.; Hou, Z. Acetalization of Glycerol with Acetone over $Co[II](Co[III]_XAl_{2-x})O_4$ Derived from Layered Double Hydroxide. *Fuel* **2018**, *233*, 565–571. [CrossRef]
195. Gomes, I.S.; de Carvalho, D.C.; Oliveira, A.C.; Rodríguez-Castellón, E.; Tehuacanero-Cuapa, S.; Freire, P.T.; Josué Filho, M.; Saraiva, G.D.; de Sousa, F.F.; Lang, R. On the Reasons for Deactivation of Titanate Nanotubes with Metals Catalysts in the Acetalization of Glycerol with Acetone. *Chem. Eng. J.* **2018**, *334*, 1927–1942. [CrossRef]

196. Luis, A.; Pinheiro, G.; Vitor, J.; Carmo, C.; Carvalho, D.C.; Oliveira, A.C.; Rodríguez-castellón, E.; Tehuacanero-cuapa, S.; Otubo, L.; Lang, R. Bio-Additive Fuels from Glycerol Acetalization over Metals-Containing Vanadium Oxide Nanotubes ($MeVO_x$-NT in Which, Me = Ni, Co, or Pt). *Fuel Process. Technol.* **2019**, *184*, 45–56. [CrossRef]
197. Bakuru, V.R.; Churipard, S.R.; Maradur, S.P.; Kalidindi, S.B. Exploring the Brønsted Acidity of UiO-66 (Zr, Ce, Hf) Metal-Organic Frameworks for Efficient Solketal Synthesis from Glycerol Acetalization. *Dalt. Trans.* **2019**, *48*, 843–847. [CrossRef]
198. Timofeeva, M.N.; Panchenko, V.N.; Khan, N.A.; Hasan, Z.; Prosvirin, I.P.; Tsybulya, S.V.; Jhung, S.H. Isostructural Metal-Carboxylates MIL-100(M) and MIL-53(M) (M: V, Al, Fe and Cr) as Catalysts for Condensation of Glycerol with Acetone. *Appl. Catal. A Gen.* **2017**, *529*, 167–174. [CrossRef]
199. Wang, W.; Zeng, X.; He, S.; Zhang, H.; Jiang, G.; He, Y.; Liu, Y.; Dong, F.; Zhang, X.; Suib, S.L. Understanding How the Crystalline Nature of Fe-Promoted Alumino-Borate PKU-1 Catalyst Affects Glycerin Ketalization: The Systematic Control of Surface Composition and Acidity. *Appl. Catal. A Gen.* **2023**, *649*, 118945. [CrossRef]
200. De Carvalho, D.C.; Oliveira, A.C.; Ferreira, O.P.; Josué Filho, M.; Tehuacanero-Cuapa, S.; Oliveira, A.C. Titanate Nanotubes as Acid Catalysts for Acetalization of Glycerol with Acetone: Influence of the Synthesis Time and the Role of Structure on the Catalytic Performance. *Chem. Eng. J.* **2017**, *313*, 1454–1467. [CrossRef]
201. Hu, W.; Zhang, Y.; Huang, Y.; Wang, J.; Gao, J.; Xu, J. Selective Esterification of Glycerol with Acetic Acid to Diacetin Using Antimony Pentoxide as Reusable Catalyst. *J. Energy Chem.* **2015**, *24*, 632–636. [CrossRef]
202. da Silva, D.S.; Altino, F.M.R.S.; Bortoluzzi, J.H.; Meneghetti, S.M.P. Investigation of Sn(IV) Catalysts in Glycerol Acetylation. *Mol. Catal.* **2020**, *494*, 111130. [CrossRef]
203. Abida, K.; Chudasama, B.; Ali, A. Development and Functionalization of Magnetic Nanoparticles as Stable and Reusable Catalysts for Triacetin Synthesis. *New J. Chem.* **2020**, *44*, 9365–9376. [CrossRef]
204. Altino, F.M.R.S.; da Silva, D.S.; Bortoluzzi, J.H.; Meneghetti, S.M.P. Investigation of Glycerol Acetylation in the Presence of Sb Catalysts. *Biomass Convers. Biorefinery* **2021**, *13*, 3237–3246. [CrossRef]
205. Serafim, H.; Fonseca, I.M.; Ramos, A.M.; Vital, J.; Castanheiro, J.E. Valorization of Glycerol into Fuel Additives over Zeolites as Catalysts. *Chem. Eng. J.* **2011**, *178*, 291–296. [CrossRef]
206. Hong, G.H.; Li, Z.; Park, J.S.; Li, Z.; Kim, K.Y.; Li, C.; Lee, J.; Jin, M.; Stucky, G.D.; Kim, J.M. Glycerol Acetalization over Highly Ordered Mesoporous Molybdenum Dioxide: Excellent Catalytic Performance, Recyclability and Water-Tolerance. *J. Ind. Eng. Chem.* **2022**, *107*, 354–364. [CrossRef]
207. Nanda, M.R.; Yuan, Z.; Qin, W.; Ghaziaskar, H.S.; Poirier, M.A.; Xu, C.C. A New Continuous-Flow Process for Catalytic Conversion of Glycerol to Oxygenated Fuel Additive: Catalyst Screening. *Appl. Energy* **2014**, *123*, 75–81. [CrossRef]
208. Arun, P.; Pudi, S.M.; Biswas, P. Acetylation of Glycerol over Sulfated Alumina: Reaction Parameter Study and Optimization Using Response Surface Methodology. *Energy Fuels* **2016**, *30*, 584–593. [CrossRef]
209. Nda-Umar, U.I.; Ramli, I.; Muhamad, E.N.; Azri, N.; Taufiq-Yap, Y.H. Optimization and Characterization of Mesoporous Sulfonated Carbon Catalyst and Its Application in Modeling and Optimization of Acetin Production. *Molecules* **2020**, *25*, 5221. [CrossRef]
210. Dmitriev, G.S.; Terekhov, A.V.; Zanaveskin, L.N.; Maksimov, A.L.; Khadzhiev, S.N. Kinetics of the Formation of Solketal in the Presence of Sulfuric Acid. *Kinet. Catal.* **2018**, *59*, 504–508. [CrossRef]
211. Rane, S.A.; Pudi, S.M.; Biswas, P. Esterification of Glycerol with Acetic Acid over Highly Active and Stable Alumina-Based Catalysts: A Reaction Kinetics Study. *Chem. Biochem. Eng. Q.* **2016**, *30*, 33–45. [CrossRef]
212. Veluturla, S.; Shetty, S.; Rao, D.S.; Archna, A. Kinetic Study of Synthesis of Bio-Fuel Additives from Glycerol Using a Hetropolyacid. *Resour. Technol.* **2017**, *3*, 337–341. [CrossRef]
213. Banu, I.; Bumbac, G.; Bombos, D.; Velea, S.; Gălan, A.M.; Bozga, G. Glycerol Acetylation with Acetic Acid over Purolite CT-275. Product Yields and Process Kinetics. *Renew. Energy* **2020**, *148*, 548–557. [CrossRef]
214. Keogh, J.; Jeffrey, C.; Tiwari, M.S.; Manyar, H. Kinetic Analysis of Glycerol Esterification Using Tin Exchanged Tungstophosphoric Acid on K-10. *Ind. Eng. Chem. Res.* **2022**. [CrossRef]
215. Reinoso, D.M.; Boldrini, D.E. Kinetic Study of Fuel Bio-Additive Synthesis from Glycerol Esterification with Acetic Acid over Acid Polymeric Resin as Catalyst. *Fuel* **2020**, *264*, 116879. [CrossRef]
216. Maksimov, A.L.; Nekhaev, A.I.; Ramazanov, D.N.; Arinicheva, Y.A.; Dzyubenko, A.A.; Khadzhiev, S.N. Preparation of High Octane Oxygenate Fuel Components from Plant Derived Polyols. *Pet. Chem.* **2011**, *51*, 61–69. [CrossRef]
217. Shirani, M.; Ghaziaskar, H.S.; Xu, C. Optimization of Glycerol Ketalization to Produce Solketal as Biodiesel Additive in a Continuous Reactor with Subcritical Acetone Using Purolite® PD206 as Catalyst. *Fuel Process. Technol.* **2014**, *124*, 206–211. [CrossRef]
218. Oliveira, P.A.; Souza, R.O.M.A.; Mota, C.J.A. Atmospheric Pressure Continuous Production of Solketal from the Acid-Catalyzed Reaction of Glycerol with Acetone. *J. Braz. Chem. Soc.* **2016**, *27*, 1832–1837. [CrossRef]
219. Aghbashlo, M.; Tabatabaei, M.; Hosseinpour, S.; Rastegari, H.; Ghaziaskar, H.S. Multi-Objective Exergy-Based Optimization of Continuous Glycerol Ketalization to Synthesize Solketal as a Biodiesel Additive in Subcritical Acetone. *Energy Convers. Manag.* **2018**, *160*, 251–261. [CrossRef]
220. Domínguez-Barroso, V.; Herrera, C.; Larrubia, M.Á.; González-Gil, R.; Cortés-Reyes, M.; Alemany, L.J. Continuous-Flow Process for Glycerol Conversion to Solketal Using a Brönsted Acid Functionalized Carbon-Based Catalyst. *Catalysts* **2019**, *9*, 609. [CrossRef]

221. Rastegari, H.; Ghaziaskar, H.S. From Glycerol as the By-Product of Biodiesel Production to Value-Added Monoacetin by Continuous and Selective Esterification in Acetic Acid. *J. Ind. Eng. Chem.* **2015**, *21*, 856–861. [CrossRef]
222. Esteban, J.; Vorholt, A.J.; Behr, A.; Ladero, M.; Garcia-ochoa, F. Liquid − Liquid Equilibria for the System Acetone + Solketal + Glycerol at (303.2, 313.2, and 323.2) K. *J. Chem. Eng. Data* **2014**, *59*, 2850–2855. [CrossRef]
223. Mahreni; Azimatun Nur, M.M. Investigation of Ferri-Alginate (Fe-Alg) as Environmentally Friendly Catalyst on the Formation of Solketal from Glycerol and Acetone. *IOP Conf. Ser. Mater. Sci. Eng.* **2020**, *742*, 012010. [CrossRef]
224. Fischer, E.; Pfähler, E. Über Glycerin-aceton Und Seine Verwendbarkeit Zur Reindarstellung von A-Glyceriden; Über Eine Phosphorsäure-Verbindung Des Glykols. *Berichte Dtsch. Chem. Gesellschaft* **1920**, *53*, 1606–1621. [CrossRef]
225. Newman, M.S.; Renoll, M. Improved Preparation of Isopropylidene Glycerol. *J. Am. Chem. Soc.* **1945**, *67*, 1621. [CrossRef]
226. Deutsch, J.; Martin, A.; Lieske, H. Investigations on Heterogeneously Catalysed Condensations of Glycerol to Cyclic Acetals. *J. Catal.* **2007**, *245*, 428–435. [CrossRef]
227. Roldán, L.; Mallada, R.; Fraile, J.M.; Mayoral, J.A.; Menéndez, M. Glycerol Upgrading b y Ketalization in a Zeolite m Embrane Reactor. *Asia-Pacific J. Chem. Eng.* **2009**, *4*, 279–284. [CrossRef]
228. Esposito, R.; Raucci, U.; Cucciolito, M.E.; Di Guida, R.; Scamardella, C.; Rega, N.; Ruffo, F. Iron(III) Complexes for Highly Efficient and Sustainable Ketalization of Glycerol: A Combined Experimental and Theoretical Study. *ACS Omega* **2019**, *4*, 688–698. [CrossRef]
229. Li, X.; Lai, J.; Cong, H.; Shu, C.; Zhao, R.; Wang, Y.; Li, H.; Gao, X. Toward Sustainable and Eco-Efficient Novel Catalytic Distillation Process for Production of Solketal Using Seepage Catalytic Packing Internal. *Catal. Today* **2022**, *388–389*, 92–108. [CrossRef]
230. Liu, J.; Wang, Z.; Sun, Y.; Jian, R.; Jian, P.; Wang, D. Selective Synthesis of Triacetin from Glycerol Catalyzed by HZSM-5/MCM-41 Micro/Mesoporous Molecular Sieve. *Chin. J. Chem. Eng.* **2019**, *27*, 1073–1078. [CrossRef]
231. Li, H.; Li, J.; Li, X.; Gao, X. Esterification of Glycerol and Acetic Acid in a Pilot-Scale Reactive Distillation Column: Experimental Investigation, Model Validation, and Process Analysis. *J. Taiwan Inst. Chem. Eng.* **2018**, *89*, 56–66. [CrossRef]
232. Bhaduri, K.; Chatterjee, R.; Bhaumik, A.; Chowdhury, B. Metal-Free Phosphate Modified Hierarchically Porous Carbon-Silica Nanocomposites for Solvent-Free Glycerol Carbonylation and Esterification Reactions. *ACS Sustain. Chem. Eng.* **2022**, *10*, 11242–11256. [CrossRef]
233. Gatti, M.N.; Pompeo, F.; Nichio, N.N.; Santori, G.F. Crude Glycerol Hydrogenolysis to Bio-Propylene Glycol: Effect of Its Impurities on Activity, Selectivity and Stability. *Processes* **2023**, *11*, 1731. [CrossRef]
234. Da Silva, C.X.A.; Mota, C.J.A. The Influence of Impurities on the Acid-Catalyzed Reaction of Glycerol with Acetone. *Biomass Bioenergy* **2011**, *35*, 3547–3551. [CrossRef]
235. Kowalska-Kuś, J.; Held, A.; Nowińska, K. A Continuous-Flow Process for the Acetalization of Crude Glycerol with Acetone on Zeolite Catalysts. *Chem. Eng. J.* **2020**, *401*, 126143. [CrossRef]
236. Popova, M.; Szegedi, Á.; Ristić, A.; Tušar, N.N. Glycerol Acetylation on Mesoporous KIL-2 Supported Sulphated Zirconia Catalysts. *Catal. Sci. Technol.* **2014**, *4*, 3993–4000. [CrossRef]
237. Oh, S.; Park, C. Enzymatic Production of Glycerol Acetate from Glycerol. *Enzyme Microb. Technol.* **2015**, *69*, 19–23. [CrossRef]
238. Avilés-García, O.; Mendoza-Zepeda, A.; Regalado-Méndez, A.; Espino-Valencia, J.; Martínez-Vargas, S.L.; Romero, R.; Natividad, R. Photo-Oxidation of Glycerol Catalyzed by Cu/TiO_2. *Catalysts* **2022**, *12*, 835. [CrossRef]
239. Hidalgo-Carrillo, J.; Estévez-Toledano, R.C.; López-Tenllado, F.J.; Bautista, F.M.; Urbano, F.J.; Marinas, A. Fourth Generation Synthesis of Solketal by Glycerol Acetalization with Acetone: A Solar-Light Photocatalytic Approach. *J. Taiwan Inst. Chem. Eng.* **2021**, *125*, 297–303. [CrossRef]
240. Gomes, G.H.M.; Gabriel, J.B.; Bruziquesi, C.G.O.; Victoria, H.V.; Krambrock, K.; Oliveira, L.C.A.; Mohallem, N.D.S. The Role of Oxygen Vacancies in TT-Nb_2O_5 Nanoparticles for the Photoconversion of Glycerol into Solketal. *Ceram. Int.* **2023**, *49*, 14719–14732. [CrossRef]
241. Vannucci, J.A.; Gatti, M.N.; Cardaci, N.; Nichio, N.N. Economic Feasibility of a Solketal Production Process from Glycerol at Small Industrial Scale. *Renew. Energy* **2022**, *190*, 540–547. [CrossRef]
242. Avila Alcántara, J.R.; Yang Kong, Z.; Lee, H.-Y.; Sunarso, J. Advancements in Optimization and Control Techniques for Intensifying Processes. *Processes* **2021**, *9*, 2150. [CrossRef]
243. Corrêa, I.; Faria, R.P.V.; Rodrigues, A.E. Continuous Valorization of Glycerol into Solketal: From the Fixed-Bed Adsorptive Reactor to the Simulated Moving-Bed Reactor. *Ind. Eng. Chem. Res.* **2022**, *61*, 4017–4030. [CrossRef]
244. Faria, R.P.V.; Gonçalves, J.C.; Corrêa, I.; Ribeiro, A.M.; Rodrigues, A.E. Improving the Performance of a Simulated Moving Bed Reactor for the Synthesis of Solketal by Implementing Multifeed Strategy. *Ind. Eng. Chem. Res.* **2022**, *61*, 14531–14545. [CrossRef]